

**AIRCRAFT STABILITY ANALYSIS AND CONTROL  
SYSTEMS DESIGN: AN ADAPTIVE APPROACH**

**M.Sc. Thesis by  
Kamuran TÜRKOĞLU, B.Sc.**

**Department : Aeronautical and Astronautical Engineering**

**Programme: Flight Control Systems and Avionics**

**Supervisor : Prof. Dr. Elbrus M. CAFEROV**

**JUNE 2007**

**AIRCRAFT STABILITY ANALYSIS AND CONTROL  
SYSTEMS DESIGN: AN ADAPTIVE APPROACH**

**M.Sc. Thesis by  
Kamuran TÜRKOĞLU, B.Sc.  
511051017**

**Date of submission : 07 May 2007  
Date of defence examination: 13 June 2007**

**Supervisor (Chairman): Prof. Dr. Elbrus M. Caferov  
Members of the Examining Committee Prof. Dr. Mehmet Ş. Kavsaoglu (İTÜ)  
Assoc. Prof. Dr. Fuat Gürleyen (İTÜ)**

**JUNE 2007**

**BİR UÇAĞIN KARARLILIK ANALİZİ VE  
OTOMATİK KONTROL SİSTEMİ TASARIMLARI:  
UYARLAMALI (ADAPTİF) KONTROL YAKLAŞIMI**

**YÜKSEK LİSANS TEZİ  
Müh. Kamuran TÜRKOĞLU  
511051017**

**Tezin Enstitüye Verildiği Tarih : 07 Mayıs 2007  
Tezin Savunulduğu Tarih : 13 Haziran 2007**

**Tez Danışmanı : Prof. Dr. Elbrus M. Caferov  
Diğer Jüri Üyeleri Prof. Dr. Mehmet Ş. Kavsaoğlu (İTÜ)  
Doç. Dr. Fuat Gürleyen (İTÜ)**

**HAZİRAN 2007**

## **FOREWORD**

In the thesis, longitudinal and lateral dynamic modes of an Unmanned Aerial Vehicle (UAV) have been analyzed and different kind of automatic control systems consisted of Model Reference Adaptive System Design: PI adjustment based on Normalized MIT rule, PI adjustment based on Lyapunov stability theory and Augmented Optimal LQR Control System design procedures have been discussed. During the research, necessary calculations and analyses have been conducted with the help of MATLAB v7.1.

I would like to express my gratitude to Prof. Dr. Elbrous M. Jafarov for his guidance and support during my B.Sc., M.Sc. studies and the thesis.

As a last word, I would like to express my special thanks to my family for their invaluable support during the most difficult times that I have been experiencing throughout 2006 and 2007.

İstanbul, June 2007.

Kâmran Türkođlu

<b>FOREWORD</b>	ii
<b>CONTENTS</b>	iii
<b>ABBREVIATIONS</b>	v
<b>TABLE LIST</b>	vi
<b>FIGURE LIST</b>	vii
<b>NOTATION LIST</b>	ix
<b>SUMMARY</b>	x
<b>ÖZET</b>	xi
<b>1. INTRODUCTION</b>	
1.1. Components of an Aircraft	4
1.1.1. Control surfaces	4
1.1.2. Servo mechanisms	5
1.1.3. Rate gyroscopes	5
1.1.4. Integrating gyroscopes	6
<b>2. LONGITUDINAL DYNAMIC MODELING</b>	
2.1. Equations of Motion	7
2.2. Derivation the Longitudinal Dynamic Model of the Aircraft	13
2.3. Model Reference Adaptive Control System Design for the Longitudinal Dynamics of the UAV	23
2.3.1. PI Adjustment based on MIT rule	27
2.3.2. PI Adjustment based on Lyapunov Stability Theory	32
2.4. Augmented Optimal LQR Control System Design: Longitudinal Dynamics	41
2.4.1. Observability and controllability of system dynamics: Longitudinal flight	42
2.4.2. Augmented optimal LQR control system design: Integral control	44
2.5. Comparison of Automatic Control System Designs: Longitudinal Dynamics	49
<b>3. LATERAL DYNAMIC MODELING</b>	
3.1. Equations of Motion	51
3.2. Model Reference Adaptive Control System Design for the Lateral Dynamics of the UAV	60
3.2.1. MRAS Design based on Lyapunov stability	60
3.3. Optimal LQR Control System Design: Lateral Dynamics	64
3.3.1. Observability and controllability of system dynamics: Lateral flight	64
3.3.2. Optimal LQR control system design: Classical approach	64
3.4. Comparison of Automatic Control Systems Design: Lateral Dynamics	67

<b>4. RESULTS AND DISCUSSION</b>	69
<b>REFERENCES</b>	71
<b>APPENDIX</b>	74
<b>CURRICULUM VITAE</b>	86

## ABBREVIATIONS

<b>EOM</b>	:	Equations of motion
<b>LT</b>	:	Laplace transform
<b>CE</b>	:	Characteristic equation
<b>UAV</b>	:	Unmanned aerial vehicle
<b>TF</b>	:	Transfer function
<b>MRAS</b>	:	Model reference adaptive system
<b>PI</b>	:	Proportional-Integral
<b>PM</b>	:	Phase margin
<b>GM</b>	:	Gain margin
<b>OL</b>	:	Open-Loop
<b>CL</b>	:	Closed-Loop
<b>LTI</b>	:	Linear time-invariant
<b>KE</b>	:	Kinetic energy
<b>PE</b>	:	Potential energy
<b>LQR</b>	:	Linear quadratic regulator
<b>DRM</b>	:	Dutch-Roll mode
<b>MIMO</b>	:	Multi Input Multi Output
<b>SISO</b>	:	Single Input Single Output

## TABLE LIST

	<b><u>Page No.</u></b>
<b>Table 1.1</b>	Constants of longitudinal EOM ..... 14
<b>Table 1.2</b>	Stability derivatives of longitudinal EOMs ..... 16
<b>Table 1.3</b>	Elevator displacements (inputs) of the UAV system ..... 16
<b>Table 2.1</b>	Comparison of characteristic properties of designed controllers: Longitudinal dynamics ..... 48
<b>Table 2.2</b>	Lateral stability derivatives and inputs of the UAV ..... 52
<b>Table 3.1</b>	Comparison of characteristic properties of designed controllers: Lateral dynamics ..... 66



## FIGURE LIST

	<u>Page No.</u>
<b>Figure 1.1</b> : Control surfaces on the aircraft .....	4
<b>Figure 1.2</b> : Rate gyroscopes .....	6
<b>Figure 1.3</b> : Integrating gyroscopes .....	6
<b>Figure 2.1</b> : Body axis system .....	9
<b>Figure 2.2</b> : Bode and time domain response plot of $u(s)/\delta_e(s)$ .....	20
<b>Figure 2.3</b> : Bode and time domain response plot of $\alpha(s)/\delta_e(s)$ .....	21
<b>Figure 2.4</b> : Bode plot and time domain response of $\theta(s)/\delta_e(s)$ ...	22
<b>Figure 2.5</b> : A sample adaptive control system block diagram .....	23
<b>Figure 2.6</b> : Sample block diagram of a model-reference adaptive system (MRAS) .....	24
<b>Figure 2.7</b> : Detailed Bode plot of open loop $\theta/\delta_e$ transfer function .	25
<b>Figure 2.8</b> : Lead compensated nominal plant and bode diagram plots	27
<b>Figure 2.9</b> : Suggested MRAS simulink block diagram for MIT rule .	28
<b>Figure 2.10</b> : Closed-loop time domain responses of model-reference adaptive control system design: PI adjustment based on normalized MIT rule .....	32
<b>Figure 2.11</b> : Lyapunov stability theory representation in phase domain	34
<b>Figure 2.12</b> : Simulink block diagram of PI adjustment based on Lyapunov Stability .....	38
<b>Figure 2.13</b> : Closed-loop time domain responses of model-reference adaptive control system design: PI adjustment based on Lyapunov stability .....	39
<b>Figure 2.14</b> : Nominal plant and observer mechanism .....	40
<b>Figure 2.15</b> : Integral control block diagram for robust tracking and disturbance rejection .....	44
<b>Figure 2.16</b> : Simulink block diagram of augmented optimal control system design .....	46
<b>Figure 2.17</b> : Simulink block diagram of estimation (observer) mechanism .....	47
<b>Figure 2.18</b> : Time domain response of augmented optimal LQR control system design .....	47
<b>Figure 2.19</b> : Closed-loop time domain responses of designed automatic control systems: Comparison analysis .....	48
<b>Figure 3.1</b> : Open-loop time domain step responses for a given deflection .....	57
<b>Figure 3.2</b> : Simulink block diagram of MRAS based on Lyapunov stability .....	60

<b>Figure 3.3</b>	: Closed-loop time domain response of model-reference adaptive control system design: Based on Lyapunov stability .....	61
<b>Figure 3.4</b>	: Simulink block diagram of optimal LQR control system design .....	64
<b>Figure 3.5</b>	: Time domain response of optimal LQR control system design .....	64
<b>Figure 3.6</b>	: Closed-loop time domain responses of designed automatic control systems: Comparison analysis .....	65
<b>Figure A1</b>	: Simulink block diagram of PI adjustment algorithm based on normalized MIT rule .....	72
<b>Figure A2</b>	: Simulink block diagram of adjustment parameter- $\theta_1$ based on normalized MIT rule .....	72
<b>Figure A3</b>	: Simulink block diagram of adjustment parameter- $\theta_2$ based on normalized MIT rule .....	73

## NOTATION LIST

$u$	:	Steady state velocity
$\alpha$	:	Angle of attack
$\delta_e$	:	Elevator-control surface displacement
$\delta_a$	:	Aileron-control surface displacement
$\delta_r$	:	Rudder-control surface displacement
$\theta$	:	Pitch angle
$V_T$	:	Translational velocity
$H$	:	Angular momentum
$\omega$	:	Angular velocity
$\mathcal{L}$	:	Roll moment
$\mathcal{M}$	:	Pitch moment
$\mathcal{N}$	:	Yaw moment
$\xi$	:	Damping ratio
$\omega_n$	:	Natural frequency
$\tilde{\theta}_n$	:	n-th parameter adjustment algorithm
$e$	:	Error signal
$G(s)$	:	Transfer function of nominal plant
$G_m(s)$	:	Transfer function pf reference model
$\hat{G}_o(s)$	:	Estimated (observed) nominal plant
$\tau_n$	:	Time constant of n-th mode
$L$	:	Parameter adjustment-feedback gain
$L^*$	:	Feedback gain satisfying perfect matching conditions
$\Delta L$	:	Parameter adjustment uncertainties

## **SUMMARY**

In this study, stability analysis of an Unmanned Aerial Vehicle (UAV) has been conducted and several control system designs have been suggested for autonomous flight. In the study, firstly, stability analyses have been carried out for the longitudinal and lateral flight dynamics. Additionally, for automatic control system designs, Model Reference Adaptive and Augmented Optimal LQR have been used, control algorithms have been developed and simulations have been conducted. UAV flight dynamics have been linearized and linearized equations of motion have been used in analyses. Adaptive control system design implemented on longitudinal flight dynamics has been investigated in two parts, where firstly PI adjustment algorithm based on MIT rule has been executed. Afterwards, PI adjustment algorithm based on Lyapunov stability theory has been applied and results have been analyzed. Moreover, Augmented Optimal LQR control system design approach has been introduced in longitudinal dynamics and in this way the first part of the study has been concluded. In the second part of the study, equations of motion in lateral flight have been obtained and stability analyses have been conducted. In this section, Model Reference Adaptive control system design based on Lyapunov stability theory has been applied to lateral system dynamics. And finally, with the implementation of Optimal LQR control system design on the lateral flight dynamics, the study has been concluded. When obtained results have been compared with the existing results in the literature, it is witnessed that designed control systems are able to present remarkable time domain and closed-loop performance characteristics.

## **ÖZET**

### **BİR UÇAĞIN KARARLILIK ANALİZİ VE OTOMATİK KONTROL SİSTEMİ TASARIMLARI: UYARLAMALI (ADAPTİF) KONTROL YAKLAŞIMI**

Bu çalışmada, temel olarak bir İnsansız Hava Aracı (İHA)'nın kararlılığı incelenmiş ve otonom uçuş için çeşitli kontrol yöntemleri önerilmiştir. Çalışmada ilk olarak, İHA'nın uzunlamasına ve yanlamasına hareketi için kararlılık analizleri gerçekleştirilmiştir. Buna ek olarak, yanlamasına uçuş ve uzunlamasına uçuşun otomatik idaresi için, Uyarlamalı (Adaptif) Model Referans ve Yeniden Şekillendirilmiş Optimal Lineer Kuadratik Regülâtör yöntemleri kullanılmış, çeşitli otomatik uçuş kontrol algoritmaları geliştirilmiş ve bilgisayar ortamında uygulamaları yapılmıştır. Tezde incelenen insansız hava aracı doğrusal (lineer) bir model olarak ele alınmıştır ve denklemleri buna göre elde edilmişlerdir. Uzunlamasına hareket için gerçekleştirilen Uyarlamalı Model Referans kontrol yöntemi uygulamaları iki başlık altında incelenmiş olup ilk aşamada MIT kuralına dayalı orantı-integral uyarlama algoritması uygulanmış ve sonuçları analiz edilmiştir. Daha sonrasında ise Lyapunov kararlılık teorisine dayalı orantı-integral algoritması uzunlamasına hareket dinamiklerine uygulanmış ve sonuçları analiz edilmiştir. Ayrıca, Yeniden Şekillendirilmiş Optimal Lineer Kuadratik Regülâtör yöntemi ile uzunlamasına kontrol sistemi tasarlanarak tezin birinci kısmı sonlandırılmıştır. Tezin ikinci bölümünde, yanlamasına hareket dinamikleri elde edilmiş ve kararlılık analizleri gerçekleştirilmiştir. Bu bölümde Uyarlamalı kontrol yöntemleri içerisinde sadece Lyapunov kararlılık teorisine dayalı model referans adaptif kontrol tasarımı gerçekleştirilmiştir. Ve son olarak yanlamasına hareket için tasarlanan optimal lineer kuadratik regülâtör tasarımı ile tez sonlandırılmıştır. Elde edilen sonuçlar literatürdeki çalışmalarla karşılaştırıldığında, önerilen yöntemlerle geliştirilen otomatik kontrol sistem tasarımlarının, kayda değer sonuçlar sergilediği ve performans kriterlerini fazlasıyla sağladığı gözlenmiştir.

## INTRODUCTION

In recent years, Unmanned Aerial Vehicles (UAVs) are increasingly useful in different kind of operations starting from observations up to remote sensing operations. They are cheaper than the manned vehicles and are very suitable for unsafe missions that would be inevitable for a human pilot, where some specific applications of UAVs could be summarized as border patrol, search and rescue, surveillance, communications relaying, and mapping of hostile territory.

The capabilities of UAVs continue to grow with advances in wireless communications and computing power. Accordingly, research topics in control of UAVs include efficient vision for real-time computer based computing and communication strategies for different kind of control techniques, as well as traditional aircraft-related topics such as collision avoidance and formation flight. Emerging results in control of UAVs are presented via discussion of different topics, including particular requirements, challenges, and some promising strategies relating to each topic. Case studies presented in the thesis, highlight specific solutions and recent results, ranging from pure simulation to control strategies for UAVs. This study serves as an overview of current problems of interest [1].

Control system design of small and inexpensive Unmanned Aerial Vehicles (UAVs) is of great interest in military and civilian applications, including mapping, patrolling, search and rescue. These tasks sometimes could be dangerous and recurring, which makes them ideal for autonomous vehicles. In these types of applications, control system design, as well as dynamic modeling, has a crucial role in the behavior of the UAV and in mission accomplishment. Therefore it is vital to gain knowledge about dynamic properties of the UAV in order to be used in control system design procedure. In literature, there are several conducted researches on automatic control system designs of UAVs such as receding horizon control [18], variable horizon model predictive control [19], control system design using evolutionary algorithms [20], feedback linearization and linear observer design [21], cooperative receding horizon control [22], adaptive control system design [23],

control system design using MIMO QFT [24], decentralized non-linear control [25], robust control system design using coupled stabilities [26], H infinity control and inverse dynamic system approach [27] and non-linear autopilot design using dynamic inversion [28], are some of the studies [29]. After an intensive search in several publications, there were found very limited amount of adaptive control applications on UAVs and therefore the main goal of the thesis was to demonstrate the implementation of model reference adaptive control algorithms on UAV dynamics.

In the first part of the thesis, as an introduction to dynamic modeling, some important components existing on an aircraft/UAV have been introduced. Following to that, in the second section of the thesis, a general overview over longitudinal dynamic modeling of an aircraft (specifically an UAV) will be presented. In modeling part, firstly, equations of motion of UAV will be obtained, afterwards stability derivatives will be derived and subsequently longitudinal flight dynamics of UAV will be originated. During this examination, transfer functions (TFs) of velocity ( $u$ ), angle of attack ( $\alpha$ ) and pitching angle ( $\theta$ ) for a given elevator displacement ( $\delta_e$ ) have been investigated and obtained results have been analyzed in both time and frequency domains. In order to construct a fundamental for the automatic control design part, short period and long (phugoid) period characteristics have been inspected and the approximated phases have been examined. For each phase, natural frequencies and corresponding periods have been calculated, TFs of velocity ( $u$ ), angle of attack ( $\alpha$ ) and pitching angle ( $\theta$ ) versus elevator displacement ( $\delta_e$ ) have been obtained, later bode diagrams have been plotted and necessary comments have been presented in the conclusion part of the chapter.

As a natural consequence of conducted analyses, the necessity of feedback control system has aroused. Following to that, in order to improve the stability characteristics and time domain results of the open loop-nominal plant, two different control system design procedures have been suggested on the open loop dynamics of UAV: Model Reference Adaptive Control System Design (MRAS) and Augmented Optimal LQR control system design. In MRAS control system design, two different approaches have been presented: PI adjustment based on MIT rule and PI adjustment based on Lyapunov stability theory. In augmented optimal LQR control system

design, inner loop and outer loop concepts have been used, where the inner loop (together with an observer mechanism) has been constructed for stability and the outer loop has been introduced with augmentation in order to improve the performance characteristics. In each section, performances of MRAS and augmented optimal LQR controllers have been discussed and the results have been pointed out in the consequent parts of the thesis. At last, with the presentation of necessary comments and possible further study steps, the first chapter of the thesis has been concluded.

In the second chapter, with the similar approach, lateral dynamic model of the UAV (using state space approach) has been given. Afterwards, lateral automatic control system of the UAV has been taken into account and MRAS control system design with the augmented optimal LQR control system design have been put into practice. Obtained results are given with several analyses and suggestions are presented for further analyses in the last part of the thesis.



## CHAPTER 1

### 1.1 Components of an Aircraft

#### 1.1.1 Control surfaces

It is a commonly known fact that if the body of an aircraft is required to be changed from its equilibrium state, external forces and moments should be applied to the aircraft. Every aircraft needs surfaces placed on the different locations on the aircraft body, so that when a force is applied to the system through the specified surfaces, a force or a moment is generated on the aircraft and the body is accelerating in the desired direction. Such surfaces are called control surfaces and could be mainly divided into three groups: pitch control surfaces (elevators), yaw control surface (rudder) and roll control surfaces (ailerons). It is possible to see the defined control surfaces (elevators, ailerons and rudder) on a conventional aircraft in Figure 1.1.

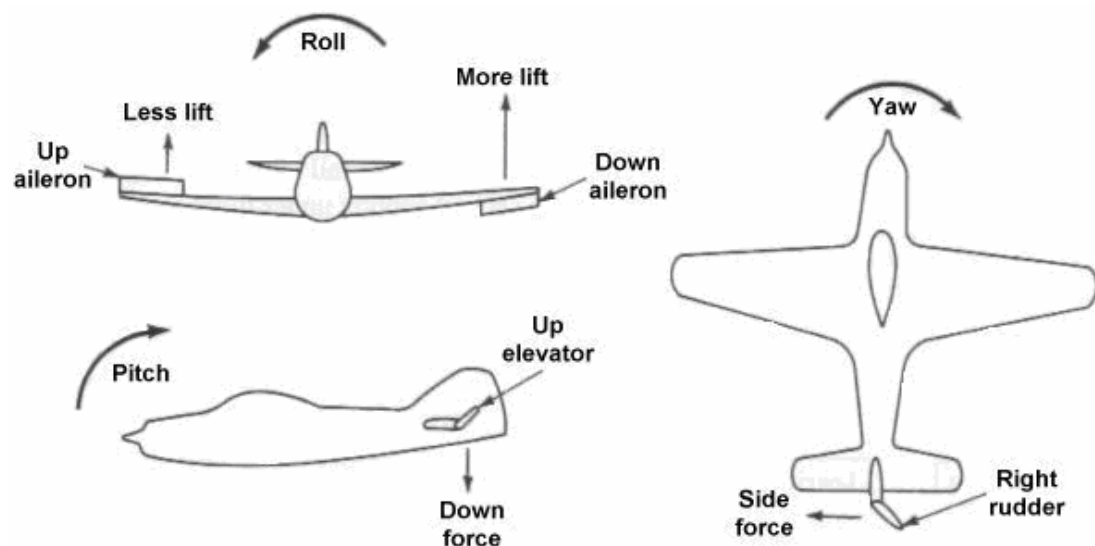


**Figure 1.1** Control surfaces on the aircraft.

Many modern aircrafts, especially combat aircrafts, are including more control surfaces than the conventional aircrafts in order to produce additional control forces or moments. Some of these additional surfaces include horizontal and vertical

canards, spoilers, variable cambered wings, reaction jets, differentially operating horizontal tails and moveable fins [2]. One of the critical and most important properties of flight control is that it needs simultaneous usage of different control surfaces at the same time. When two or more control surfaces are used simultaneously, the coupling effects are occurring and the system becomes complicated for control action. The control surfaces are controlled by actuators which are being fed by electrical signals (fly-by-wire) or by optical devices (fly-by-light) [2]. But in a conventional aircraft, pilot has links to the control surfaces and is able to control the surfaces manually in case of emergency.

### **1.1.2 Servo mechanisms**

A servomechanism, usually shortened just as servo, is a device used to provide mechanical control on the aircraft surface. For example, a servo can be used at a remote location to proportionally follow the angular position of a control knob. The connection between the two is not mechanical, but electrical or wireless [3]. The most common type of servo is that which gives positional control. Servos are commonly electrical or partially electronic and they are using an electric motor as the primary means of creating mechanical force, though other types that operate on hydraulic or magnetic principles are available. Usually, servos operate on the principle of negative feedback, where the control input is compared to the actual position of the mechanical system as measured by some sort of transducer at the output. Any difference between the actual and wanted values (an "error signal") is amplified and used to drive the system in the direction necessary to reduce or eliminate the error. A whole science of this type of system has been developed, known as control theory [2].

### **1.1.3 Rate gyroscopes**

Rate gyroscopes are simple mechanical and rotating systems used in aircrafts. They use Coriolis Effect of sensor element (vibrating resonator chip) to sense the speed of rotation (rate of turn) and as a result of the measurement, the signal is being fed into the control system, where rate gyros are generally used in negative feedback loops. Rate gyros are single degree of freedom gyros different than the free rotating (two degree of freedom) gyros and a sample diagram of a rate gyro is shown in Figure 1.2 [4]. The elastic restraint in rate gyros is provided by a torsion bar, fixed to the inner

gimbal and the case. The viscous damper is also added to provide damping of the transient state [5].

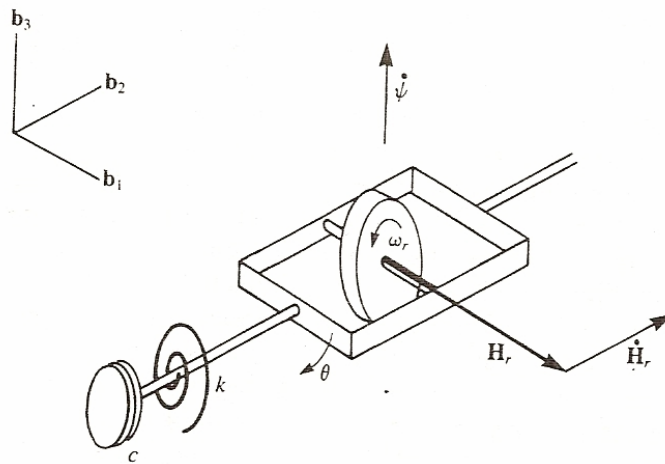


**Figure 1.2** Rate gyroscopes have single degree of freedom.

#### 1.1.4 Integrating gyroscopes

If the elastic restraint ( $k$ ) is removed from the rate gyro, leaving only the viscous damper, the result is referred to as a “rate integrating gyro” or just an “integrating gyro”. The name integrating gyro arises from the fact that the gimbal angle is proportional to the time integral of the input angular velocity. Because the integral of the input angular velocity is the total angle through which the gyro has rotated about its input axis with respect to inertial space, steady state value of the gyro is proportional to this angle [5].

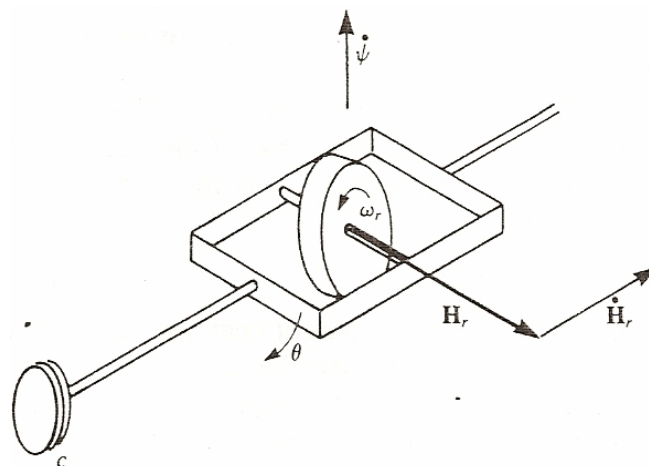


**Figure 1.3** Integrating gyroscope.

## CHAPTER 2

### 2. Longitudinal Dynamic Modeling

In this section of the thesis, longitudinal equations of motion will be summarized.

#### 2.1 Equations of Motion (EOMs)

In longitudinal dynamic modeling segment, first of all EOM will be derived. If the Newton's 2<sup>nd</sup> Law is taken into account:

$$\vec{F} = m \vec{a} \quad (2.1)$$

and by taking all the forces and moments acting on the aircraft into consideration, general form of EOMs could be expressed as in (2.2) and (2.3).

$$\sum \vec{F} = \frac{d}{dt} (m \vec{V}_T) \Big]_I \quad (2.2)$$

$$\sum \vec{M} = \frac{d \vec{H}}{dt} \Big]_I \quad (2.3)$$

If the forces and moments including the steady state values and disturbance values are redefined, it is found as shown in (2.4a) and (2.4b),

$$\sum \vec{F} = \sum \vec{F}_0 + \sum \Delta \vec{F} \quad (2.4a)$$

$$\sum \vec{M} = \sum \vec{M}_0 + \sum \Delta \vec{M} \quad (2.4b)$$

where  $\sum \vec{F}_0$  and  $\sum \vec{M}_0$  are summations of the equilibrium forces/moments and

$\sum \Delta \vec{F}_0$  and  $\sum \Delta \vec{M}_0$  are disturbances (from steady state condition) values [5, 6].

Here, it is assumed that the aircraft is flying in an unaccelerated (stick-fixed) flight

regime and all the disturbances are occurring as a result of control surface deflections or atmospheric effects (wind, gust, turbulence ... etc.). With respect to the mentioned postulations, equations in (2.2) and (2.3) could be defined as in (2.5) and (2.6).

$$\sum \Delta \vec{F} = \left. \frac{d}{dt} (m \vec{V}_T) \right]_I \quad (2.5)$$

$$\sum \Delta \vec{M} = \left. \frac{d \vec{H}}{dt} \right]_I \quad (2.6)$$

Before continuing in derivation of EOMs for the longitudinal flight, assumptions such as the mass of the aircraft is not changing with time, the aircraft is a rigid body and the earth is an inertial reference system has been taken into account. If the given formulations are considered with respect to the earth, it should be obtained

$$\sum \Delta \vec{F} = m \left. \frac{d \vec{V}_T}{dt} \right]_E \quad (2.7)$$

From here, if the time rate of change of the velocity vector ( $\vec{V}_T$ ) with respect to the earth is calculated, the result is being as given in (2.8),

$$\left. \frac{d \vec{V}_T}{dt} \right]_E = \vec{1}_{V_T} \frac{d \vec{V}_T}{dt} + \omega \otimes \vec{V}_T \quad (2.8)$$

where  $\vec{1}_{V_T} (d\vec{V}_T/dt)$  is the change in linear velocity,  $\omega$  is the total angular velocity of the aircraft with respect to the earth, and  $\otimes$  defines the cross product [5, 6]. If  $\vec{V}_T$  and  $\omega$  is written in expanded form (with respect to the aircraft body axes system given in Figure 2.1),  $\vec{V}_T$  could be defined as (2.9)

$$\vec{V}_T = iU + jV + kW \quad (2.9)$$

and in the same way  $\vec{\omega}$  could be found as (2.10),

$$\vec{\omega} = \vec{i}P + \vec{j}Q + \vec{k}R \quad (2.10)$$

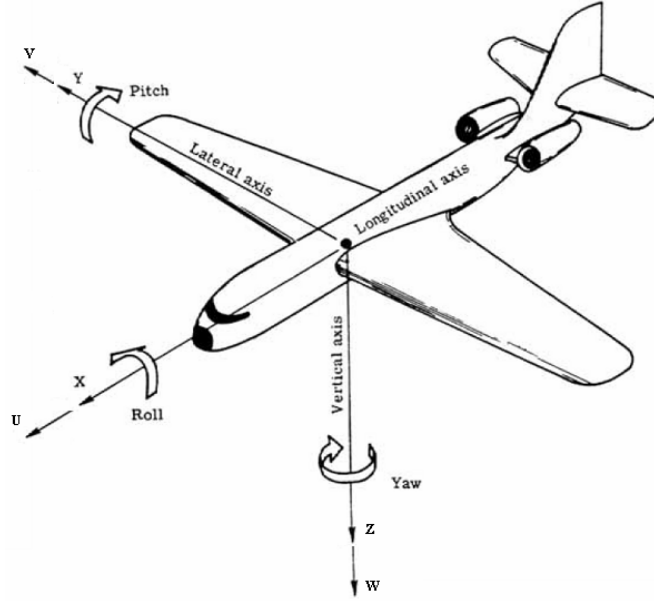


**Figure 2.1** Body fixed axes system.

where  $i, j$  and  $k$  are unit vectors;  $U, V$  and  $W$  are directional velocities and  $P, Q$  and  $R$  are rates of change along the aircraft's  $X, Y$  and  $Z$  axes, respectively. Then from (2.8), the acceleration term could be written as (2.11)

$$\vec{1}_{V_T} \frac{d}{dt} \vec{V}_T = \vec{i} \dot{U} + \vec{j} \dot{V} + \vec{k} \dot{W} \quad (2.11)$$

and the cross product term is found as (2.12).

$$\vec{\omega} \otimes \vec{V}_T = \begin{vmatrix} \vec{i} & \vec{j} & \vec{k} \\ P & Q & R \\ U & V & W \end{vmatrix} \quad (2.12)$$

If the determinant in (2.12) is calculated, the result leads to (2.13)

$$\vec{\omega} \otimes \vec{V}_T = \vec{i}(QW - RV) - \vec{j}(PW - RU) + \vec{k}(PV - QU) \quad (2.13)$$

Disturbance forces ( $\sum \Delta \vec{F}$ ) acting on the airplane could be written as

$$\sum \Delta \vec{F} = \vec{i} \sum \Delta F_x + \vec{j} \sum \Delta F_y + \vec{k} \sum \Delta F_z \quad (2.14)$$

If equations (2.11) and (2.13) are placed in (2.14), then force equations governing the directional motion turn into their final states as given in (2.15).

$$\begin{aligned}
\sum \Delta F_x &= m(\dot{U} + QW - RV) \\
\sum \Delta F_y &= m(\dot{V} + RU - PW) \\
\sum \Delta F_z &= m(\dot{W} + PV - QU)
\end{aligned} \tag{2.15}$$

Similarly, in order to obtain the equations governing the angular motion, it is needed to define the tangential velocity at first as in (2.16).

$$\vec{V}_{\text{tan}} = \vec{\omega} \otimes \vec{R} \tag{2.16}$$

Following to this, the incremental momentum resulting from this tangential velocity of the element mass can be expressed as shown in (2.17) [5, 6].

$$d\vec{M} = (\vec{\omega} \otimes \vec{R}) dm \tag{2.17}$$

Then the differential angular momentum becomes

$$d\vec{H} = \vec{r} \otimes (\vec{\omega} \otimes \vec{R}) dm \Rightarrow \vec{H} = \int \vec{r} \otimes (\vec{\omega} \otimes \vec{R}) dm \tag{2.18}$$

If the extended form of moment arm is introduced

$$\vec{r} = \vec{i} x + \vec{j} y + \vec{k} z \tag{2.19}$$

then the product term becomes

$$\vec{\omega} \otimes \vec{r} = \begin{vmatrix} \vec{i} & \vec{j} & \vec{k} \\ P & Q & R \\ x & y & z \end{vmatrix} \tag{2.20}$$

If the determinant in (2.20) is calculated

$$\vec{\omega} \otimes \vec{r} = \vec{i}(Qz - Ry) - \vec{j}(Pz - Rx) + \vec{k}(Py - Qx) \tag{2.21}$$

And if the outer cross product term is introduced into (2.21), the results are being as shown in (2.22).

$$\vec{r} \otimes (\vec{\omega} \otimes \vec{r}) = \begin{vmatrix} \vec{i} & \vec{j} & \vec{k} \\ x & y & z \\ (Qz - Ry) & (Pz - Rx) & (Py - Qx) \end{vmatrix} \quad (2.22)$$

If the determinant in (2.22) is calculated, the outer cross product is found as in (2.23).

$$\begin{aligned} \vec{r} \otimes (\vec{\omega} \otimes \vec{r}) = & \vec{i} [P(y^2 + z^2) - xyQ - xzR] + \vec{j} [Q(z^2 + x^2) - yzR - xyP] \\ & + \vec{k} [R(x^2 + z^2) - xzP - yzQ] \end{aligned} \quad (2.23)$$

By replacing (2.23) in angular momentum term in (2.18), angular momentum (H) is found as in (2.24),

$$\begin{aligned} H = & \int i [P(y^2 + z^2) - xyQ - xzR] \\ & + \int j [Q(z^2 + x^2) - yzR - xyP] \\ & + \int k [R(x^2 + z^2) - xzP - yzQ] \end{aligned} \quad (2.24)$$

where  $\int (y^2 + z^2) dm$  is defined as the moment of inertia  $I_x$ , and  $\int xy dm$  is defined as the product of inertia  $J_{xy}$ . By remembering the assumptions taken into account at the beginning, the product inertias in xy and yz coordinates are leading to  $J_{xy} = J_{yz} = 0$ , so that the resulting angular momentum equations are found as in (2.25).

$$\begin{aligned} H_x &= PI_x - RJ_{xz} \\ H_y &= QI_y \\ H_z &= RI_z - PJ_{xz} \end{aligned} \quad (2.25)$$

It is possible to rewrite (2.3) as

$$\sum \Delta \vec{M} = \vec{1}_H \frac{dH}{dt} + \vec{\omega} \otimes \vec{H} \quad (2.26)$$

where the components of  $\vec{1}_H dH / dt$  are



$$\begin{aligned}
\frac{dH_x}{dt} &= \dot{P}I_x - \dot{R}J_{xz} \\
\frac{dH_y}{dt} &= \dot{Q}I_y \\
\frac{dH_z}{dt} &= \dot{R}I_z - \dot{P}J_{xz}
\end{aligned} \tag{2.27}$$

If the rigid body assumption for our aircraft is remembered, the time rates of change of the moments and products of inertias are going to be zero [5, 6]. So that

$$\vec{\omega} \otimes \vec{H} = \begin{vmatrix} \vec{i} & \vec{j} & \vec{k} \\ P & Q & R \\ H_x & H_y & H_z \end{vmatrix} \tag{2.28}$$

If the determinant in (2.28) is calculated

$$\vec{\omega} \otimes \vec{H} = \vec{i}(QH_z - RH_y) - \vec{j}(PH_z - RH_x) + \vec{k}(PH_y - QH_x) \tag{2.29}$$

Also  $\sum \Delta \vec{M}$  can be written as

$$\sum \Delta \vec{M} = \vec{i} \sum \Delta \mathcal{L} + \vec{j} \sum \Delta \mathcal{M} + \vec{k} \sum \Delta \mathcal{N} \tag{2.30}$$

By replacing the necessary values in the right hand side, the final equations of angular motion are found as in (2.31).

$$\begin{aligned}
\sum \Delta \mathcal{L} &= \dot{P}I_x - \dot{R}J_{xz} + QR(I_z - I_y) - PQJ_{xz} \\
\sum \Delta \mathcal{M} &= \dot{Q}I_y + PR(I_x - I_z) - (P^2 + R^2)J_{xz} \\
\sum \Delta \mathcal{N} &= \dot{R}I_z - \dot{P}J_{xz} + PQ(I_y - I_x) + QRJ_{xz}
\end{aligned} \tag{2.31}$$

and equations of linear motion has been previously obtained in (2.15) as

$$\begin{aligned}
\sum \Delta F_x &= m(\dot{U} + QW - RV) \\
\sum \Delta F_y &= m(\dot{V} + RU - PW) \\
\sum \Delta F_z &= m(\dot{W} + PV - QU)
\end{aligned}$$

Equations in (2.15) and (2.31) are the complete equations of motion for the longitudinal motion of the aircraft. Next, it will be necessary to linearize and to expand the left hand-sides of equations in order to obtain the final states of EOMs. Even if, it is possible to derive the linearized equations of motion and stability derivatives from beginning, this will not be performed here. At this point, only the final states of Longitudinal EOMs will be given in the following sections. The reader could find further and detailed information related with the development of EOMs and longitudinal stability derivatives in [5, 7-9].

## 2.2 Derivation the Longitudinal Dynamic Model of the Aircraft

Although it is possible to derive longitudinal equations of motion (EOM) of an aircraft from (2.15) and (2.31); here, only the final state of the longitudinal EOM will be presented. The entire derivation could be investigated step by step from [5, 7-9].

While presenting the final values of the longitudinal EOM, firstly the transient response will be considered and homogenous solution will be evaluated. By neglecting  $C_{x\dot{\alpha}}$ ,  $C_{xq}$  and  $C_{m\dot{u}}$  in homogeneous solution, one should obtain Linearized and Laplace Transformed longitudinal EOMs as shown in (2.32)

$$\begin{aligned}
x: & \left(\frac{mu}{Sq}s - C_{XU}\right)'u(s) - C_{X\alpha}'\alpha(s) - C_W(\cos\Theta)\theta(s) = C_{F_{X_a}} = 0 \\
z: & -C_{ZU}'u(s) + \left[\left(\frac{mu}{Sq} - \frac{c \cdot C_{Z\dot{\alpha}}}{2u}\right)s - C_{Z\alpha}\right]'\alpha(s) \\
& + \left[\left(-\frac{mu}{Sq} - \frac{c \cdot C_{Zq}}{2u}\right)s - C_W \sin\Theta\right]\theta(s) = C_{F_{Z_a}} = 0 \\
M: & \left(-\frac{c \cdot C_{m\dot{\alpha}}}{2u}s - C_{M\alpha}\right)'\alpha(s) + \left(\frac{I_y}{Sqc}s^2 - \frac{c \cdot C_{Mq}}{2u}s\right)\theta(s) = C_{m_a} = 0
\end{aligned} \tag{2.32}$$

where ( $u$ ,  $w$ ) are perturbation velocities in (X, Z) axis's respectively and

' $u = u/U_0$  = Change of velocity in longitudinal flight

' $\alpha = w/U_0$  = Change of angle of attack in longitudinal flight

$\theta$  = Change of pitch angle from equilibrium condition

Characteristic properties of UAV in Sea Level (~100m) conditions are presented in Table 1.1.

**Table 1.1** Constants of longitudinal EOMs.

<b>Mass:</b> $m = 5$ [kg]	$\partial C_L / \partial \alpha = 0.1249$
<b>Velocity:</b> $u = 12$ [m/sec]	$\partial C_D / \partial \alpha = 0.0389$
<b>Gravity:</b> $g = 9.807$ [m/sec <sup>2</sup> ]	$\partial C_m / \partial i_t = -1.5$
<b>Wing area:</b> $S = 0.4805$ [m <sup>2</sup> ]	<b>Wing span:</b> $b = 1.7$ [m]
<b>Air density:</b> $\rho = 1.225$ [kg/m <sup>3</sup> ]	<b>Aspect Ratio:</b> $AR = 6.0146$
<b>Dynamic pressure:</b> $q = 88.2$ [kg/m.sec <sup>2</sup> ]	<b>Washout respect to <math>\alpha</math>:</b> $d\varepsilon / d\alpha = 0.0116$
<b>Moment of Inertia<sub>y</sub>:</b> $I_y = 0.1204$ [m <sup>4</sup> ]	<b>Allowance factor:</b> $K = 1.1$
<b>Chord length:</b> $c = 0.235$ [m]	<b>Dist. CG to N. Point:</b> $x = 0.0587$
<b>Length to c/4 of tail:</b> $L_t = 0.235$ [m]	<b>Static Margin:</b> $SM = -0.25$
<b>Equilibrium state:</b> $\Theta = 0$ [deg]	<b>Dist. from tail to c:</b> $L_{tc} = 1$

Corresponding stability derivatives in longitudinal flight are considered as shown in the followings, where

$$C_{x_u} = -2C_D - U_0 \frac{\partial C_D}{\partial u} \quad (2.33)$$

is the change in force in X direction due to the change in forward velocity, so that  $U_0$  is the steady state velocity,  $C_D$  is drag coefficient and  $\partial C_D / \partial u$  is the change in drag coefficient with respect to perturbation velocity.

$$C_{x_\alpha} = C_L - \frac{\partial C_D}{\partial \alpha} \quad (2.34)$$

is the change in force in X direction due to the change in angle of attack, where  $C_L$  is lift coefficient and  $\partial C_D / \partial \alpha$  is the change in drag coefficient with respect to angle of attack.

$$C_{z_u} = -2C_L - U_0 \frac{\partial C_L}{\partial u} \quad (2.35)$$

is the change in force in Z direction due to the change in forward velocity, where  $\partial C_L / \partial u$  is the change in lift coefficient with respect to perturbation velocity.

$$C_{z_\alpha} = -C_D - \frac{\partial C_L}{\partial \alpha} \cong -\frac{\partial C_L}{\partial \alpha} \quad (2.36)$$

is the change in force in Z direction due to the change in angle of attack, where  $\partial C_L / \partial \alpha$  is the change in lift coefficient with respect to angle of attack.

$$C_{Z_{\dot{\alpha}}} = 2 \left( \frac{\partial C_m}{\partial i_t} \right) \left( \frac{d\varepsilon}{d\alpha} \right) \quad (2.37)$$

is the effect of rate of change in angle of attack on Z force, where  $(\partial C_m / \partial i_t)$  is the rate of change of the pitching moment coefficient of the tail with respect to the angle of incidence and  $d\varepsilon / d\alpha$  is the change in downwash with respect to angle of attack. Theoretical value of  $d\varepsilon / d\alpha$  is

$$\frac{d\varepsilon}{d\alpha} = \frac{2}{\pi AR} \left( \frac{dC_L}{d\alpha} \right) \quad (2.38)$$

where  $AR$  is the aspect ratio of the aircraft.

$$C_{Z_q} = 2K \left( \frac{\partial C_m}{\partial i_t} \right) \quad (2.39)$$

is the change in the Z force due to change in pitching velocity, where  $K$  is the approximate allowance factor for the contribution of the rest of the aircraft to  $C_{Z_q}$  and is usually about 1.1 [5].

$$C_{m_{\dot{\alpha}}} = (SM) \left( \frac{\partial C_L}{\partial \alpha} \right)_{\delta}^a \quad (2.40)$$

is the change in pitching moment due to the change in angle of attack, where  $SM$  is static margin which is equal to  $x/c$ , so that  $x$  is the distance between the fixed control neutral point and the center of gravity of the aircraft and  $c$  is the mean aerodynamic chord length of the wing.

$$C_{m_{\dot{\alpha}}} = 2 \left( \frac{\partial C_m}{\partial i_t} \right) \frac{d\varepsilon}{d\alpha} \frac{l_t}{c} \quad (2.41)$$

is the effect of rate of change in angle of attack on pitching moment coefficient, where  $l_t$  is the distance between the center of gravity of the aircraft and the aerodynamic center of tail.

$$C_{m_q} = 2K \left( \frac{\partial C_m}{\partial i_t} \right) \frac{l_t}{c} \quad (2.42)$$

is the effect on the pitching moment due to a pitching rate.

$$C_w = -\frac{mg}{Sq} \cong -C_L \quad (2.43)$$

is the weight coefficient, where it is generally assumed as equal to  $-C_L$ .

After obtaining necessary formulations of stability derivatives, by using characteristic properties of UAV given in Table 1.1, it is possible to calculate the numerical values of stability derivatives as given in Table 1.2.

**Table 1.2** Stability derivatives of longitudinal EOM.

$C_{X_u} = -0.0264$	$C_{Z_{\alpha'}} = -0.0397$
$C_{X_{\alpha}} = 1.1181$	$C_{Z_{\alpha}} = -0.1381$
$C_D = 0.0132$	$C_{Z_q} = -3.3000$
$C_L = 1.1570$	$C_{M_{\alpha'}} = -0.0397$
$C_W = -1.1570$	$C_{M_{\alpha}} = -0.0312$
$C_{Z_u} = -2.3141$	$C_{M_q} = -3.3000$

And finally, elevator displacements (inputs) of the system are given as

**Table 1.3** Elevator displacements (inputs) of the UAV system.

$C_{X_{\delta e}} = 0$
$C_{Z_{\delta e}} = -0.71$
$C_{m_{\delta e}} = -0.71$

At this point, if the calculated values given in Table-1 and Table-2 are placed in (2.32), it is expected to obtain the homogeneous solution of Laplace transformed EOMs as in (2.44).

$$\begin{aligned}
x: & (1.4158s + 0.0264)'u(s) - 1.1181'\alpha(s) + 1.1570\theta(s) = 0 \\
z: & 2.3141'u(s) + (1.4161s + 0.1381)'\alpha(s) - 1.3834s\theta(s) = 0 \\
M: & 0 + (0.0003s + 0.0312)'\alpha(s) + (0.0121s^2 + 0.0323s)\theta(s) = 0
\end{aligned} \tag{2.44}$$

If (2.44) is rewritten in matrix form,

$$\begin{bmatrix} (1.4158s + 0.0264) & -1.1181 & 1.1570 \\ 2.3141 & (1.4161s + 0.1381) & -1.3834 \\ 0 & (0.0003s + 0.0312) & (0.0121s^2 + 0.0323s) \end{bmatrix} \begin{bmatrix} 'u(s) \\ '\alpha(s) \\ \theta(s) \end{bmatrix} = 0 \tag{2.45}$$

and using (2.45), it is possible to obtain the characteristic equation (CE) of the UAV system simply by taking the determinant as shown in (2.46).

$$\begin{vmatrix} (1.4158s + 0.0264) & -1.1181 & 1.1570 \\ 2.3141 & (1.4161s + 0.1381) & -1.3834 \\ 0 & (0.0003s + 0.0312) & (0.0121s^2 + 0.0323s) \end{vmatrix} = 0 \tag{2.46}$$

By expanding the determinant in (47), the CE is found as

$$\begin{aligned}
0.0242s^4 + 0.0684s^3 + 0.1s^2 + 0.0859s + 0.0836 &= 0 \\
s^4 + 2.8264s^3 + 4.1322s^2 + 3.5496s + 3.4545 &= 0
\end{aligned} \tag{2.47}$$

In order to have better idea related with the open loop characteristic of the aircraft, using (2.47), it is possible to obtain the roots (poles) of the system such as

$$\begin{aligned}
s_{1,2} &= -1.3921 \pm 0.9226i \\
s_{3,4} &= -0.0181 \pm 1.1119i
\end{aligned} \tag{2.48}$$

From the corresponding poles of CE, it is likely to see that the system is stable but has very close complex conjugate poles to the origin, which will lead to highly oscillatory manner and relatively low damping with frequent oscillations. If complex conjugate poles ( $s_{1,2}$ ,  $s_{3,4}$ ) are grouped, a compact form is obtained as in (2.49).

$$\begin{aligned}
[(s + 1.3921 - 0.9226i)(s + 1.3921 + 0.9226i)][(s + 0.0181 - 1.1119i)(s + 0.0181 + 1.1119i)] &= 0 \\
(s^2 + 2.7842s + 2.7892)(s^2 + 0.0362s + 1.2367) &= 0
\end{aligned} \tag{2.49}$$

Next, it is possible to introduce the natural frequency and damping ratio concepts using the general representation as

$$s^2 + 2\xi\omega_n s + \omega_n^2 = 0$$

$$(s^2 + 2\xi_s\omega_{ns}s + \omega_{ns}^2)(s^2 + 2\xi_p\omega_{np}s + \omega_{np}^2) = 0 \quad (2.50)$$

and adapting (2.50) to the obtained system, it is found

$$(s^2 + 2\xi_s\omega_{ns}s + \omega_{ns}^2) = (s^2 + 2.7842s + 2.7892) \quad (2.51)$$

$$(s^2 + 2\xi_p\omega_{np}s + \omega_{np}^2) = (s^2 + 0.0362s + 1.2367) \quad (2.52)$$

Using (2.51) and (2.52), one could find the natural frequencies and damping ratios for both short period and phugoid mode. If the necessary calculations are conducted, it is possible to obtain  $\omega_n$  (natural frequency) and  $\xi$  (damping ratio) values such as

$$\left. \begin{array}{l} \xi_{pm} = 0.0163 \\ \omega_{n\_pm} = 1.1121 \text{ rad/sec} \\ T_{pm} = 55.2007 \text{ sec} \end{array} \right\} \text{ long period oscillation} \quad (2.53)$$

$$\left. \begin{array}{l} \xi_{sp} = 0.8336 \\ \omega_{n\_sp} = 1.6701 \text{ rad/sec} \\ T_{sp} = 0.7183 \text{ sec} \end{array} \right\} \text{ short period oscillation} \quad (2.54)$$

From (2.53) and (2.54), it is apparent that the characteristic behaviours of both modes are as

- ✓ Short period mode of the UAV is adequately damped.
- ✓ Phugoid mode of the UAV is lightly damped which indicates an under-damped case in our situation.

Additionally, another indicator of damping ratio is the time required for one period of the oscillations, which is commonly defined as

$$T = \frac{1}{\xi\omega_n} \quad (2.55)$$

Using (2.55), it is credible to obtain the time required for one period such as

$$T_{sp} = \frac{1}{0.8336 \times 1.6701} = 0.7183 \text{ s} \quad (2.56)$$

$$T_{pm} = \frac{1}{0.0163 \times 1.1121} = 55.2007 \text{ s} \quad (2.57)$$

From (2.56), it is expected that the short period mode, oscillations with period of  $2T$ , are occurring within every second and a half; while in phugoid mode, time required for one period is relatively high, nearly 1 minute. In phugoid mode, structures of the aircraft would be affected seriously due to high oscillations, forces (due to vibration) and moments, therefore investigation of modes is taking an important role.

In order to obtain related transfer functions (TFs) for given elevator displacements, elevator deflections/inputs has been introduced in (2.32), where  $C_{z\delta_e} = -0.71$ ,  $C_{m\delta_e} = -0.71$  and  $C_{x\delta_e} = 0$  (which has been neglected) [5, 6], which yields to

$$\begin{aligned} x: & (1.4158s + 0.0264)'u(s) - 1.1181'\alpha(s) + 1.1570\theta(s) = 0 \\ z: & 2.3141'u(s) + (1.4161s + 0.1381)'\alpha(s) - 1.3834s\theta(s) = -0.71\delta_e \\ M: & 0 + (0.0003s + 0.0312)'\alpha(s) + (0.0121s^2 + 0.0323s)\theta(s) = -0.71\delta_e \end{aligned} \quad (2.58)$$

where  $\delta_e$  is elevator deflection (rad). The matrix representation is as

$$\begin{bmatrix} (1.4158s + 0.0264) & -1.1181 & 1.1570 \\ 2.3141 & (1.4161s + 0.1381) & -1.3834 \\ 0 & (0.0003s + 0.0312) & (0.0121s^2 + 0.0323s) \end{bmatrix} \begin{bmatrix} 'u(s) \\ '\alpha(s) \\ \theta(s) \end{bmatrix} = \begin{bmatrix} 0 \\ -0.71 \\ -0.71 \end{bmatrix} \delta_e(s) \quad (2.59)$$

After obtaining the matrix representation, it is a relatively easy task to obtain TFs for Longitudinal dynamics. Starting with (2.59) and by using the Cramer's Rule,

$$\frac{'u(s)}{\delta_e(s)} = \frac{\begin{vmatrix} 0 & -1.1181 & 1.1570 \\ -0.71 & (1.4161s + 0.1381) & -1.3834 \\ -0.71 & (0.0003s + 0.0312) & (0.0121s^2 + 0.0323s) \end{vmatrix}}{\begin{vmatrix} (1.4158s + 0.0264) & -1.1181 & 1.1570 \\ 2.3141 & (1.4161s + 0.1381) & -1.3834 \\ 0 & (0.0003s + 0.0312) & (0.0121s^2 + 0.0323s) \end{vmatrix}} \quad (2.60)$$

it is possible to obtain the TFs  $'u(s)/\delta_e(s)$  such as



$$\frac{u(s)}{\delta_e(s)} = \frac{0.009597 s^2 - 0.0391 s - 0.0878}{0.02424 s^4 + 0.06836 s^3 + 0.1 s^2 + 0.0859 s + 0.0836} \quad (2.61)$$

Corresponding bode plot of  $u(s)/\delta_e(s)$  could be obtained as shown in Figure 2.2.

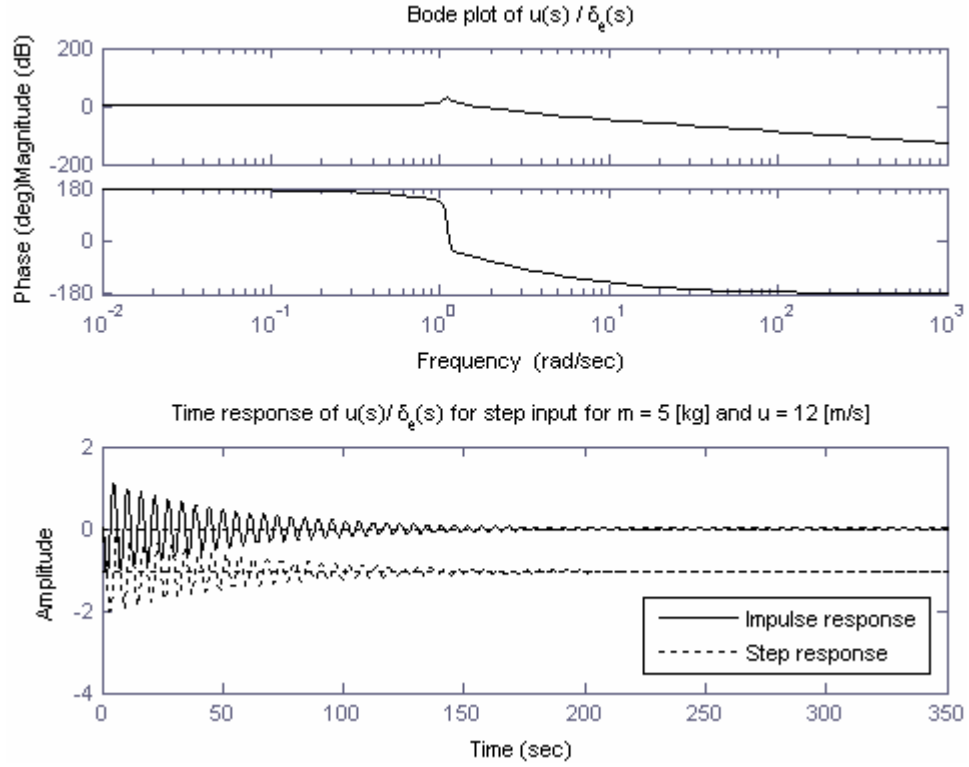


**Figure 2.2** Bode and time domain response plot of  $u(s)/\delta_e(s)$ .

As it is likely to see from Figure 2.2, for a given  $\delta_e$  deflection (input), steady state velocity of the system is considerably affected in phugoid mode, but in short period mode is not affected critically. If time domain step and impulse responses of  $u(s)/\delta_e(s)$  are investigated from Figure 2.2, it can be said that the behaviour of  $u(s)$  is highly oscillatory as a result of very close poles (2.48) to the imaginary axis.

$$\frac{\alpha(s)}{\delta_e(s)} = \frac{\begin{vmatrix} (1.4158s + 0.0264) & 0 & 1.1570 \\ 2.3141 & -0.71 & -1.3834 \\ 0 & -0.71 & (0.0121s^2 + 0.0323s) \end{vmatrix}}{\begin{vmatrix} (1.4158s + 0.0264) & -1.1181 & 1.1570 \\ 2.3141 & (1.4161s + 0.1381) & -1.3834 \\ 0 & (0.0003s + 0.0312) & (0.0121s^2 + 0.0323s) \end{vmatrix}} \quad (2.62)$$

it is possible to obtain the TFs  $\alpha(s)/\delta_e(s)$  such as

$$\frac{\alpha(s)}{\delta_e(s)} = \frac{-0.01215 s^3 - 1.423 s^2 - 0.02654 s - 1.901}{0.02424 s^4 + 0.06836 s^3 + 0.1 s^2 + 0.0859 s + 0.0836} \quad (2.63)$$

Corresponding bode plot and time domain response of  $\alpha(s)/\delta_e(s)$

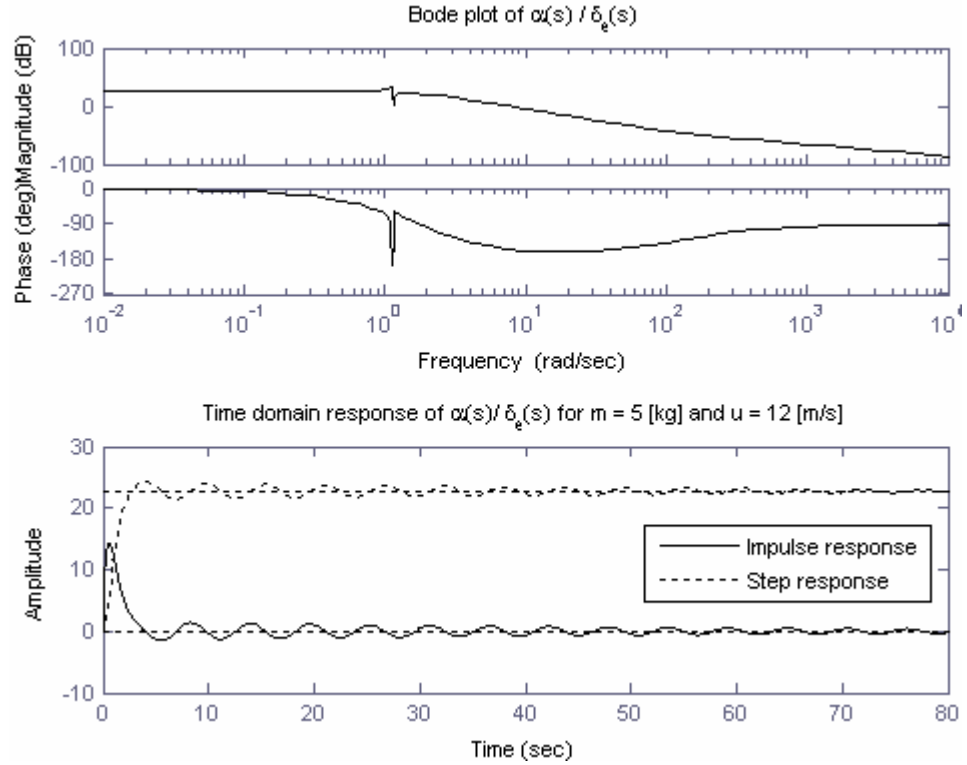


**Figure 2.3** Bode and time domain response plot of  $\alpha(s)/\delta_e(s)$ .

could be obtained as given in Figure 2.3. As it is probable to see from Figure 2.3, for a given  $\delta_e$  deflection (input), angle of attack ( $\alpha$ ) is noticeably affected in phugoid mode, but in short period mode angle of attack is changing quite smoothly. Moreover, if time domain step and impulse responses of  $\alpha(s)/\delta_e(s)$  are examined, from Figure 2.3, it can be observed that  $\alpha(s)$  has regular oscillations as a result of very close poles ( $s_{3,4}$ ) to the origin.

$$\frac{\theta(s)}{\delta_e(s)} = \frac{\begin{vmatrix} (1.4158s + 0.0264) & -1.1181 & 0 \\ 2.3141 & (1.4161s + 0.1381) & -0.71 \\ 0 & (0.0003s + 0.0312) & -0.71 \end{vmatrix}}{\begin{vmatrix} (1.4158s + 0.0264) & -1.1181 & 1.1570 \\ 2.3141 & (1.4161s + 0.1381) & -1.3834 \\ 0 & (0.0003s + 0.0312) & (0.0121s^2 + 0.0323s) \end{vmatrix}} \quad (2.64)$$

it is possible to obtain the TFs  $\theta(s)/\delta_e(s)$  such as

$$\frac{\theta(s)}{\delta_e(s)} = \frac{1.423 s^2 + 0.134 s + 1.839}{0.02424 s^4 + 0.06836 s^3 + 0.1 s^2 + 0.0859 s + 0.0836} \quad (2.65)$$

Corresponding bode plot of  $\theta(s)/\delta_e(s)$  could be obtained as

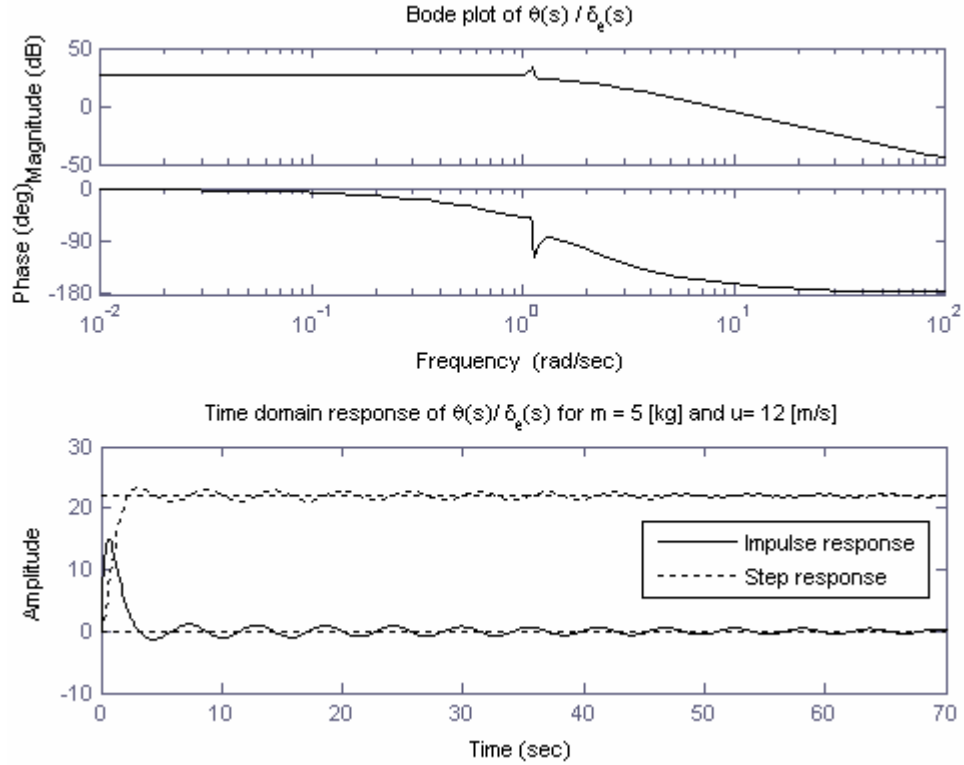


**Figure 2.4** Bode plot of  $\theta(s)/\delta_e(s)$  .

As it is likely to see from Figure 2.4 that for a given  $\delta_e$  deflection (input), pitching angle ( $\theta$ ) is noticeably affected in phugoid mode, but in short period mode angle of attack is changing smoothly. If time domain step and impulse responses of  $\theta(s)/\delta_e(s)$  are plotted, it is likely to find the graphs as shown in Figure 2.4. It could also be said that the behaviour of  $\theta(s)$  has frequent and long-lasting oscillations as a result of very close poles (2.48) to the imaginary axis. After such assessments, in order to get a better idea that how UAV is going to behave in short period and phugoid modes, short period and phugoid mode approximations and their characteristics might be examined, but it will not be conducted here. For detailed analysis conducted on short and long period approximations, reader is referred to [2, 5-9] for further reading.

### 2.3 Model-Reference Adaptive Control System Design for the Longitudinal Dynamics of the UAV:

Subsequent to the conclusion of longitudinal dynamic modeling part, in the following sections of the thesis, automatic control system designs based on Adaptive control approach will be introduced.

An adaptive control algorithm is simply an adaptive control system design with adjustable parameters and a mechanism for adjusting the parameters. The controller itself is becoming nonlinear in the control loop, because of the adaptive parameter adjustment mechanism. But however, it is a very special formation in terms of control. Adaptive control systems can be considered as having two different loops in the control algorithm. One of the loops is the normal feedback with plant outputs and the controller. But the other loop is for the parameter adjustment purposes. A sample block diagram for an adaptive control system design (taken from [10]) is given in Figure 2.5.

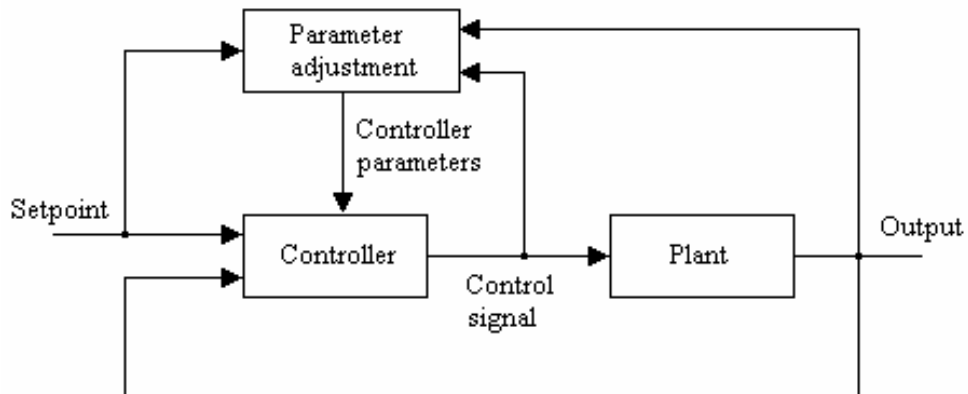


**Figure 2.5** A sample adaptive control system block diagram.

In the following parts of the thesis, as a branch of adaptive control theory, model-reference adaptive control system (MRAS) design will be introduced and subsequently will be implemented on longitudinal dynamics of the UAV in order to improve the stability and performance characteristics of the open loop system. Model-reference adaptive system (MRAS) control algorithm is an important part of the adaptive control theory. It might be considered as an adaptive servo system where the expected performance features are expressed in terms of a reference

model, which gives the desired response to a given input. A sample block diagram of a MRAS system is presented in Figure 2.6.

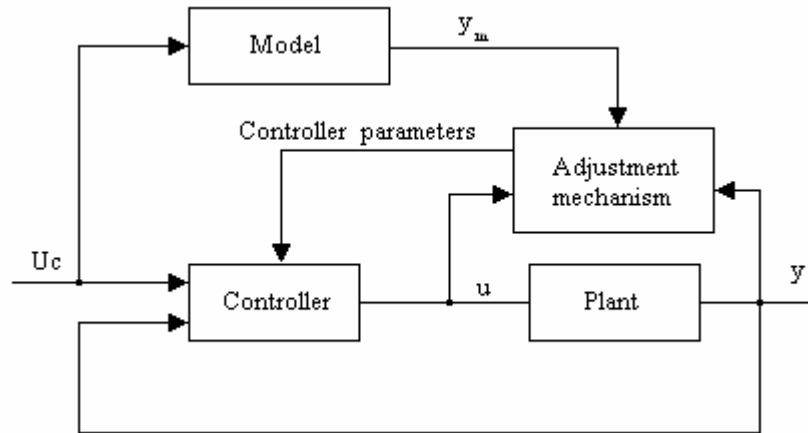


**Figure 2.6** Sample block diagram of a model-reference adaptive system (MRAS).

The MRAS system itself owns an ordinary feedback loop which is consisted of the plant-controller and another feedback loop that is used to adjust the controller parameters in order to reach to the perfect following conditions with the reference model. Parameters in the adjustment loop are tuned on the basis of feedback from the error ( $e$ ), which has been defined as the difference between the output of the plant ( $y$ ) and the output of the reference model ( $y_m$ ). In this concept, the ordinary feedback loop is named as the inner loop, while the parameter adjustment loop is called as the outer loop. The mechanism for tuning the parameters in a model-reference system can be obtained in two different ways: by using a gradient method or by applying stability theory [10, 11].

In the following parts of the thesis, two different control algorithms will be introduced: PI adjustment based on MIT rule and PI adjustment based on Lyapunov Stability Theory. But before getting through the adaptive control system design process, a closer (and a detailed) look into the frequency domain responses of the nominal plant is necessary and crucial in terms of improving the open-loop time domain performance specifications. As it is possible to remember from previous sections, longitudinal flight regime is characterized by  $\theta/\delta_e$  transfer function and by inspecting frequency domain response of  $\theta/\delta_e$  given in Figure 2.4, it is possible to see that the Phase Margin (PM) and Gain Margin (GM) characteristics are relatively weak. By examining the Bode Diagram (Figure 2.7) of  $\theta/\delta_e$ ,

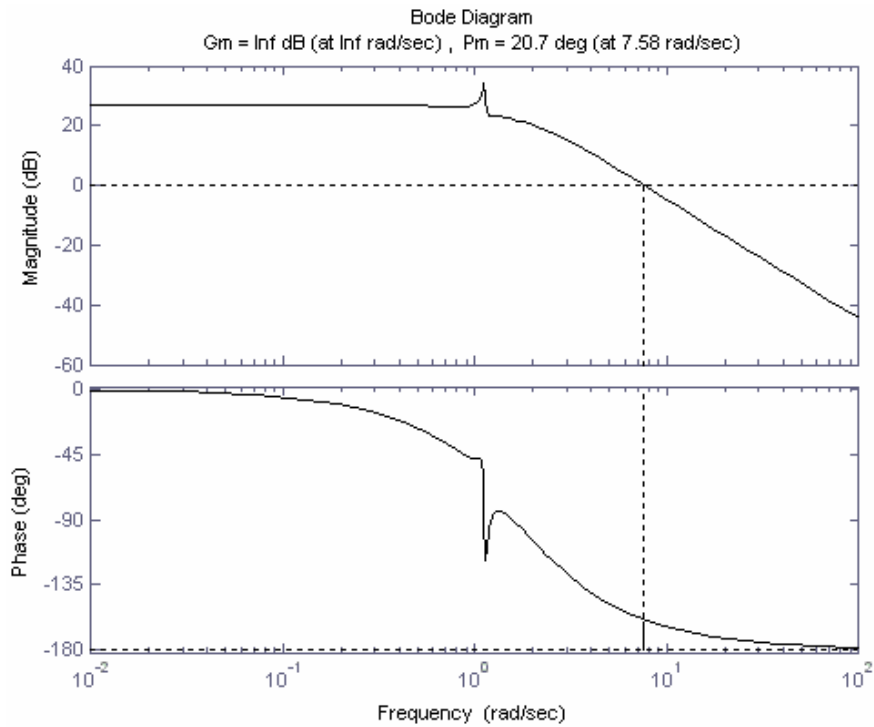


**Figure 2.7** Detailed Bode plot of open loop  $\theta / \delta_e$  transfer function.

it is easy to see that the PM value of nominal plant is 20.7 degree (at 7.58 rad/sec) and the GM is obtained as Infinity dB. With observed characteristic values of frequency domain, it is possible to mention that the PM and GM characteristics are inadequate for a control system design and therefore time domain responses of nominal plant are being quite slow and long lasting. In order to have better performance index in terms of frequency domain values, compensation of PM and GM will be suggested in the following lines with the help of Lead compensation technique.

The main characteristic of lead compensation is that it is used to reshape the frequency-response curve in order to maintain adequate phase-lead angle to offset the excessive phase lag associated with the components of the fixed system [13]. The procedure of designing a lead compensator by the frequency response approach for lead compensation has been given in [13] in detail and it is only going to be summarized for the longitudinal flight as the followings:

- 1) Transfer function of the lead compensator has been considered as

$$G_c(s) = K_c \frac{s + \frac{1}{T}}{s + \frac{1}{\alpha T}} \text{ where } 0 < \alpha < 1 \quad (2.66)$$

- 2) From Figure 2.7 it is possible to see that the PM of the nominal plant is 20.7 degrees and relatively insufficient. The main aim will be to pull PM over 50° and to have GM greater than 7dB. In this case necessary PM value is  $\phi_m = 50 - 20.7 \approx 30^\circ + 5^\circ = 35^\circ$  (5° has been added for the compensation for the shift in gain cross over frequency.)
- 3) Since  $\sin \phi_m = \frac{1 - \alpha}{1 + \alpha}$ , after some iterative procedures, it is found that  $\sin(35^\circ)$  corresponds to  $\alpha = 0.2792$ .
- 4) Once the attenuating factor  $-\alpha$  is obtained, the next step will be to obtain the corner frequencies ( $\omega = 1/T$  and  $\omega = 1/(\alpha T)$ ) of the lead compensator.  $\frac{1}{\sqrt{\alpha}} = \frac{1}{\sqrt{0.2792}} = 1.8927$  dB and  $|G(j\omega)| = -1.8927$  dB corresponds to  $\omega = 6.78$  rad/sec =  $\omega_c$ . This is going to be the new cross over frequency  $\omega_c = 1/(\alpha T)$  and following to that it is found  $1/T = \omega_c \sqrt{\alpha} = 3.5823$  and  $1/\alpha = \omega_c / \sqrt{\alpha} = 12.8323$ .

Using (2.66) the lead compensator, with preferred  $K_c = 1.6428$ , is found as

$$G_c(s) = K_c \frac{s + \frac{1}{T}}{s + \frac{1}{\alpha T}} = \frac{1.6428(s + 3.5823)}{s + 12.8323} \Rightarrow G_c(s) = \frac{1.6428s + 5.885}{s + 12.8323} \quad (2.67)$$

After deriving the lead compensation transfer function, time domain plots could be obtained of compensated and uncompensated plants as shown in Figure 2.8.

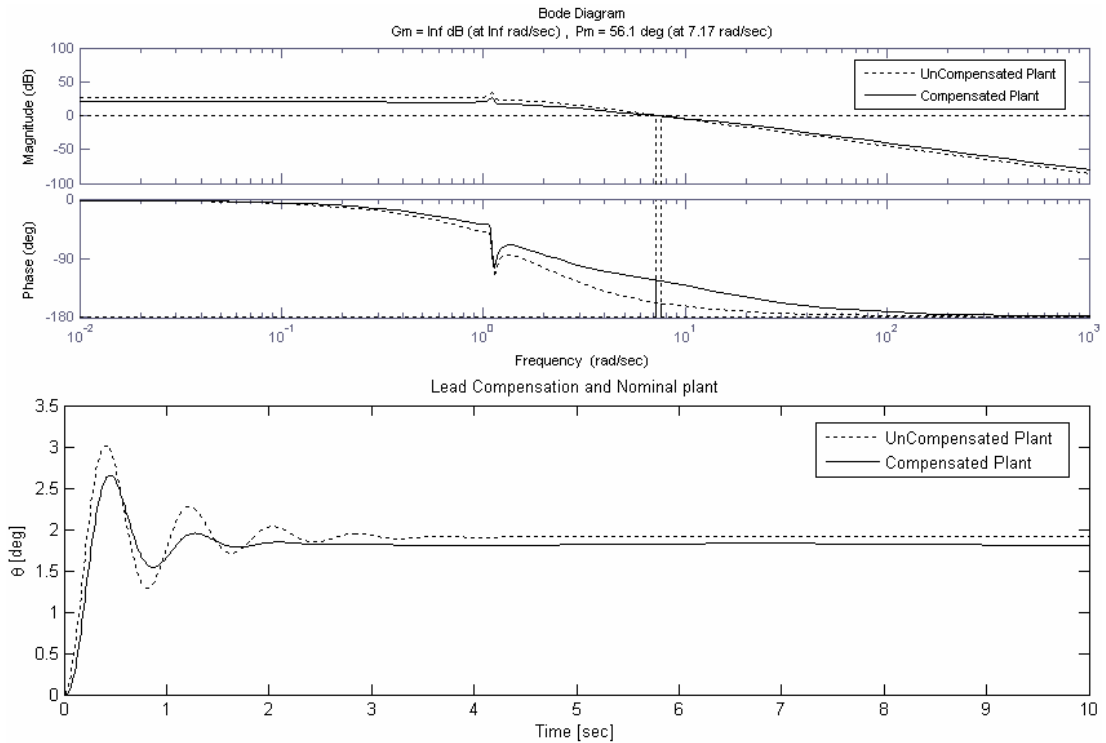


**Figure 2.8** Lead compensated nominal plant and bode diagram plots.

From Figure 2.8, it is quite easy to see the phase shift effect of the lead compensator in frequency domain. This property also influences the time domain response as well and the transient behaviour is more considerable than the uncompensated plant. After obtaining such an improvement in frequency domain characteristics and in open-loop system dynamics, it is possible to go through the automatic control system design procedures based on model-reference adaptive control algorithms.

### 2.3.1 PI Adjustment Based on MIT Rule

The MIT rule is the original approach to model-reference adaptive control system design, where it is mainly based on gradient evaluation. The name of the rule is given in this way because the theory of the method has been derived in the Instrumentation (now Drapper) Laboratory of Massachusetts Institute of Technology (MIT) for the first time; therefore it has been named like the MIT Rule.

In the presentation of MIT rule, an adjustable parameter  $\theta$  will be taken into account. In system dynamics, desired closed performance is defined as the output of the reference model-  $y_m$ . In MIT rule, it is considered that the error,  $e$ , is defined as the difference between the plant output,  $y$ , and reference model,  $y_m$ . Considering an



optimal control approach to the problem, it is possible to tune the parameters of the systems in a way so that the loss function

$$J(\theta) = \frac{1}{2} e^2 \quad (2.68)$$

is minimized. In order to be able to make  $J$  small enough, system parameters should be changed in the descending direction (negative gradient) of  $J$ , leading to

$$\frac{d\theta}{dt} = -\hat{\gamma} \frac{\partial J}{\partial \theta} = -\hat{\gamma} e \frac{\partial e}{\partial \theta} \quad (2.69)$$

and (2.69) is called as the MIT rule, where  $\hat{\gamma}$  is gain constant,  $J$  is the cost function (described in (2.68)) and  $e$  is the error between output of the reference model ( $y_m$ ) and nominal plant ( $y$ ). Here  $\partial e / \partial \theta$  partial derivative is called the sensitivity derivative of the system and is telling how the error is affected by the adjustable parameter,  $\theta$ .

Considering the given mathematical foundation related with the MIT rule, in the following sections, it is possible to obtain the adaptive control law necessary to shape the open loop dynamics. For this purpose, a MATLAB<sup>®</sup> Simulink block diagram has been suggested as shown in Figure 2.9.

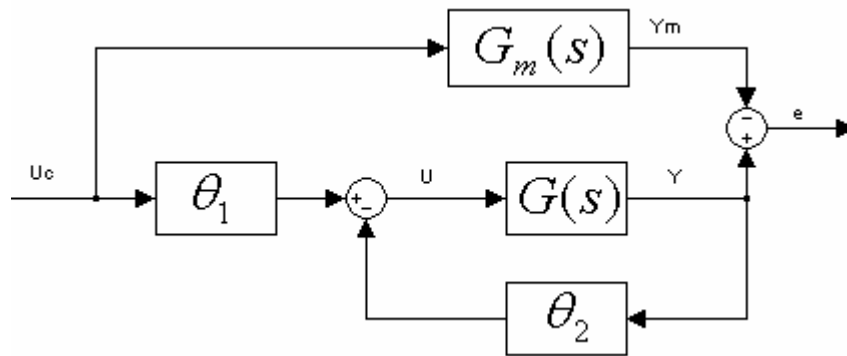


**Figure 2.9** Partial simulink block diagram for MIT rule.

With the help of Figure 2.9, it is possible to figure out that the control law has been suggested as  $u = \theta_1 u_c - \theta_2 y$ . Also the plant output could be easily obtained as  $y = G(s)u$  and reference model output is gained as  $y_m = G_m(s)u_c$ , where  $u_c$  is the command input,  $u$  is the control signal,  $G(s)$  is the transfer function of the nominal

plant (including elevator servo TF-[15/(s+15)]),  $G_m(s)$  is the transfer function of the reference model,  $\theta_1$  is the command signal adjustment parameter and  $\theta_2$  is the closed loop feedback adjustment parameter. In order to be able to obtain the MIT rule for the closed-loop system, sensitivity derivatives ( $\partial e/\partial\theta_1$  and  $\partial e/\partial\theta_2$ ) should be obtained, and for this purpose a step-by-step procedure in obtaining sensitivity derivatives has been summarized as the followings:

$$y = G(s)u, y_m = G_m(s)u_c, y = G(s)(\theta_1 u_c - \theta_2 y) \Rightarrow y + G(s)\theta_2 y = G(s)\theta_1 u_c$$

$$y = \frac{G(s)\theta_1}{1 + G(s)\theta_2} u_c, e = y - y_m \Rightarrow e = \frac{G(s)\theta_1}{1 + G(s)\theta_2} u_c - G_m(s)u_c \quad (2.70)$$

From (2.70), sensitivity derivatives could be obtained as

$$e = \frac{G(s)\theta_1}{1 + G(s)\theta_2} u_c - G_m(s)u_c, \frac{\partial e}{\partial\theta_{1,2}} = \frac{\partial}{\partial\theta_{1,2}} \left[ \frac{G(s)\theta_1}{1 + G(s)\theta_2} u_c - G_m(s)u_c \right]$$

$$\frac{\partial e}{\partial\theta_1} = \frac{G(s)(1 + G(s)\theta_2)}{(1 + G(s)\theta_2)^2} u_c \Rightarrow \frac{\partial e}{\partial\theta_1} = \frac{G(s)}{1 + G(s)\theta_2} u_c$$

$$\frac{\partial e}{\partial\theta_2} = - \frac{G(s)\theta_1 G(s)}{(1 + G(s)\theta_2)^2} u_c = \frac{-G(s)}{1 + G(s)\theta_2} \left( \underbrace{\frac{\theta_1 G(s)}{1 + G(s)\theta_2} u_c}_y \right) \quad (2.71)$$

$$\frac{\partial e}{\partial\theta_2} = \frac{-G(s)}{1 + G(s)\theta_2} Y$$

It is known that using pole placement technique from classical control theory, it is possible to find such a feedback gain like  $\tilde{\gamma}$ , which will shape the open loop eigenvalues (poles) and lead to  $G_m(s) \equiv \tilde{\gamma} G(s)/(1 + G(s)\theta_2)$ . If (2.71) is recomposed in the light of the given information, it is possible to obtain such representation as shown in (2.72).

$$\frac{\partial e}{\partial\theta_1} = \frac{G(s)}{1 + G(s)\theta_2} u_c = \frac{\tilde{\gamma}}{\tilde{\gamma}} \frac{G(s)}{1 + G(s)\theta_2} u_c = \frac{1}{\tilde{\gamma}} \left( \underbrace{\frac{\tilde{\gamma} G(s)}{1 + G(s)\theta_2}}_{G_m(s)} \right) u_c \Rightarrow \frac{\partial e}{\partial\theta_1} = \frac{G_m(s)u_c}{\tilde{\gamma}} \quad (2.72)$$

$$\frac{\partial e}{\partial\theta_2} = \frac{-G(s)}{1 + G(s)\theta_2} y = \frac{\tilde{\gamma}}{\tilde{\gamma}} \frac{-G(s)}{1 + G(s)\theta_2} y = \frac{-1}{\tilde{\gamma}} \left( \underbrace{\frac{\tilde{\gamma} G(s)}{1 + G(s)\theta_2}}_{G_m(s)} \right) y \Rightarrow \frac{\partial e}{\partial\theta_2} = \frac{-G_m(s)y}{\tilde{\gamma}}$$

After obtaining the theoretical demonstration of sensitivity derivatives, by using the MIT Rule (2.69), it is possible to obtain the adaptive control algorithm based on the MIT rule as shown in (2.73).

$$\begin{aligned} \frac{d\theta}{dt} &= -\hat{\gamma} e \frac{\partial e}{\partial \theta} \Rightarrow \frac{d\theta_1}{dt} = -\hat{\gamma} e \frac{\partial e}{\partial \theta_1} \text{ and } \frac{d\theta_2}{dt} = -\hat{\gamma} e \frac{\partial e}{\partial \theta_2} \\ \frac{d\theta_1}{dt} &= -\hat{\gamma} e \frac{\partial e}{\partial \theta_1} = -\hat{\gamma} e \left[ \frac{G_m(s)u_c}{\tilde{\gamma}} \right] = -\frac{\hat{\gamma}}{\tilde{\gamma}} e G_m(s)u_c \Rightarrow \frac{d\theta_1}{dt} = -\gamma e G_m(s)u_c \\ \frac{d\theta_2}{dt} &= -\hat{\gamma} e \frac{\partial e}{\partial \theta_2} = -\hat{\gamma} e \left[ -\frac{G_m(s)y}{\tilde{\gamma}} \right] = \frac{\hat{\gamma}}{\tilde{\gamma}} e G_m(s)y \Rightarrow \frac{d\theta_2}{dt} = \gamma e G_m(s)y \end{aligned} \quad (2.73)$$

where  $\gamma = \hat{\gamma} / \tilde{\gamma}$ . As it could be easily seen from (2.73), the adaptation rule is dependent *only* on the *reference model* parameters, which clearly indicates that even if the nominal plant- $G(s)$  parameters become unknown at certain time  $t$ , the controller will still be able to control the system and adjust the system parameters to reach the desired reference model parameters. But in (2.73) the selection of adaptation gain ( $\gamma$ ) is crucial and the preferred gain value usually depends on the command signal levels. In order to make the MIT rule less dependent on the command signal levels, it has been modified as shown in (2.74) and has been named as ‘Normalized MIT Rule’.

$$\frac{d\theta}{dt} = \frac{\hat{\gamma} \varphi e}{\alpha + \varphi^T \varphi} \text{ where } \varphi = -\partial e / \partial \theta \text{ and } \alpha > 0 \quad (2.74)$$

In (2.74), parameter  $\alpha > 0$  has been introduced to avoid difficulties when  $\varphi$  is small. It should also be noticed that (2.74) has been written in a way so that when  $\theta$  is a vector,  $\varphi$  also becomes a vector in the same size and dimension [10]. By applying the given rules in (2.74), it is possible to obtain adjustment parameters of the nominal plant as shown in (2.75).

$$\frac{d\theta_1}{dt} = \frac{\hat{\gamma}\varphi_1 e}{\alpha + \varphi_1^T \varphi_1} = \frac{\hat{\gamma}\left(-\frac{\partial e}{\partial \theta_1}\right)e}{\alpha + \left(-\frac{\partial e}{\partial \theta_1}\right)\left(-\frac{\partial e}{\partial \theta_1}\right)} = \frac{\hat{\gamma}\left(-\frac{G_m(s)u_c}{\tilde{\gamma}}\right)e}{\alpha + \left(-\frac{G_m(s)u_c}{\tilde{\gamma}}\right)\left(-\frac{G_m(s)u_c}{\tilde{\gamma}}\right)} \quad (2.75a)$$

$$\left(\frac{d\theta_1}{dt}\right)_{norm} = -\frac{\gamma_1 G_m(s)u_c e}{\alpha + (\gamma_2 G_m(s)u_c)^2} \Rightarrow (\theta_1)_{norm} = -\int \left(\frac{\gamma_1 G_m(s)u_c e}{\alpha + (\gamma_2 G_m(s)u_c)^2}\right) dt$$

where  $\gamma_1 = \hat{\gamma}/\tilde{\gamma}$  and  $\gamma_2 = 1/\tilde{\gamma}$  and

$$\frac{d\theta_2}{dt} = \frac{\hat{\gamma}\varphi e}{\alpha + \varphi^T \varphi} = \frac{\hat{\gamma}\left(-\frac{\partial e}{\partial \theta_2}\right)e}{\alpha + \left(-\frac{\partial e}{\partial \theta_2}\right)\left(-\frac{\partial e}{\partial \theta_2}\right)} = \frac{\hat{\gamma}\left(-\left(-\frac{G_m(s)y}{\tilde{\gamma}}\right)\right)e}{\alpha + \left(\frac{G_m(s)y}{\tilde{\gamma}}\right)\left(\frac{G_m(s)y}{\tilde{\gamma}}\right)} \quad (2.75b)$$

$$\left(\frac{d\theta_2}{dt}\right)_{norm} = \frac{\gamma_3 G_m(s)y e}{\alpha + (\gamma_4 G_m(s)y)^2} \Rightarrow (\theta_2)_{norm} = \int \left(\frac{\gamma_3 G_m(s)y e}{\alpha + (\gamma_4 G_m(s)y)^2}\right) dt$$

where  $\gamma_3 = \hat{\gamma}/\tilde{\gamma}$  and  $\gamma_4 = 1/\tilde{\gamma}$ . Having a closer look at the adjustment parameters ( $d\theta_1/dt$  and  $d\theta_2/dt$ ) will give valuable information, so that the adjustment algorithm is consisted just of an ‘integral’ action, which could only be used to improve the steady state error of the closed-loop system. Therefore, in order to be able to enhance the performance specifications and to increase the bandwidth of the closed loop system, ‘proportional’ part should be introduced beside obtained ‘integral’ control action, which will lead to a ‘PI adjustment’ control algorithm in adaptive control theory and is shown in (2.76) [10].

$$\begin{aligned} \tilde{\theta}(t) &= \underbrace{-\gamma_1 u_c(t) e(t)}_{\text{Proportional part}} - \underbrace{\gamma_2 \int u_c(\tau) e(\tau) d\tau}_{\text{Integral part}} \\ \tilde{\theta}_1(t) &= -\gamma_1 u_c(t) e(t) - \gamma_2 \int \frac{d\theta_1}{dt} dt \\ \tilde{\theta}_2(t) &= -\gamma_3 u_c(t) e(t) - \gamma_4 \int \frac{d\theta_2}{dt} dt \end{aligned} \quad (2.76)$$

After obtaining necessary information related with the parameter adjustment algorithms, Simulink block diagram of PI adjustment algorithm based on MIT rule has been constructed and is given in Appendix-A.

If obtained PI adjustment algorithms based on normalized MIT rules are going to be applied to the nominal plant dynamics, obtained control system performance and time domain results are being as shown in Figure 2.10.

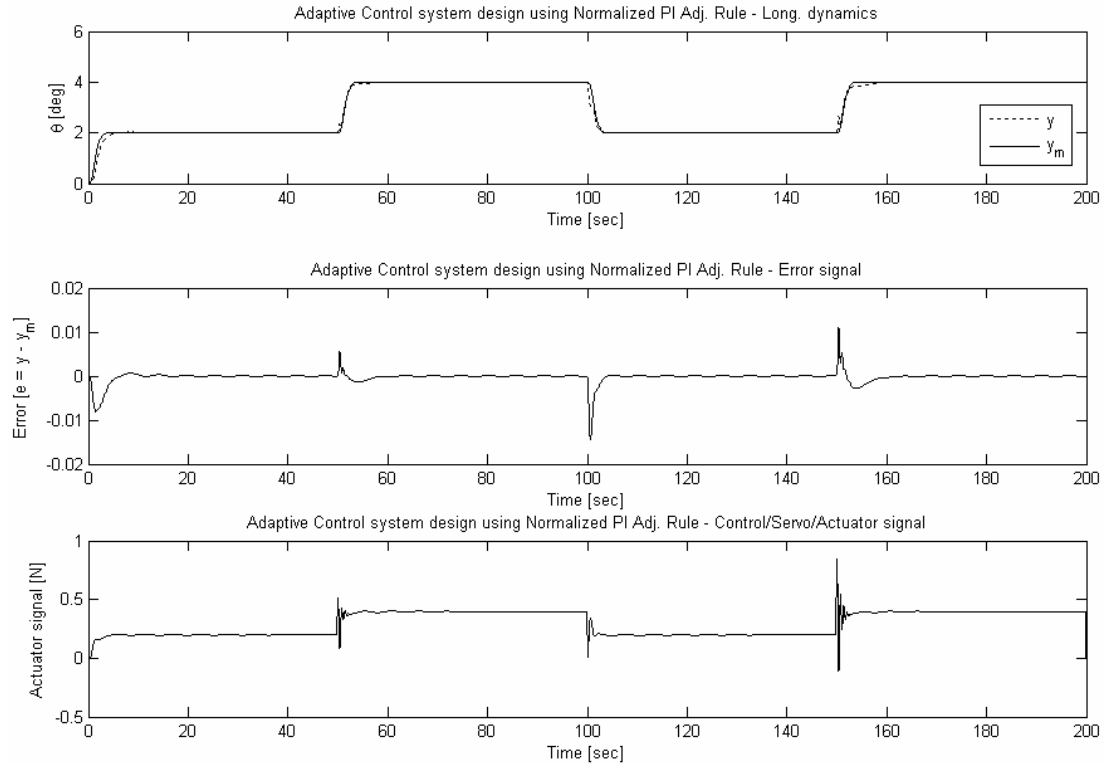


**Figure 2.10** Closed-loop time domain responses of model-reference adaptive control system design: PI adjustment based on normalized MIT rule.

From Figure 2.10, it is easy to see that the PI adjustment based on normalized MIT rule adaptation algorithm is working properly and remarkably. It is also possible to see that adaptive control rule is able to adapt and control the system parameters and match them with the desired closed loop states, so that the settling time is approximately 10 seconds and the maximum actuator effort is nearly 0.2 Newton, which are acceptable values for a control system design. Additionally, from the second plot in Figure 2.10, the change of error signal, where it is adapting itself to stay at zero (0) and fixed to the reference model, could be observed as well.

### 2.3.2 PI Adjustment Based on Lyapunov Stability Theory

There is no guarantee that an adaptive controller based on the MIT rule will give a stable closed-loop system. For this purpose Lyapunov Stability Theory has been introduced in order to guarantee stability in model-reference adaptive control

systems. In this section only the main characteristics of Lyapunov Stability Theory will be presented, but for further and detailed information one could refer to [13, 14].

Let's consider nonlinear and Linear Time-Invariant (LTI) differential equation  $dx/dt = f(x)$ . Let's assume that the system has a solution like  $f(0) = 0$  for  $x_i = 0$ , where this kind of conditions are called "equilibrium state conditions". In order to guarantee the stability for states starting out of range of equilibrium conditions, some conditions are needed. For the existence and uniqueness of the solution, there are some restrictions on  $f(x)$  for  $x_0 \neq 0$ , which guarantee the existence and the uniqueness of the solution. A necessary condition could be defined like  $f(x)$  is satisfying Lipschitz conditions as  $\|f(x) - f(y)\| < L\|x - y\|$ , where  $L$  is a number small enough for the analysis and  $0 < L < \infty$ . Here a stability analysis could be conducted for non-linear functions satisfying Lipschitz conditions. Also stability analysis could be conducted for perturbed systems whether they are going to turn back to their equilibrium states or not. But there is a boundary for going through the equilibrium states and if this boundary is overtaken, system dynamics may not be able to come back to old equilibrium points and could find some other equilibrium points. In other words, if a ball is going to be released from an arbitrary point and following to that if it comes to stability at a certain point and if this point is within the boundary of equilibrium conditions, then this is called "asymptotic stability condition" for systems. Another interesting situation is that if the ball doesn't come to stability but also if it doesn't get far away from the equilibrium states as well (in other words, if it exhibits periodic motion), in this situation the motion is stable as well. But this is only stable condition (not asymptotically stable). If a ball is released from an arbitrary point, it will stop when its kinetic energy decreases to "0". In that case, the equilibrium stability point is the point where the kinetic energy becomes "0". If the ball is shifted somewhere in the neighborhood of the equilibrium point, it will gain energy and motion will occur. However, if it loses its energy again and stops as a result of this motion, then it is called asymptotically stable. But for example, let's consider that the ball stopped in another equilibrium point, where its kinetic energy becomes "0" and turn into potential energy. Then this equilibrium point is stable but it is not asymptotically stable.

In all of the stated discussions, energy functions are positive definite functions. But the rest condition of a system is representing that its kinetic energy is “0”. From here it can be summarized that if kinetic energy of a system is changing in a descending direction (-) with time, then it corresponds to an “asymptotically stable” equilibrium point. Also Lyapunov stability theory depends on the property that the kinetic function of a system is descending and changing in a descending direction with time (Figure 2.11).

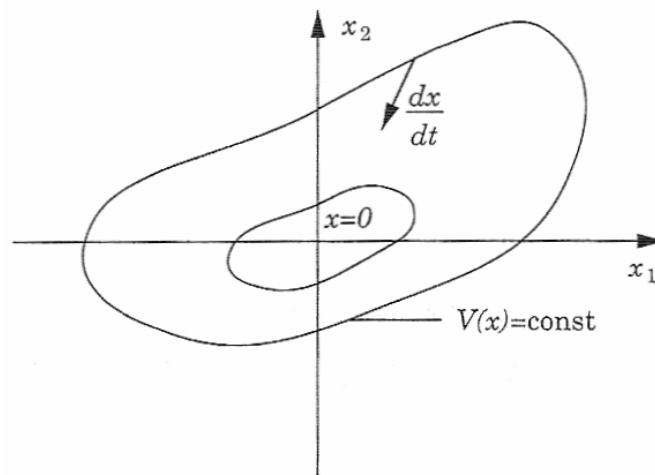


**Figure 2.11** Lyapunov stability theory representation in phase domain.

Thus, if KE of a system is decreasing, it means that the system is approaching to an asymptotic stability point. And Lyapunov stability simply is based on characteristic of a decreasing (descending) KE function. Since it is very hard to derive KE function of a complex system, if one can define such functions ( $V(x)$ ) representing the characteristics of KE functions, and if those functions are in a decreasing characteristic along the trajectory of KE functions, then one can guarantee that the solution of the differential equation will always give us stable solutions and then  $V(x)$  will be called Lyapunov function.

In other words, with the language of mathematics, if  $V(x)$  is suggested as  $V(x) = x^T P x$  and  $\dot{x} = A x + B u$ , where  $u = -K x$  and  $\bar{A} = A - B K$ , then for each symmetric positive-definite matrix  $Q$ , there exists a unique symmetric positive-definite matrix  $P$  such that

$$\bar{A}^T P + P \bar{A} = -Q \text{ leading to } \dot{V}(x) = -x^T Q x \text{ and } \dot{V}(x) < 0 \text{ for } t > 0 \quad (2.77)$$

then the system is called asymptotically stable and  $V(x)$  is called a Lyapunov function satisfying  $\dot{V}(x) < 0$  condition.

Next step, after a brief introduction of the Lyapunov stability theory, is the derivation of parameter adjustment rules for longitudinal flight control system design based on Lyapunov stability theory. In order to do this and in order to satisfy perfect matching conditions (between  $A$  and  $A_m$ ), the candidate Lyapunov function (taken from [15]) has been suggested as given in (2.78).

$$V(x) = e^T P e + Tr[(A - BL - A_m)^T N (A - BL - A_m)] \quad (2.78)$$

where  $N$  is the weighting matrix and  $Tr$  is the ‘‘Trace’’ of a matrix, which has been defined as the sum of the diagonal elements of a matrix such as

$$A = \begin{bmatrix} a_{11} & a_{12} & a_{13} \\ a_{21} & a_{22} & a_{23} \\ a_{31} & a_{32} & a_{33} \end{bmatrix} \Rightarrow Tr(A) = (a_{11} + a_{22} + a_{33}) \quad (2.79)$$

Under *perfect matching conditions*, it has been assumed (and calculated) that there exists such  $L^*$  which will lead nominal system dynamics to  $A - BL^* \rightarrow A_m$ , so that  $L^*$  is the *constant* feedback gain obtained by LQR or a similar control algorithm. And adaptive parameter adjustment algorithm-L in (2.78) has been defined as  $L = L^* + \Delta L$ , where  $\Delta L$  is representing the parameter adjustment uncertainties [29-31]. In this way, by simply introducing adjustment parameter uncertainties, robustness characteristics have also been also introduced in adjustment system dynamics of adaptive control system design.

It is easy to see from (2.78) that the main aim is to find such feedback parameter  $L = L^* + \Delta L$ , which will shape and help the nominal plant to reach the system parameters to the desired level, which is the reference-model. In this way, perfect



matching conditions will be satisfied and as it has been mentioned in previous lines, the main goal will be satisfied. Therefore, the derivative of Lyapunov function will always be negative ( $\dot{V}(x) < 0$ ) and will lead to guaranteed stability. For this purpose, derivative of the candidate Lyapunov function has been taken and the procedure has been summarized step-by-step in (2.81). But before that step, change of error function ( $e$ ) with respect to time ( $\dot{e}$ ) should be obtained as shown in (2.80).

$$\begin{aligned}
e &= y - y_m \Rightarrow \dot{e} = \dot{y} - \dot{y}_m = (Ay + Bu) - (A_m y_m + B_m u_c) \\
u &= u_c - Ly, \quad L = L^* + \Delta L \\
\dot{e} &= Ay + B(u_c - Ly) - A_m y_m - B_m u_c = Ay + Bu_c - BLy - A_m y_m - B_m u_c \Rightarrow y_m = y - e \\
\dot{e} &= Ay + Bu_c - BLy - A_m(y - e) - B_m u_c = Ay + Bu_c - BLy - A_m y + A_m e - B_m u_c \quad (2.80) \\
\dot{e} &= A_m e + (A - BL - A_m)y + (B - B_m)u_c \Rightarrow B = B_m \\
\dot{e} &= A_m e + (A - BL - A_m)y \Rightarrow L = L^* + \Delta L \text{ and } A - A_m = BL^* \\
\dot{e} &= A_m e + (A - A_m - B(L^* + \Delta L))y = A_m e + (BL^* - BL^* - B\Delta L)y \\
\dot{e} &= A_m e - B\Delta Ly
\end{aligned}$$

And derivative of the candidate Lyapunov function has been constructed as in (2.81a-b).

$$\begin{aligned}
V(x) &= e^T P e + Tr[(A - BL - A_m)^T N(A - BL - A_m)] \\
A - BL - A_m &= (A - A_m) - BL = BL^* - BL = B(L - \Delta L) - BL = BL - B\Delta L - BL \\
V(x) &= e^T P e + Tr[(-B\Delta L)^T N(-B\Delta L)] = e^T P e + Tr[(B\Delta L)^T N(B\Delta L)] \\
\dot{V}(x) &= \dot{e}^T P e + e^T P \dot{e} + Tr[(B\Delta \dot{L})^T N(B\Delta L) + (B\Delta L)^T N(B\Delta \dot{L})] \\
\dot{V}(x) &= [A_m e - B\Delta Ly]^T P e + e^T P [A_m e - B\Delta Ly] \\
&\quad + Tr[(B\Delta \dot{L})^T N(B\Delta L) + (B\Delta L)^T N(B\Delta \dot{L})] \\
\dot{V}(x) &= e^T A_m^T P e - y^T \Delta L^T B^T P e + e^T P A_m e - e^T P B\Delta Ly \\
&\quad + Tr[(B\Delta \dot{L})^T N(B\Delta L) + (B\Delta L)^T N(B\Delta \dot{L})] \quad (2.81a)
\end{aligned}$$

$$y^T \Delta L^T B^T P e = e^T P B\Delta Ly \quad \text{and} \quad Tr[(B\Delta \dot{L})^T N(B\Delta L)] = Tr[(B\Delta L)^T N(B\Delta \dot{L})]$$

therefore,

$$\dot{V}(x) = e^T \underbrace{(A_m^T P + P A_m)}_{-Q} e - 2y^T \Delta L^T B^T P e + 2Tr[(B\Delta L)^T N(B\Delta \dot{L})]$$

$$\dot{V}(x) = -e^T Q e - 2y^T \Delta L^T B^T P e + 2Tr(\Delta L^T \overbrace{(B^T N B)}^T \Delta \dot{L})$$

$$\begin{aligned}\dot{V}(x) &= -e^T Q e - 2y^T \Delta L^T B^T P e + 2Tr[\Delta L^T T \Delta \dot{L}] \\ \dot{V}(x) &= -e^T Q e + 2Tr[-\Delta L^T B^T P e y^T + \Delta L^T T \Delta \dot{L}]\end{aligned}\quad (2.81b)$$

One of the most important point that should be stressed on in (2.81b) is the definition of  $T = (B^T N B)_{n \times n}$ . It is a very important term, because if it hadn't been defined in this way (i.e. as a square matrix), in the following sections of derivation of parameter adjustment rule,  $(B^T)_{m \times n}$  term would be left alone, where the *Pseudo Inverse* operation would be necessary due to the reason that the term  $B^T$  is not a square matrix (it is actually a matrix in dimensions of  $m \times n$ ). As it is known from linear algebra, if a matrix is not a square matrix, the inverse of the matrix cannot be found very easily. For that reason, in order to be able to find the inverse of a *non-square* matrix, *Pseudo Inverse* has been defined in literature and the reader can refer to [10, 14] for further and detailed information related with Pseudo Inverse. By simply defining  $T = (B^T N B)_{n \times n}$ , the complexity of the equation has been reduced and a non-square matrix possibility has been wiped out.

In (2.81b)  $e$  is the error function between output of the nominal plant ( $y$ ) and reference model ( $y_m$ ),  $P$  and  $Q$  are the symmetric positive definite matrices obtained and defined in Lyapunov function, respectively. From (2.81b) it is possible to see that if the term

$$Tr[-\Delta L^T B^T P e y^T + \Delta L^T T \Delta \dot{L}] = 0 \Rightarrow \Delta L^T (-B^T P e y^T + T \Delta \dot{L}) = 0 \quad (2.82)$$

then the candidate Lyapunov function becomes  $\dot{V}(x) = -e^T Q e$ , so that  $\dot{V}(x)$  will always be  $\dot{V}(x) < 0$  and stable. For that reason, equality  $\Delta L^T (-B^T P e y^T + T \Delta \dot{L}) = 0$  should be satisfied. If it is remembered that the main goal was to derive such  $L = L^* + \Delta L$ , which will lead to perfect matching conditions; only  $\Delta L^T (-B^T P e y^T + T \Delta \dot{L}) = 0$  will be taken into account, because when such  $L$ 's are obtained from  $\Delta L^T (-B^T P e y^T + T \Delta \dot{L}) = 0$ , and then  $\dot{V}(x) = -e^T Q e$  will automatically satisfy Lyapunov stability condition ( $\dot{V}(x) < 0$ ).

After such analyses, it is time to apply the given theoretical background into the longitudinal flight dynamics, but before getting into the process, it will be suitable to present the state-space matrices of the longitudinal flight system for simplicity in calculations. State-space matrixes of longitudinal flight system dynamics (including elevator servo TF,  $15/(s+15)$ ) has been obtained from  $\theta(s)/\delta_e(s)$  TF and are as shown in (2.83).

$$A_{long} = \begin{bmatrix} -30.6528 & -275.1114 & -661.2977 & -896.4313 & -778.2264 & -663.9486 \\ 1.0000 & 0 & 0 & 0 & 0 & 0 \\ 0 & 1.0000 & 0 & 0 & 0 & 0 \\ 0 & 0 & 1.0000 & 0 & 0 & 0 \\ 0 & 0 & 0 & 1.0000 & 0 & 0 \\ 0 & 0 & 0 & 0 & 1.0000 & 0 \end{bmatrix} \Rightarrow eig(A_{long}) = \begin{bmatrix} -15.0 \\ -12.83 \\ -1.39 + 0.92i \\ -1.39 - 0.92i \\ -0.01 + 1.11i \\ -0.01 - 1.11i \end{bmatrix} \quad (2.83)$$

$$B_{long} = [1 \ 0 \ 0 \ 0 \ 0 \ 0]^T \quad \text{and} \quad C_{long} = [0 \ 0 \ 566,14 \ 2081,4 \ 922,53 \ 2620,9]$$

From (2.83), it is likely to see that A-(compensated) state matrix is 6x6 and B-input (control) matrix is (6x1), which leads the parameter adjustment matrix-L to be (1x6)

$$L = [L_{11} \ L_{12} \ L_{13} \ L_{14} \ L_{15} \ L_{16}]_{(1 \times 6)}$$

for compatibility of dimensions. Next, if the necessary calculations are conducted in (2.82), the adaptive parameter adjustment rule based on Lyapunov stability is obtained as

$$\begin{aligned} Tr[-\Delta L^T B^T P e y^T + \Delta L^T T \Delta \dot{L}] &= 0 \Rightarrow \Delta L^T (-B^T P e y^T + T \Delta \dot{L}) = 0 \\ -B^T P e y^T + T \Delta \dot{L} &= 0 \Rightarrow T \Delta \dot{L} = B^T P e y^T \\ \Delta \dot{L} &= T^{-1} B^T P e y^T = (B^T N B)^{-1} B^T P e y^T \\ L &= L^* + \Delta L \Rightarrow \dot{L} = \Delta \dot{L} \\ \Delta \dot{L} = \dot{L} &= T^{-1} B^T P e y^T = (B^T N B)^{-1} B^T P e y^T \end{aligned} \quad (2.84)$$

Here  $\dot{L}$  has been found as  $\dot{L} = \Delta \dot{L}$ , because  $L^*$  is a constant parameter and is not changing with time. From (2.84), it is also possible to see that the parameter adjustment rule is only dependent on the output of the plant ( $y$ ) and the error function ( $e$ ), which makes the parameter adjustment system dynamics independent of information related to A-state matrix.

From here it is possible to see that the PI adjustment rule based on Lyapunov stability theory is obtained as the followings, where the control law is defined as  $u = u_c - \tilde{\theta}y$ .

$$\tilde{\theta}(t) = \underbrace{\gamma_1 u_c(t) e(t)}_{\text{Proportional part}} + \underbrace{\gamma_2 \int u_c(\tau) e(\tau) d\tau}_{\text{Integral part}} \Rightarrow \quad (2.85)$$

$$\tilde{\theta}(t) = \gamma_1 u_c(t) e(t) + \gamma_2 Ly(t)$$

Before getting into the time domain analysis of closed-loop system response, MATLAB<sup>®</sup> Simulink block diagram has been constructed (Figure 2.12) for PI adjustment control algorithm.

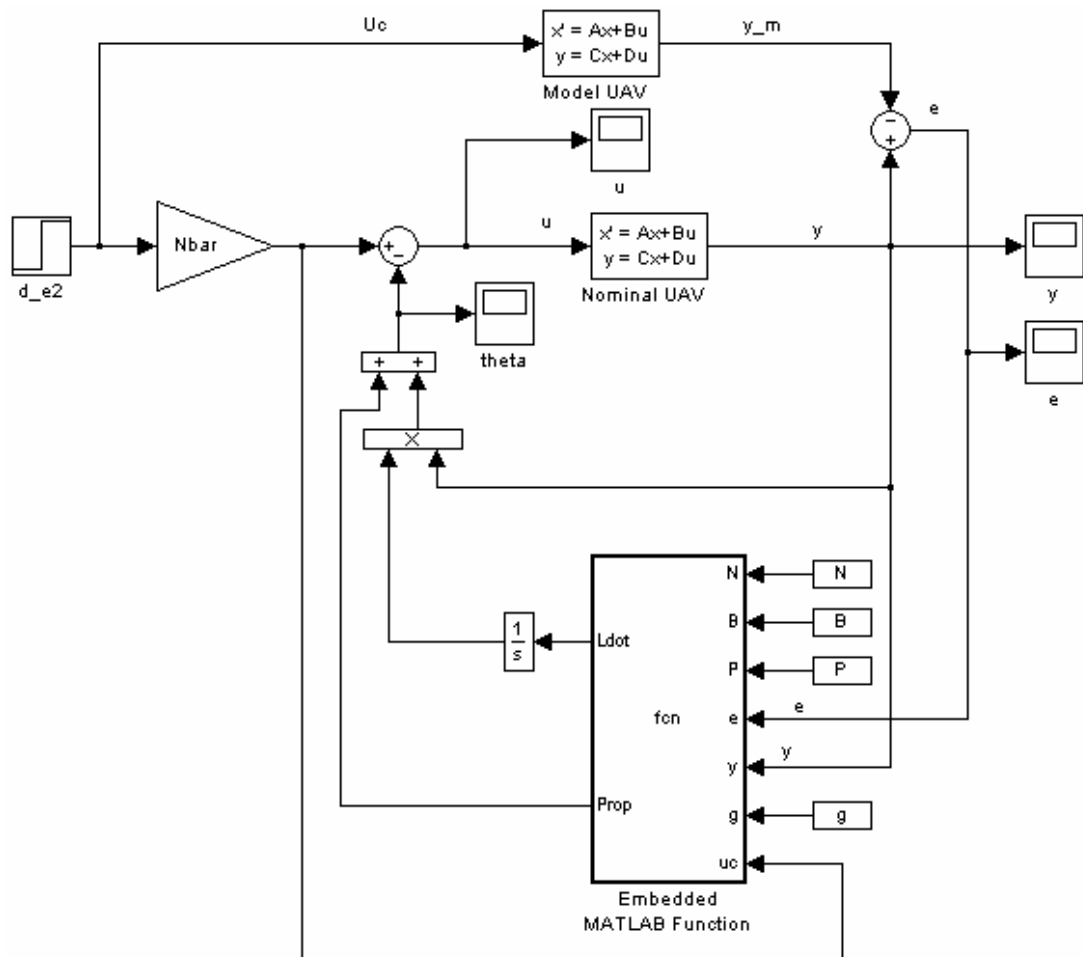


**Figure 2.12** Simulink block diagram of PI adjustment based on Lyapunov Stability.

In some cases, output of the nominal plant may have some difference from the reference signal, which is called as steady state error ( $e_{ss}$ ) and which is also the case in our system dynamics for longitudinal flight. In order to eliminate the occurring

steady state error it is possible to scale the input to make it equal to the steady state response. This scaling factor is often called as  $Nbar$  and it has been introduced into the system dynamics as shown in Figure 2.12.  $Nbar$  has been calculated using a Matlab program which has been taken from [32]. Following to that, if time domain responses of adaptive control system design based on Lyapunov stability are plotted, they should be obtained as given in Figure 2.13.

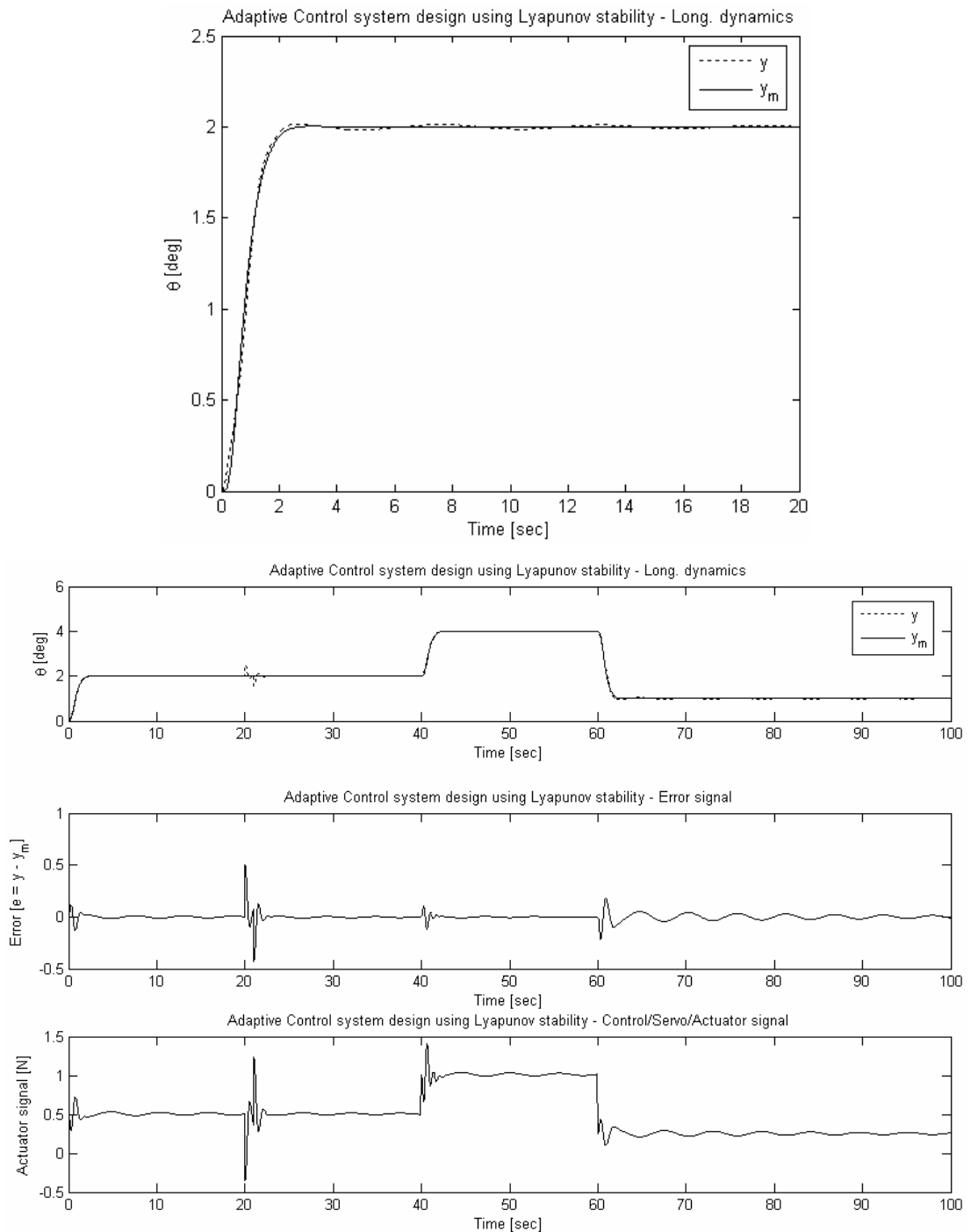


**Figure 2.13** Closed-loop time domain responses of model-reference adaptive control system design: PI adjustment based on Lyapunov stability.

From Figure 2.13, it is possible to see that time domain responses of PI adjustment rule based on Lyapunov stability are remarkable, so that the settling time is nearly 2.5 seconds and the maximum actuator signal is obtained as 1.5 Newton. Also the evolution of error signal is considerable and given in the second plot of Figure 2.13. Moreover, tracking and disturbance rejection characteristics are noteworthy, where a disturbance to the output has been introduced with a 25% magnitude of input signal at  $t = 20$  sec.

## 2.4 Augmented Optimal LQR Control System Design: Longitudinal Dynamics

In this part of the thesis, an augmented optimal LQR control system design, taken from [16], will be investigated with further details, and afterwards using derived mathematical model, the theory will be implemented on the longitudinal flight dynamics of the UAV.

In physical environment, it is not always possible to measure all the states of an aircraft during the flight and because of that reason, sometimes complexities and several anomalies could arise in automatic control process due to lack of state and feedback information. Therefore, in order to suppress the effects of lack of measurement, an observer mechanism is used in order to compensate measurement insufficiencies and to obtain a theoretical estimation of necessary states those couldn't be measured. This option will also be used in augmented optimal LQR control system design in order to suppress measurement effects and in order to obtain an estimated model for better performance characteristics.

In general sense, state-space mathematical model of a system is defined as

$$G(s) \Leftrightarrow \begin{cases} \dot{x}(t) = Ax(t) + Bu(t) \\ y(t) = Cx(t) \end{cases} \quad (2.85)$$

and estimation mechanism transfer function could be named as  $\hat{G}(s)$ , where nominal states of the plant are classified as  $x$  and estimated plant states are named as  $\hat{x}$ . As a result of the observer mechanism, it is expected to have  $\lim_{t \rightarrow \infty} \hat{x} - x = 0$  [12], which leads to adequate observation condition. Following to that, it is possible to construct

a MATLAB© Simulink block diagram of estimated (observed) system as shown in Figure 2.14.

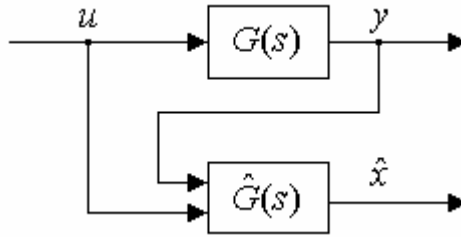


**Figure 2.14** Nominal plant and observer mechanism.

But before getting into control system design process, due to the reason that the observer mechanism has been suggested to be included in system dynamics, it has to be checked and guaranteed that the nominal plant is fully observable and controllable.

#### 2.4.1 Observability and controllability of system dynamics: Longitudinal flight

During the optimal control system design process, which is going to be presented in the next section, an observer scheme will be used in order to estimate the outputs those may not be measured during the flight. And just before getting into the control system design part, the observability and the controllability characteristics of the UAV system will be investigated in the following parts.

Observability matrix of a system is defined as,

$$Obs = O_n = [C \quad CA \quad CA^2 \quad \dots \quad CA^{n-1}]^T \quad (2.86)$$

where C is the output matrix and A is the state matrix of the nominal plant [13]. In the light of the observability matrix ( $O_n$ ), a system is described observable if (2.87) is satisfied.

$$Rank(O_n) = n \quad (2.87)$$

Using the  $\theta(s)/\delta_e(s)$  TF and elevator servo TF  $[15/(s+15)]$  of system dynamics, it is possible to obtain state space system representation of longitudinal flight dynamics

with the help of `tf2ss` MATLAB© command. If necessary calculations are conducted, state matrix-A and output matrix-C of longitudinal flight dynamics are obtained as shown in (2.83). Using (2.83) and replacing in (2.86), observability matrix is attained as

$$Obs = O_n = \begin{bmatrix} C \\ CA \\ CA^2 \\ \dots \\ CA^{n-1} \end{bmatrix} = 10^5 * \begin{bmatrix} 0 & 0 & 0.0088 & 0.0008 & 0.0114 \\ 0 & 0.0088 & 0.0008 & 0.0114 & 0 \\ 0.0088 & 0.0008 & 0.0114 & 0 & 0 \\ -0.1561 & -0.3976 & -0.5764 & -0.4986 & -0.4557 \\ 2.3846 & 6.6729 & 9.7189 & 8.3830 & 8.0778 \end{bmatrix} \quad (2.88)$$

where the rank of the system becomes  $Rank(O_n) = 5 = n$  showing that the system is fully observable. As a confirmation, it is also possible to calculate the number of unobservable states from (2.89),

$$UnOb = Length(A_{n \times n}) - Rank(O_n) = 5 - 5 = 0 \quad (2.89)$$

which simply states that there are no unobservable states (i.e. all of the states could be observed). Thus, it is feasible to verify that an observer mechanism can be used in estimation of the states of open-loop dynamics in longitudinal flight, where mathematical model of an observer mechanism can be simply defined as [12],

$$\hat{G}(s) \Leftrightarrow \begin{cases} \hat{x}(t) = A\hat{x}(t) + Bu(t) + H(y(t) - \hat{y}(t)), \\ \quad = \underbrace{(A - HC)}_{\hat{A}(t)} \hat{x}(t) + Bu(t) + H y(t) \\ \hat{y}(t) = C \hat{x}(t) \end{cases} \quad (2.90)$$

Additionally, controllability of the system dynamics should be verified as well, so that there will be no theoretical obstacle to get into the optimal control system design process. It is known that controllability matrix of a system is defined in [13] as

$$C_t = [B \quad AB \quad A^2B \quad \dots \quad A^{n-1}B] \quad (2.91)$$

so that the controllability matrix must satisfy (2.92)



$$\text{Rank}(C_i) = n \quad (2.92)$$

and in this way the system is called reachable or controllable. If the given controllability conditions are applied, controllability matrix is obtained as

$$C_i = [B \ AB \ A^2B \ \dots \ A^{n-1}B] = 10^4 * \begin{bmatrix} 0.0001 & -0.0018 & 0.0271 & -0.4070 & 6.1044 \\ 0 & 0.0001 & -0.0018 & 0.0271 & -0.4070 \\ 0 & 0 & 0.0001 & -0.0018 & 0.0271 \\ 0 & 0 & 0 & 0.0001 & -0.0018 \\ 0 & 0 & 0 & 0 & 0.0001 \end{bmatrix} \quad (2.93)$$

where the rank of the system is calculated as  $\text{Rank}(C_i) = 5 = n$  leading to a fully controllable system dynamics.

With such observability and controllability analyses, it has been proved that the longitudinal UAV system is both controllable and observable, which grants the opportunity to use an observer (estimation) mechanism in control system design process.

#### 2.4.2 Augmented optimal LQR control system design: Integral control

In this section of the thesis, an augmented optimal LQR control system design with an observer (estimation) mechanism will be presented using integral control technique and subsequently will be implemented on longitudinal flight dynamics of an UAV.

Generally speaking, state space representation of a system could be given like

$$\begin{aligned} \dot{x} &= Ax + Bu + Gw \\ y &= Cx \end{aligned} \quad (2.94)$$

and the feedback error could be given such as  $e = y - r$ , which is negative in sign (and different) than the usual feedback convention,  $e = r - y$ . It can be shown that the feedback control rule could be obtained in a way so that the plant could be augmented with an extra integral state ( $x_I$ ), which simply obeys the integral equation

$$\dot{x}_I = Hx - r = e \quad (2.95)$$

and leading to

$$x_I = \int e dt \quad (2.95)$$

Then the augmented state equations become

$$\begin{bmatrix} \dot{x}_I \\ \dot{x} \end{bmatrix} = \begin{bmatrix} 0 & C \\ 0 & A \end{bmatrix} \begin{bmatrix} x_I \\ x \end{bmatrix} + \begin{bmatrix} 0 \\ B \end{bmatrix} u + \begin{bmatrix} 0 \\ G \end{bmatrix} w \quad (2.96)$$

where the feedback control law becomes

$$u = -\begin{bmatrix} K_1 & K_0 \end{bmatrix} \begin{bmatrix} x_I \\ x \end{bmatrix} \quad (2.97)$$

Accordingly, control structure using the integral control action design technique results in as showed in Figure 2.15 [12, 16].

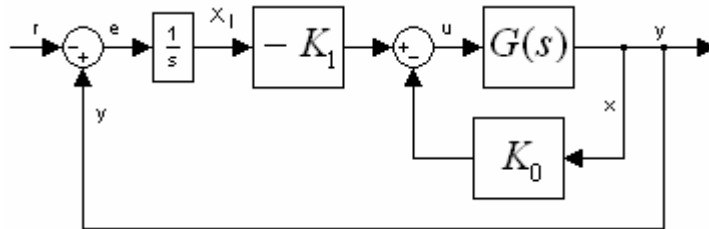


**Figure 2.15** Integral control block diagram for robust tracking and disturbance rejection.

After obtaining some mathematical background related with the robust tracking and disturbance rejection in system dynamics, it is time to implement it inside the optimal LQR control system design. In optimal control system design process, the main goal will be to determine the optimal feedback gain

$$u = -K_{LQR} \hat{x}(t) \quad (2.98)$$

which will eliminate the error between the reference and the feedback signals, so that the cost function will become

$$J(u(t)) = \int_0^{\infty} (y(t) - r(t))^T Q (y(t) - r(t)) - u(t)^T R u(t) dt \quad (2.99)$$

where  $Q$  and  $R$  are positive-definite weighting matrices. This problem cannot be solved without each a-priori-knowledge and/or without restriction of the reference signal  $r(t)$ , because  $r(t)$  can be for example an unstable signal and therefore the integral (2.99) will result in no finite value [12]. However, the problem can be solved as a modified sequence regulation problem for unknown  $r(t)$ . The solution exists within the expansion of the closed-loop through a filter  $K_{filt}$ , so that using general formula of a closed TF from input to output

$$\frac{Y(s)}{R(s)} = C [sI - (A - BK_{LQR})]^{-1} BK_{filt} := G_{CL}(s) \quad (2.100)$$

it is possible to obtain the value of  $K_{filt}$  as

$$K_{filt} = -\{C[(A - BK_{LQR})]^{-1}B\}^{-1} \quad (2.101)$$

The just described regulator design is for undisturbed rule as well as for rule without and/or with small model uncertainties well suited. A demand often placed in the practice is the capacity of the closed-loop to be able to compensate constant-not measurable disturbances [12]. The well known idea out of the classic theory in compensation of disturbances is to expand the regulator around an Integral-control loop, where the structure of integral control had been given previously in Figure 2.15.

If augmented system dynamics are going to be reorganized from (2.96), it should be obtained

$$\tilde{\dot{x}} = \begin{bmatrix} 0 & -C \\ 0 & A \end{bmatrix} \tilde{x}(t) + \begin{bmatrix} 0 \\ B \end{bmatrix} \tilde{u}(t) = \tilde{A} \tilde{x}(t) + \tilde{B} \tilde{u}(t) \quad (2.102a)$$

$$\tilde{y}(t) = [\gamma \quad C] \tilde{x}(t) = \tilde{C} \tilde{x}(t)$$

where  $\gamma$  is a scalar weighting factor ( $\gamma > 0$ ) and

$$\tilde{u}(t) = K_{LQR} \tilde{x}(t) = [-K_I \quad K_0] \tilde{x}(t) \quad (2.102b)$$

It should be noted that, in order to have a usual sign convention ( $e = r - y$ ) in the outer loop of the augmented plant dynamics (Figure 2.16), output matrix-C has been assigned with a negative (-) sign convention in (2.102a).

After having implemented classical integral control method into optimal LQR control system dynamics, it is time to see the results in longitudinal flight dynamics. In optimal control system design procedure, nominal plant parameters, (2.83), has been used and corresponding  $K_{flt}$  gain value has been calculated from (2.101) as  $K_{flt} = 0.8664$ . Positive-definite weighting functions ( $Q$  and  $R$ ), which are going to minimize the cost function- $J$ , and  $\gamma$  parameter have been selected as

$$Q = \text{diag}([1 \quad 1 \quad 200 \quad 200 \quad 20 \quad 20]), R = 0.3800 \text{ and } \gamma = 10 \quad (2.103)$$

Using the chosen  $Q$ ,  $R$  and  $\gamma$  values, calculated  $K_{LQR}$  has been obtained with the help of `lqr` command in MATLAB<sup>®</sup> as

$$\begin{aligned} K &= [1.6222 \quad 6.7195 \quad 141.0039 \quad 711.8341 \quad 254.3036 \quad 894.9278] \\ K_I &= 1.6222 \\ K_{LQR} &= [6.7195 \quad 141.0039 \quad 711.8341 \quad 254.3036 \quad 894.9278] \end{aligned} \quad (2.104)$$

The last thing to do before getting into the time domain responses is to define the characteristics of observer (estimation) mechanism. As it is possible to see from (2.90), observer mechanism is included with a pole placement weighting matrix- $H$ , which is going to place the nominal plant poles to the desired places. It is desired to place poles of the estimation mechanism at

$$\text{eig}(\hat{G}(s)) = \begin{bmatrix} -15.0000 \\ -1.7925 + 1.1873i \\ -1.7925 - 1.1873i \\ -0.7070 + 0.7072i \\ -0.7070 - 0.7072i \end{bmatrix} \quad (2.105)$$

and corresponding pole placement gain ( $H$ ) is obtained as



damped modes of the nominal plant and to shape system dynamics efficiently. Disturbance rejection and signal tracking properties of controller are also significant.

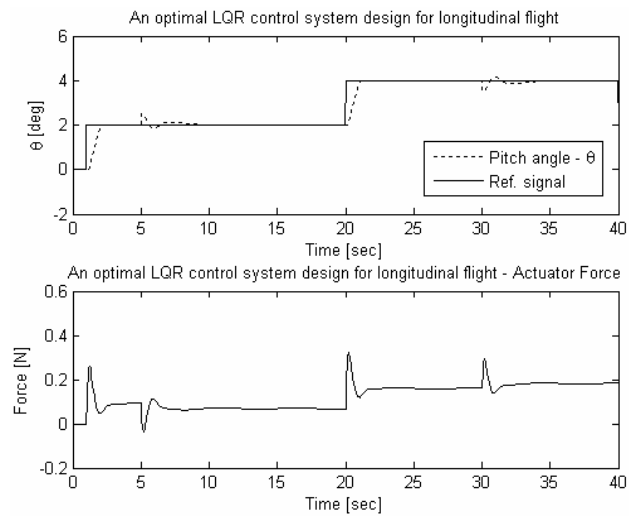


**Figure 2.18** Time domain response of augmented optimal LQR control system design.

## 2.5 Comparison of Automatic Control System Designs: Longitudinal Dynamics

After obtaining time domain responses of each automatic control system designs, it will be suitable to plot responses all together for comparison purposes (Figure 2.19).

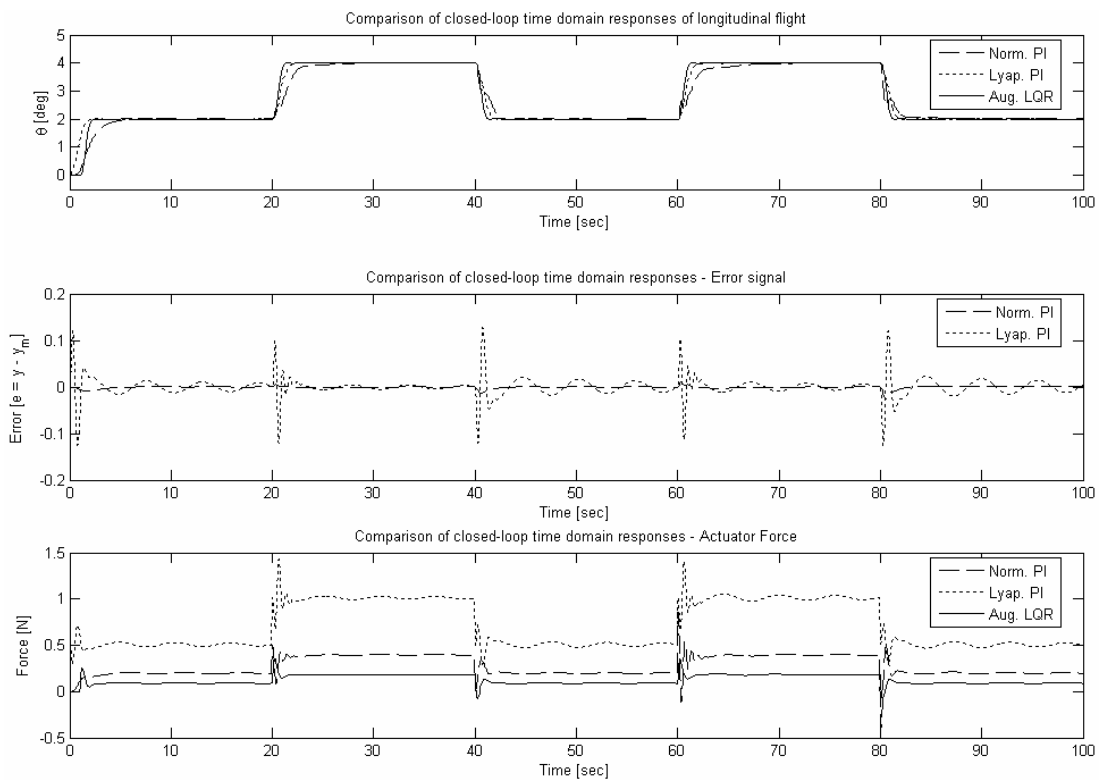


**Figure 2.19** Closed-loop time domain responses of designed automatic control systems: Comparison analysis.

Furthermore, it is possible to present performance characteristics of obtained controllers as given in Table 2.1.

<b>Table 2.1</b> Comparison of characteristic properties of designed controllers: Longitudinal dynamics					
	<b>RiseTime</b>	<b>PeakTime</b>	<b>SettlingTime</b>	<b>Max.Overshoot</b>	<b>Max.Actuator</b>
	[sec]	[sec]	[sec]	[%]	Force [N]
<b>Norm. PI Adj.</b>	5.5	7.6	10	1.86	0.2
<b>Lyap. PI Adj.</b>	-	1	2	2	1.5
<b>Aug. LQR.</b>	1.33	1.45	1.56	0.24	0.26

As it is possible to see from Table 2.1, best performance has been obtained with the augmented optimal LQR control system design together with the adaptive PI adjustment based on Lyapunov stability.

## CHAPTER 3

### 3. Lateral Dynamic Modeling

In this section of the thesis, lateral equations of motion will be summarized. In this part, state space approach has been preferred in dynamical modeling of lateral flight in order to have a convenient representation of EOMs for the automatic control system design part. In that sense, state space equations, which have been derived and used in this section of the thesis, have been taken from [2, 6]. By using the given representation, the lateral dynamic state space equations could be obtained easily and TFs could be derived straightforwardly.

#### 3.1 Equations of Motion (EOMs)

Using the fundamental state space representation as shown in (2.85), it is possible to construct the state-space form of the lateral flight model. For the lateral flight case, the matching state vector has been defined as

$$x = [\beta \quad p \quad r \quad \phi \quad \psi]^T \quad (3.1)$$

where  $\beta$  is the side slip angle,  $p$  is the roll rate,  $r$  is the yaw rate,  $\phi$  is the roll angle and  $\psi$  is the yaw angle. The input vector has been defined as

$$u = [\delta_a \quad \delta_r]^T \quad (3.2)$$

where  $\delta_a$  is the aileron input and  $\delta_r$  is the rudder input. For the lateral dynamic system, state matrix-A has been given as



$$A_{lat} = \begin{bmatrix} Y_v & 0 & -1 & \frac{g}{U_0} & 0 \\ L'_\beta & L'_p & L'_r & 0 & 0 \\ N'_\beta & N'_p & N'_r & 0 & 0 \\ 0 & 1 & 0 & 0 & 0 \\ 0 & 0 & 1 & 0 & 0 \end{bmatrix} \quad (3.3)$$

where primed stability derivatives are defined as

$$\begin{aligned} L'_\beta &= L_\beta + I_B N_\beta & N'_\beta &= N_\beta + I_A L_\beta \\ L'_p &= L_p + I_B N_p & N'_p &= N_p + I_A L_p \\ L'_r &= L_r + I_B N_r & N'_r &= N_r + I_A L_r \\ L'_{\delta_A} &= L_{\delta_A} + I_B N_{\delta_A} & N'_{\delta_A} &= N_{\delta_A} + I_A L_{\delta_A} \\ L'_{\delta_R} &= L_{\delta_R} + I_B N_{\delta_R} & N'_{\delta_R} &= N_{\delta_R} + I_A L_{\delta_R} \end{aligned} \quad (3.4)$$

$$\begin{aligned} I_A &\equiv I_{xz} / I_{xx} \\ I_B &\equiv I_{xz} / I_{zz} \end{aligned} \quad (3.5)$$

and the accompanying stability derivatives are given below, so that

$$Y_v = \frac{\rho U_0 S}{2m} C_{y\beta} \quad (3.6)$$

is side force coefficient with side slip motion,

$$L_\beta = \frac{\rho U_0^2 S b}{2I_{xx}} C_{l_\beta} \quad (3.7)$$

is rolling moment coefficient with a change in side slip angle,

$$\left( \text{where it should be noted that } L'_\beta = \frac{L_\beta + (I_{xz} / I_{xx}) N_\beta}{1 - ((I_{xz})^2 / I_{xx} I_{zz})} \right)$$

$$N_\beta = \frac{\rho U_0^2 S b}{2I_{zz}} C_{n_\beta} \quad (3.8)$$

is yawing moment coefficient with a change in side slip angle,

$$L_p = \frac{\rho U_0 S b^2}{4I_{xx}} C_{l_p} \quad (3.9)$$

is rolling moment coefficient with a change in rolling velocity,

$$N_p = \frac{\rho U_0 S b^2}{4I_{zz}} C_{n_p} \quad (3.10)$$

is yawing moment coefficient with a change in rolling velocity,

$$L_r = \frac{\rho U_0 S b^2}{4I_{xx}} C_{l_r} \quad (3.11)$$

is rolling moment coefficient with a change in yawing velocity,

$$N_r = \frac{\rho U_0 S b^2}{4I_{zz}} C_{n_r} \quad (3.12)$$

is yawing moment coefficient with a change in yawing velocity, where  $\rho$  is the air density,  $U_0$  is the speed,  $S$  is the reference area of wing surface,  $b$  is the wing span,  $I_{xx}$  is the moment of inertia around x,  $I_{xz}$  is the moment of inertia around xz and  $I_{zz}$  is the moment of inertia around z of the UAV.

Next, the control matrix-B could be shown as

$$B_{lat} = \begin{bmatrix} 0 & Y^*_{\delta_R} \\ L'_{\delta_A} & L'_{\delta_R} \\ N'_{\delta_A} & N'_{\delta_R} \\ 0 & 0 \\ 0 & 0 \end{bmatrix} \Rightarrow Y^*_{\delta_R} = Y_{\delta_R} / U_0 \quad (3.12)$$

where

$$Y_{\delta} = \frac{\rho U_0^2 S}{2m} C_{y_{\delta}} \quad (3.13)$$

is the side force control coefficient with rudder/aileron deflection,

$$L_{\delta} = \frac{\rho U_0^2 S b}{2I_{xx}} C_{l_{\delta}} \quad (3.14)$$

is the rolling moment control coefficient with rudder/aileron deflection,

$$N_{\delta} = \frac{\rho U_0^2 S b}{2I_{zz}} C_{n_{\delta}} \quad (3.15)$$

is the yawing moment control coefficient with rudder/aileron deflection. The output matrix-C can be presented as,

$$y = C_{lat} x \Rightarrow \begin{aligned} C_{\beta} &= [1 \ 0 \ 0 \ 0 \ 0] \\ C_p &= [0 \ 1 \ 0 \ 0 \ 0] \\ C_r &= [0 \ 0 \ 1 \ 0 \ 0] \\ C_{\phi} &= [0 \ 0 \ 0 \ 1 \ 0] \\ C_{\psi} &= [0 \ 0 \ 0 \ 0 \ 1] \end{aligned} \quad (3.16)$$

If all the given state space matrixes ( $A$ ,  $B$ ,  $C$  and  $D$ ) are going to be replaced in (2.85), the whole system representation is obtained as

$$\dot{x} = \begin{bmatrix} Y_v & 0 & -1 & \frac{g}{U_0} & 0 \\ L'_{\beta} & L'_p & L'_r & 0 & 0 \\ N'_{\beta} & N'_p & N'_r & 0 & 0 \\ 0 & 1 & 0 & 0 & 0 \\ 0 & 0 & 1 & 0 & 0 \end{bmatrix} \begin{bmatrix} \beta \\ p \\ r \\ \phi \\ \psi \end{bmatrix} + \begin{bmatrix} 0 & Y^*_{\delta_R} \\ L'_{\delta_A} & L'_{\delta_R} \\ N'_{\delta_A} & N'_{\delta_R} \\ 0 & 0 \\ 0 & 0 \end{bmatrix} \begin{bmatrix} \delta_a \\ \delta_r \end{bmatrix} \quad (3.17a)$$

$$y = \begin{bmatrix} 1 & 0 & 0 & 0 & 0 \\ 0 & 1 & 0 & 0 & 0 \\ 0 & 0 & 1 & 0 & 0 \\ 0 & 0 & 0 & 1 & 0 \\ 0 & 0 & 0 & 0 & 1 \end{bmatrix} \begin{bmatrix} \beta \\ p \\ r \\ \phi \\ \psi \end{bmatrix} \quad (3.17b)$$

Characteristic values with corresponding inputs were previously given in Table-1. Stability derivatives for lateral flight have been calculated and selected from [5] as,

<b>Table 3.1</b> Lateral stability derivatives and inputs of UAV.			
$C_{y_{\beta}} = -0.1829$	$C_{y_{\delta_r}} = 0.0158$	$C_{y_{\phi}} = 0.5765$	$C_{l_{\delta_a}} = 0.6000$
$C_{l_{\beta}} = -0.0450$	$C_{l_{\delta_r}} = 0.0131$	$C_{y_{\psi}} = 0.0000$	$C_{n_{\delta_a}} = -0.0100$
$C_{l_p} = -0.1200$	$C_{n_{\delta_r}} = -0.0800$	$C_{n_p} = -0.0710$	$I_{xx} = 0.0860$
$C_{l_r} = 0.1441$	$C_{y_{\delta_a}} = 0.0000$	$I_{zz} = 0.1806$	$I_{xz} = 0.0000$

but different than the longitudinal flight, it is assumed that in lateral flight the UAV is flying with the speed of 17m/s. Using the specified values in Table 1.1 and Table 2.1, it is possible to construct state space matrixes starting from state matrix-A (3.3),

$$A_{lat} = \begin{bmatrix} -0.1830 & 0 & -1.0000 & 0.5769 & 0 \\ -75.6611 & -10.0881 & 12.1165 & 0 & 0 \\ 0.8006 & -2.8416 & -0.1321 & 0 & 0 \\ 0 & 1.0000 & 0 & 0 & 0 \\ 0 & 0 & 1.0000 & 0 & 0 \end{bmatrix} \quad (3.18)$$

control matrix-B, using (3.12), is found as

$$B_{lat} = \begin{bmatrix} 0 & 0.0158 \\ 1008.8 & 22.026 \\ -8.0065 & -64.052 \\ 0 & 0 \\ 0 & 0 \end{bmatrix} \quad (3.19)$$

output matrix-C is gained as

$$C_{lat} = \begin{bmatrix} 1 & 0 & 0 & 0 & 0 \\ 0 & 1 & 0 & 0 & 0 \\ 0 & 0 & 1 & 0 & 0 \\ 0 & 0 & 0 & 1 & 0 \\ 0 & 0 & 0 & 0 & 1 \end{bmatrix} \quad (3.20)$$

and direct transmission matrix-D is attained as

$$D = 0 \quad (3.21)$$

From the calculated state space matrixes ( $A$ ,  $B$ ,  $C$  and  $D$ ), it is possible to obtain all necessary TFs,

$$\frac{\beta(s)}{\delta(s)}, \frac{p(s)}{\delta(s)}, \frac{r(s)}{\delta(s)}, \frac{\phi(s)}{\delta(s)}, \frac{\psi(s)}{\delta(s)}$$

for given  $\delta_{aileron}$  and  $\delta_{rudder}$  inputs, respectively. But before obtaining the corresponding TFs, the eigenvalues of state matrix-A should be analyzed and the

poles of the open loop system should be investigated. Using Matlab command `eig` it is possible to obtain the poles of the system such as,

$$\begin{aligned}
 p_1 &= 0.0000 \\
 p_2 &= -9.4057 \\
 p_3 &= -0.4985 + 5.3667 i \\
 p_4 &= -0.4985 - 5.3667 i \\
 p_5 &= -0.0006
 \end{aligned} \tag{3.22}$$

It should be noticed that the open loop system is stable but has a pole lying at the origin (0,0), which makes the system a marginally stable one. Such system with a pole on the origin (0,0), could easily be detonated and become unstable with a little disturbance. In order to prevent any instability and to suppress the effects of “zero type system”, automatic controller with good disturbance rejection will be required.

If the poles of the UAV are going to be named according to the modes of lateral flight, it should be found

$$\begin{aligned}
 s_{Dutch\ Roll_1} &= -0.4985 + 5.3667 i \\
 s_{Dutch\ Roll_2} &= -0.4985 - 5.3667 i \\
 s_{roll} &= -9.4057 \\
 s_{spiral} &= -0.0006
 \end{aligned} \tag{3.23}$$

In analysis of lateral dynamic model of UAV, three degree of freedom assumption will be acknowledged, which yields to a characteristic equation (CE) representation such as

$$(s^2 + 2\zeta_{DR}\omega_{n_{DR}}s + \omega_{n_{DR}}^2)\left(s + \frac{1}{\tau_r}\right)\left(s + \frac{1}{\tau_s}\right) = 0 \tag{3.24}$$

By using the representation in (3.24), the CE equation of the three-degree of freedom system could be constructed as the followings,

$$(s^2 + 0.9969s + 29.0504)(s + 9.4057)(s + 0.0006) = 0 \tag{3.25}$$

where

$$CE_{DutchRoll} = (s^2 + 0.9969s + 29.0504) = 0 \quad (3.26)$$

symbolizes the CE of the Dutch Roll Mode (DRM) of the UAV. The corresponding natural frequency ( $\omega_{n_{DR}}$ ), damping frequency ( $\omega_{D_{DR}}$ ) and damping ratio ( $\zeta_{DR}$ ) of the DRM are established as

$$\begin{aligned} \omega_{n_{DR}} &= 5.3898 \text{ rad / sec} \\ \zeta_{DR} &= 0.0925 \\ \omega_{D_{DR}} &= \omega_{n_{DR}} \sqrt{1 - \zeta_{DR}^2} = 5.1346 \text{ rad / sec} \end{aligned} \quad (3.27)$$

From (3.27), it is probable to see that the DRM of the UAV has an oscillatory behaviour with relatively small periods as

$$T_{DRM} = \frac{2\pi}{\omega_{n_{DR}}} = 1.1657 \text{ sec} \quad (3.28)$$

As a characteristic property signifying the performance of the UAV, time constants for roll ( $\tau_{roll}$ ) and spiral modes ( $\tau_{spiral}$ ) could be offered. If the time constants of both roll and spiral modes are calculated, it is possible to find the final values such as

$$\tau_{spiral} = \frac{1}{0.0002} = 1666.7 \text{ sec} \quad (3.29)$$

$$\tau_{roll} = \frac{1}{8.9677} = 0.1855 \text{ sec} \quad (3.30)$$

Additionally, in DRM

$$\frac{\phi(s)}{\delta(s)} \frac{\delta(s)}{\beta(s)} = \frac{\phi(s)}{\beta(s)} \quad (3.31)$$

ratio can tell if the DRM is composed of mostly yawing motion, mostly rolling motion or approximately equal contribution of each [8]. Via (3.31), the ratio could be calculated as

$$\frac{\phi(s)}{\beta(s)} = \left( \frac{C_{l_\beta} I_{zz}}{C_{n_\beta} I_{xx} \rho U_0} \right) = 4.5378 \quad (3.32)$$

From (3.32), it is possible to witness that the  $\phi(s)/\beta(s)$  ratio is higher than 1, which leads to a rolly Dutch Roll Mode characteristic and is generally because of a high degree of lateral stability [8].

After such analyses, it is time to get into time responses of the open loop system. But just before that, it is also possible to construct the TFs for each control surface (aileron/rudder) deflection.

Using MATLAB<sup>®</sup> and `ss2tf` command, one is able to obtain all the TFs for aileron deflection as,

$$\frac{\beta(s)}{\delta_a(s)} = \frac{-1.421 \times 10^{-14} s^4 + 8.006 s^3 + 3529 s^2 + 20.92 s}{s^5 + 10.4 s^4 + 38.43 s^3 + 273.3 s^2 + 0.1698 s} \quad (3.33)$$

$$\frac{p(s)}{\delta_a(s)} = \frac{1009 s^4 + 220.9 s^3 + 208.6 s^2 + 3.345 \times 10^{-13} s}{s^5 + 10.4 s^4 + 38.43 s^3 + 273.3 s^2 + 0.1698 s} \quad (3.34)$$

$$\frac{r(s)}{\delta_a(s)} = \frac{-8.006 s^4 - 2949 s^3 - 539.4 s^2 + 116.5 s}{s^5 + 10.4 s^4 + 38.43 s^3 + 273.3 s^2 + 0.1698 s} \quad (3.35)$$

$$\frac{\phi(s)}{\delta_a(s)} = \frac{-1.599 \times 10^{-14} s^4 + 1009 s^3 + 220.9 s^2 + 208.6 s}{s^5 + 10.4 s^4 + 38.43 s^3 + 273.3 s^2 + 0.1698 s} \quad (3.36)$$

$$\frac{\psi(s)}{\delta_a(s)} = \frac{-1.776 \times 10^{-14} s^4 - 8.006 s^3 - 2949 s^2 - 539.4 s + 116.5}{s^5 + 10.4 s^4 + 38.43 s^3 + 273.3 s^2 + 0.1698 s} \quad (3.37)$$

and the TFs for rudder deflection are gained as

$$\frac{\beta(s)}{\delta_r(s)} = \frac{0.01581 s^4 + 64.21 s^3 + 722 s^2 - 446 s}{s^5 + 10.4 s^4 + 38.43 s^3 + 273.3 s^2 + 0.1698 s} \quad (3.38)$$

$$\frac{p(s)}{\delta_r(s)} = \frac{22.03 s^4 - 770.3 s^3 - 4970 s^2 - 1.183 \times 10^{-12} s}{s^5 + 10.4 s^4 + 38.43 s^3 + 273.3 s^2 + 0.1698 s} \quad (3.39)$$

$$\frac{r(s)}{\delta_r(s)} = \frac{-64.05 s^4 - 720.5 s^3 - 126.2 s^2 - 2786 s}{s^5 + 10.4 s^4 + 38.43 s^3 + 273.3 s^2 + 0.1698 s} \quad (3.40)$$

$$\frac{\phi(s)}{\delta_r(s)} = \frac{8.882 \times 10^{-15} s^4 + 22.03 s^3 - 770.3 s^2 - 4970 s}{s^5 + 10.4 s^4 + 38.43 s^3 + 273.3 s^2 + 0.1698 s} \quad (3.41)$$

$$\frac{\psi(s)}{\delta_r(s)} = \frac{1.599 \times 10^{-14} s^4 - 64.05 s^3 - 720.5 s^2 - 126.2 s - 2786}{s^5 + 10.4 s^4 + 38.43 s^3 + 273.3 s^2 + 0.1698 s} \quad (3.42)$$

From both TF sets, it is likely to see that in the numerator part, there are zeros at the origin (0,0), which might be cancelled with the poles at the origin (0,0) in the denominator part. Due to the fact that, the cancellation of poles and zeros will reduce the order of the system and will lead to a significant change in the characteristic of the system; the elimination hasn't been done here and the obtained TFs have been used.

If the corresponding time domain step response graphs of the found TFs are plotted, they should be obtained as shown in Figure 3.1.

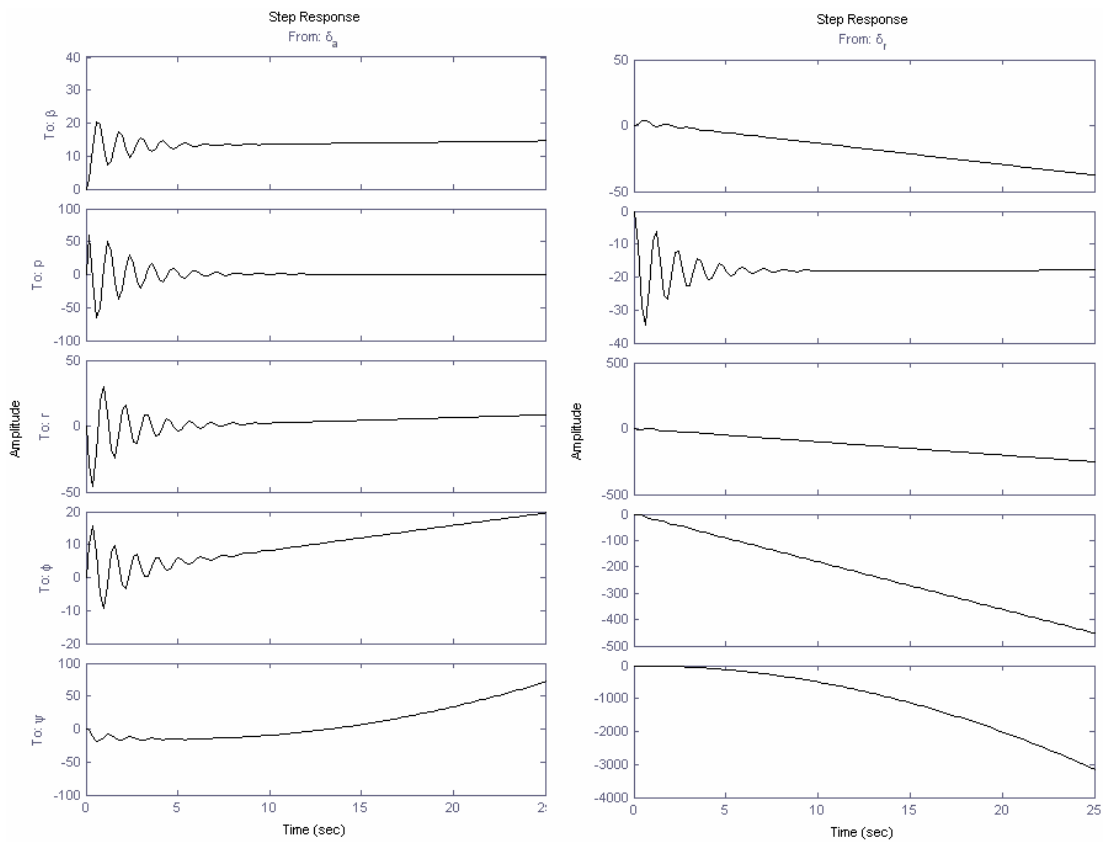


**Figure 3.1** Open-loop time domain step responses for a given deflection.

From time domain step responses, it is likely to observe that the poles at the origin are causing oscillatory, lightly damped (under-damped) and unstable behaviours in several cases. As it is also probable to witness from the open loop time domain responses, the flight control system needs an efficiently weighted control system, which can also verify the robustness of the system. As a result of this need, an adaptive control system based on Lyapunov stability and an augmented optimal LQR control system will be designed and applied to the lateral flight dynamics,



respectively. The results will also be investigated and compared in the following sections.

### **3.2 Model-Reference Adaptive Control System Design for the Lateral Dynamics of the UAV**

In the previous chapter, where longitudinal flight dynamics have been discussed, both MIT rule and Lyapunov stability approaches have been implemented on longitudinal flight dynamics. Considering the fact that the lateral flight system is a Multi-Input-Multi-Output (MIMO) system, which has two inputs and five outputs, and the longitudinal flight is a Single-Input-Single-Output (SISO) system, which has only one input and one output; in this section MIT rule will not be taken into account because of weak controllability effect in high order and complex systems (which is also the case in lateral flight dynamics). Therefore, only (more robust) adaptive control system approach based on Lyapunov stability theory, will be implemented on lateral flight dynamics.

#### **3.2.1 MRAS Design based on Lyapunov stability**

In this part of the thesis, adaptation rules based on Lyapunov stability theory will be derived.

The mathematical background of Lyapunov stability theory was simply and briefly discussed previously in section 2.3.2; therefore, here only the derivation of adaptation rules and adjustment parameters will be given.

For the lateral flight dynamics, the same candidate Lyapunov function that has been formerly used in longitudinal dynamics has been suggested as shown in (2.78).

$$V(x) = e^T P e + Tr[(A - BL - A_m)^T N (A - BL - A_m)] \quad (3.43)$$

From earlier calculations in (2.80), it is known that the time derivative of error function has been derived as

$$\dot{e} = A_m e - B \Delta L y \quad (3.44)$$

It is possible to construct the derivative of given Lyapunov function as in (2.81).

$$\dot{V}(x) = e^T \underbrace{(A_m^T P + P A_m)}_{-Q} e - 2y^T \Delta L^T B^T P e + 2Tr[(B \Delta L)^T N(B \Delta \dot{L})]$$

$$\dot{V}(x) = -e^T Q e - 2y^T \Delta L^T B^T P e + 2Tr(\Delta L^T \overbrace{(B^T N B)}^T \Delta \dot{L}) \quad (3.45)$$

$$\dot{V}(x) = -e^T Q e - 2y^T \Delta L^T B^T P e + 2Tr[\Delta L^T T \Delta \dot{L}]$$

$$\dot{V}(x) = -e^T Q e + 2Tr[-\Delta L^T B^T P e y^T + \Delta L^T T \Delta \dot{L}]$$

where  $A_m^T P + P A_m = -Q$ . From here, in order to guarantee that  $V(x)$  will always be  $\dot{V}(x) < 0$ , condition  $\Delta L^T (-B^T P e y^T + T \Delta \dot{L}) = 0$  should be satisfied. Next step will be to conduct some dimension analysis in order to obtain the size of  $L$ . If nominal plant (no servo mechanism included) state matrix-A is taken into account from (3.18), it is easy to see that the system has 5 states (5x5). If servo mechanism's TFs of aileron and rudder actuators are considered, then the system will be consisted of 7 states (7x7), where also the newly shaped output matrix-B will have 7 states (7x2) as well. In order to have compatibility in terms of matrix dimensions in (3.43), parameter adjustment feedback gain-L should be constructed in dimensions of (2x7), leading to

$$L = \begin{bmatrix} L_{11} & L_{12} & L_{13} & L_{14} & L_{15} & L_{16} & L_{17} \\ L_{21} & L_{22} & L_{23} & L_{24} & L_{25} & L_{26} & L_{27} \end{bmatrix}_{(2 \times 7)} \quad (3.46)$$

Afterwards, if necessary calculations are conducted in  $\Delta L^T (-B^T P e y^T + T \Delta \dot{L}) = 0$ , the elements of parameter adjustment matrix-L are going to be obtained as given in (3.47).

$$Tr[-\Delta L^T B^T P e y^T + \Delta L^T T \Delta \dot{L}] = 0 \Rightarrow \Delta L^T (-B^T P e y^T + T \Delta \dot{L}) = 0$$

$$-B^T P e y^T + T \Delta \dot{L} = 0 \Rightarrow T \Delta \dot{L} = B^T P e y^T$$

$$\Delta \dot{L} = T^{-1} B^T P e y^T = (B^T N B)^{-1} B^T P e y^T \quad (3.47)$$

$$L = L^* + \Delta L \Rightarrow \dot{L} = \Delta \dot{L}$$

$$\Delta \dot{L} = \dot{L} = T^{-1} B^T P e y^T = (B^T N B)^{-1} B^T P e y^T$$

Before getting into the time domain analysis of closed-loop system response, MATLAB<sup>®</sup> Simulink block diagram has been constructed (Figure 3.2) for MRAS design based on Lyapunov stability adjustment control algorithm.

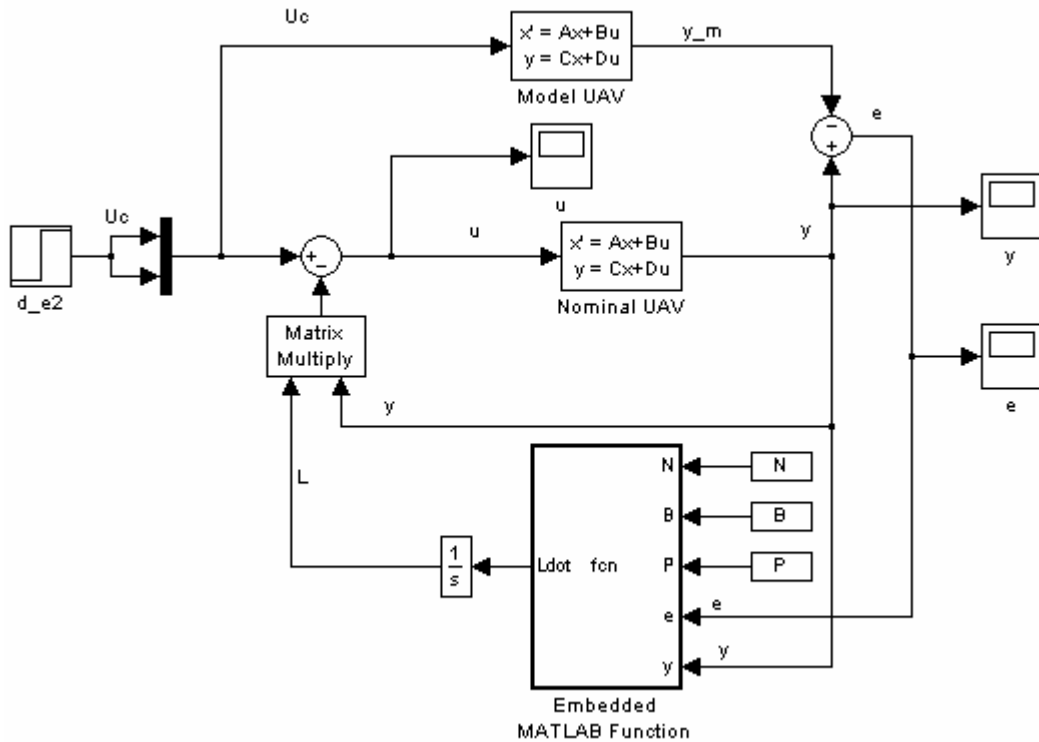


**Figure 3.2** Simulink block diagram of MRAS based on Lyapunov stability.

It should be noted that in lateral control system design process, instead of PI adjustment, only Lyapunov stability based control rules have been implemented into system dynamics. Following to that, if time domain responses of MRAS control design based on Lyapunov stability are plotted, they should be obtained as given in Figure 3.3.

As it is possible to see from Figure 3.3, perfect matching conditions have been satisfied and the nominal plant has been adapted with respect to the reference-model in a remarkable way. From error signal plot, it is also possible to see that the error signal is being diminished within 2 second and the nominal plant is behaving such as reference-model when  $t \rightarrow \infty$ . From Figure 3.3 it is possible to see that the time domain behaviours of MRAS design based on Lyapunov stability are remarkable so that the settling time is nearly 1.5 seconds and the maximum actuator signal is obtained as 1 Newton. Also the change of error signal could be easily observed from the second plot in Figure 3.3. Evolution of adjustment parameter-L has been plotted and could be investigated in Appendix-A. Also the code of Embedded Matlab Function has been given in Appendix-B.

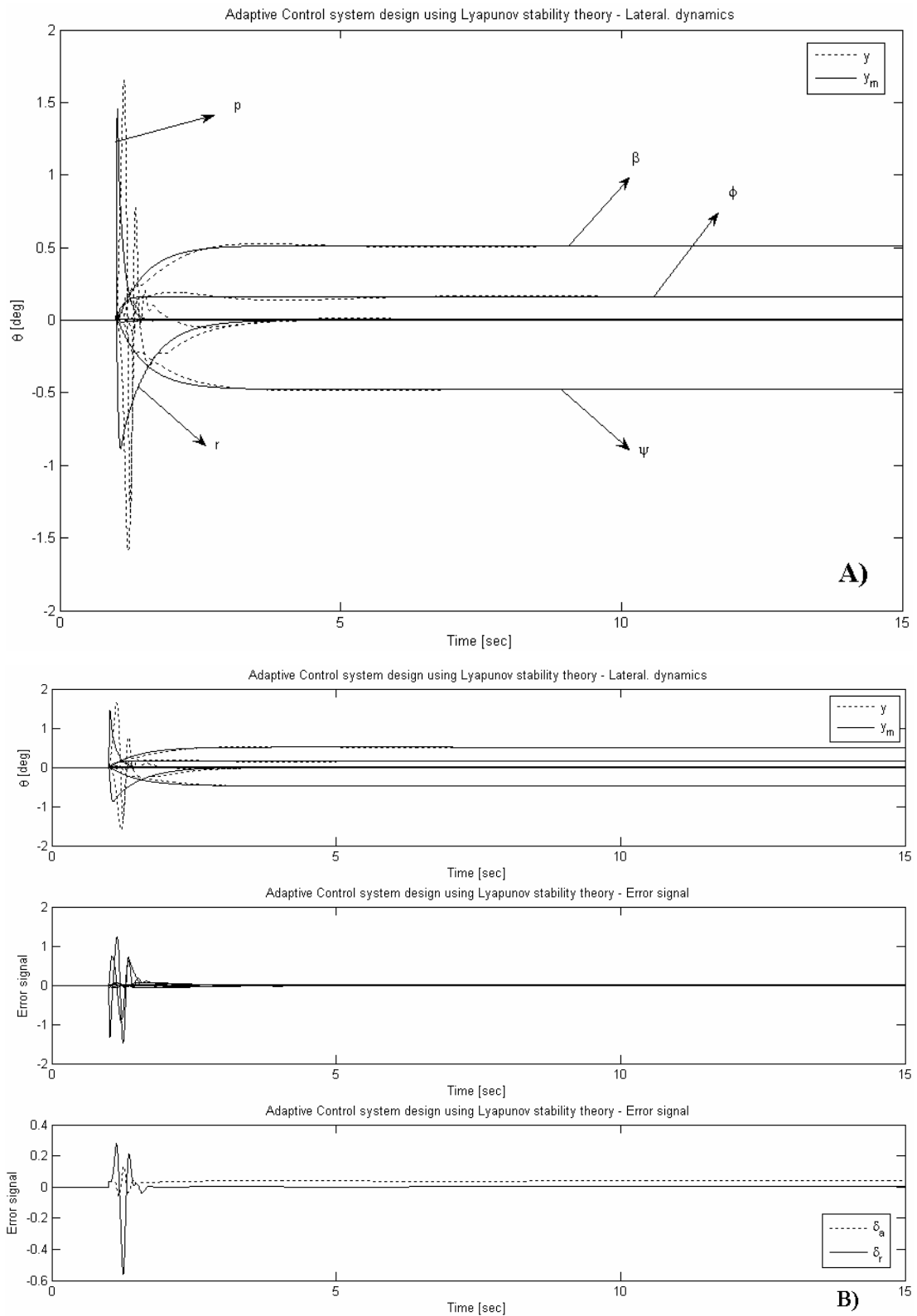


**Figure 3.3** Closed-loop time domain responses (A-B) of model-reference adaptive control system design: Based on Lyapunov stability.

### 3.3 Optimal LQR Control System Design: Lateral Dynamics

In this part of the thesis, optimal LQR control system design will be implemented on lateral dynamics of the UAV.

#### 3.3.1 Observability and controllability of system dynamics: Lateral flight

Observability matrix of a system has been previously defined in (2.83) as  $Obs = O_n = [C \ CA \ CA^2 \dots \ CA^{n-1}]^T$  and the system had been called observable if  $Rank(O_n) = n$  is satisfied. Using state matrix-A from (3.18) and identity output matrix-C from (3.20), it is possible to construct the observability matrix. It is calculated and given in Appendix-A, where the rank of the observability matrix is five and equal to the states of the nominal plant showing that the system is fully observable. As a confirmation, it is also possible to calculate unobservable states from (2.89) as  $UnOb = Length(A_{n \times n}) - Rank(O_n) = 5 - 5 = 0$  which simply states that there are no unobservable states (i.e. all of the states could be observed). Thus, it is feasible to verify that an observer mechanism can be used in estimation of the states of open-loop dynamics in lateral flight, as well. Additionally, controllability of the system dynamics should be verified as well, so that there will be no theoretical obstacle to get into the optimal control system design process. It is known from (2.91) that controllability matrix of a system is defined as  $C_t = [B \ AB \ A^2B \dots \ A^{n-1}B]$  and it must satisfy  $Rank(C_t) = n$  condition. Using state matrix-A from (3.18) and input (control) matrix-B from (3.19), controllability matrix is obtained as shown in Appendix-A, where the rank of the system is calculated as  $Rank(C_t) = 5 = n$  leading to a fully controllable system dynamics.

With such observability and controllability analyses, it has been proved that the lateral UAV system is both controllable and observable, which grants the opportunity to use an observer (estimation) mechanism in control system design process.

#### 3.3.2 Optimal LQR control system design: Classical approach

In this section of the thesis, an optimal LQR control system design with an observer (estimation) mechanism will be presented and subsequently will be implemented on lateral flight dynamics of the UAV.

Here, unfortunately augmented optimal LQR control technique based on integral control cannot be applied to lateral dynamics, because it is not possible to apply integral control action to a plant that has a zero at the origin [17], which is unfortunately the case in our lateral system dynamics. Therefore only a single optimal LQR control loop will be implemented on the lateral flight dynamics together with an observer (estimation) algorithm.

As a first step before getting into the time domain responses of closed loop system, the characteristics of observer (estimation) mechanism have been defined. As it is possible to see from (2.90), observer mechanism has been constructed with a pole placement weighting matrix- $H$  which is going to place the nominal plant poles to the desired places and estimate plant parameters. It is desired to place poles of the estimation mechanism at

$$eig(\hat{G}(s)) = \begin{bmatrix} -2 \\ -15 \\ -3.7729 + 3.8491i \\ -3.7729 - 3.8491i \\ -0.6 \\ -15.0000 \\ -15.0000 \end{bmatrix} \quad (3.48)$$

and corresponding pole placement gain - $H$  is obtained as

$$H = \begin{bmatrix} 3.5899 & -3.8491 & -1 & 0.57688 & 0 & 0 & 0.061232 \\ -71.812 & -6.3152 & 12.117 & 0 & 0 & 3907.1 & 85.305 \\ 0.80065 & -2.8416 & 1.8679 & 0 & 0 & -31.009 & -248.07 \\ 0 & 1 & 0 & 15 & 0 & 0 & 0 \\ 0 & 0 & 1 & 0 & 0.6 & 0 & 0 \\ 0 & 0 & 0 & 0 & 0 & 0 & 0 \\ 0 & 0 & 0 & 0 & 0 & 0 & 0 \end{bmatrix} \quad (3.49)$$

Positive-definite weighting functions ( $Q$  and  $R$ ), which are going to minimize the cost function- $J$  have been selected as

$$Q = \text{diag}([20 \ 20 \ 80 \ 135 \ 30 \ 10 \ 30]), \quad R = \text{diag}([1.15 \ 1.50]) \quad (3.50)$$

Using the chosen Q and R values, calculated  $K_{LQR}$  has been obtained with the help of `lqr` command in MATLAB<sup>®</sup> as

$$K_{lat\_LQR} = \begin{bmatrix} 0.0108 & 4.0024 & -0.2693 & 11.1900 & 0.9857 & 86.1137 & 2.7624 \\ 0.9985 & 0.1160 & -7.3695 & -0.4777 & -4.3881 & 2.1179 & 27.4056 \end{bmatrix} \quad (3.51)$$

After every parameter of control system has been found, Simulink block diagram of optimal LQR control system design has been suggested as shown in Figure 3.4.

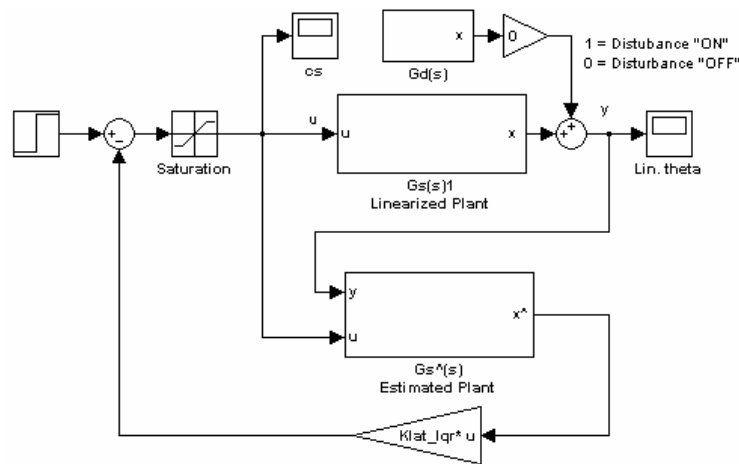


**Figure 3.4** Simulink block diagram of optimal LQR control system design.

where estimation algorithm's Simulink block diagram has been constructed as formerly shown in Figure 2.17. And now, it is time to see the closed-loop time domain results of optimal LQR control system design, and obtained results have been presented in Figure 3.5.

As it could be seen from Figure 3.5, closed-loop time domain results of optimal LQR control system design are considerable, where the settling time is approximately 7 seconds and the maximum actuator force is 1 Newton with acting time of ~0.5 seconds. It should be noted that during the construction of system dynamics, it has been considered for the lateral system dynamics that the maximum actuator force should be 1 [N] and will be limited with 1 [N], thus saturation has been used in the block diagram in the feed-forward path. Also is it likely to see that, without any (lead/lag) compensation in the nominal plant, the control system is able to suppress the frequent and sustained oscillations in nominal plant and is able to shape system dynamics efficiently.

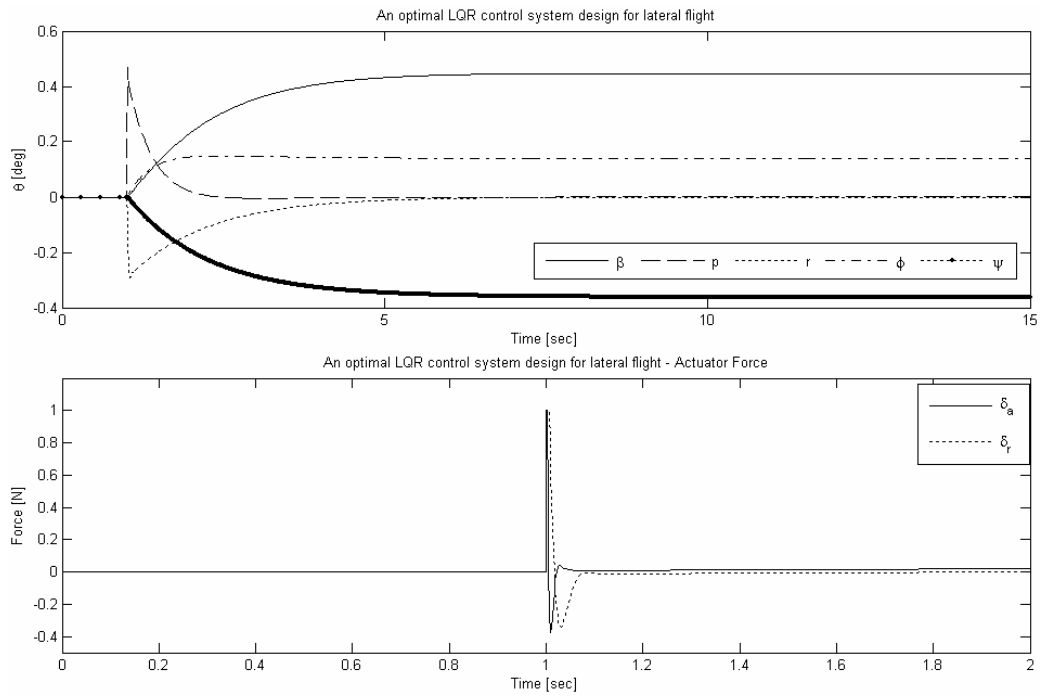


**Figure 3.5** Time domain response of optimal LQR control system design.

### 3.4 Comparison of Automatic Control System Designs: Lateral Dynamics

After obtaining the time domain responses of each automatic control system designs, it will be convenient to plot the closed-loop responses all together for comparison purposes (Figure 3.6).

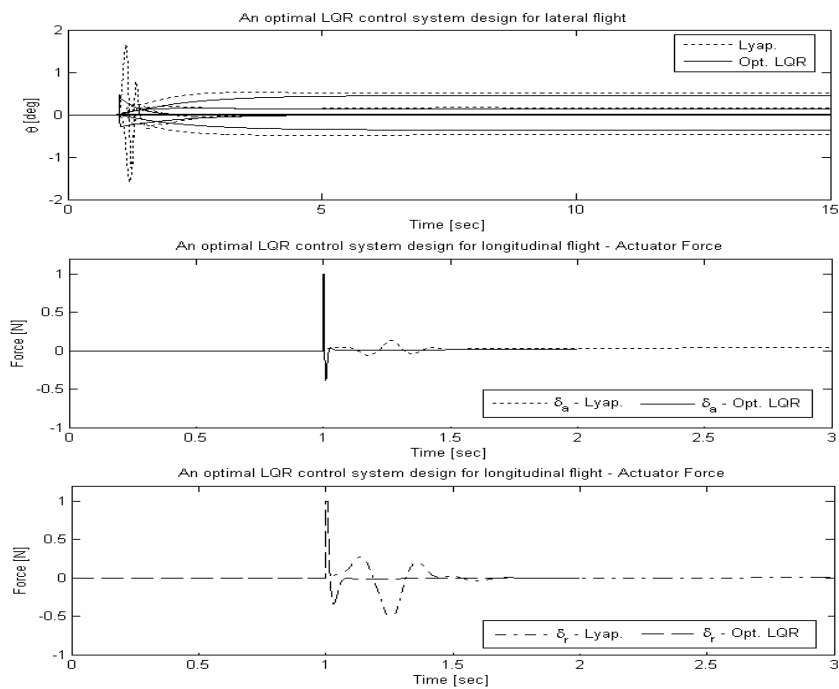


**Figure 3.6** Closed-loop time domain responses of designed automatic control systems: Comparison analysis.



Furthermore, it is possible to present performance characteristics of obtained controller as given in Table 3.1.

	<b>SettlingTime [sec]</b>	<b>Max.Actuator Force [N]</b>
<b>MRAS Lyapunov</b>	2	1
<b>Optimal LQR</b>	5	1

As it is possible to see from Table 3.1, best performance has been obtained with the MRAS design based on Lyapunov stability theory.

## **CHAPTER 4**

### **4.1 CONCLUSIONS AND DISCUSSIONS**

In the thesis, mainly, dynamical modeling of an UAV and subsequently automatic control system designs has been discussed widely.

After a short introduction in the first chapter, in the second chapter longitudinal dynamic model of the UAV has been constructed. It has been obtained from the open loop longitudinal dynamic model that the system has very close poles to the origin leading to highly oscillating behaviours. In order to suppress those oscillatory effects in open-loop dynamics two automatic control system design approaches have been implemented on longitudinal flight dynamics of the UAV: Model Reference Adaptive Control System PI Adjustment design based on MIT Rule and based on Lyapunov Stability together with Augmented Optimal LQR Control approach. Obtained time domain results of designed controllers are stating that PI adjustment based on MIT rule is not able to guarantee stability in closed-loop dynamics, but PI adjustment based on Lyapunov stability is capable of guaranteeing the stability. Moreover, the results of augmented optimal LQR control system design are stating that augmentation of open loop system dynamics is introducing robustness into the system dynamics, and therefore suppression of disturbances and tracking of reference signal is relatively better than the other approaches.

In the third chapter, lateral dynamic model of the UAV using state space approach has been obtained. Dutch roll, roll and spiral modes have been investigated and as a result of weak open loop performance, firstly, automatic control system based on adaptive PI adjustment rule based on Lyapunov stability has been introduced. It has been witnessed that the Lyapunov stability approach is able to compensate all the outputs and obtain relatively remarkable performance in time domain. In order to suppress high coupling effect and reduce the uncertainties in the system, an augmented optimal LQR control system design was supposed to be implemented on

system dynamics but because of the lateral flight dynamics were including a zero at the origin, Integral control approach couldn't be applied as a result of theoretical limitations. Thus, classical optimal LQR control approach has been introduced into the lateral dynamics, but it has been seen that it was not able to shape the open-loop system dynamics as much as adaptive control system design based on Lyapunov stability could do.

Some of the obtained results from the thesis have been published in 9<sup>th</sup> International WSEAS Conference on Automatic Control, Modeling and Simulation, May 27-29, 2007, Istanbul, Turkey.

## REFERENCES

- [1] **Ryan, A., Zennaro, M., Howell, A., Sengupta, R. and Hedrick, J. K.**, 2004.43<sup>rd</sup> IEEE Conference on Decision and Control December 14-17, 2004, Atlantis, Paradise Island, Bahamas.
- [2] **McLean D., 1990.** Automatic Flight Control Systems, Prentice Hall.
- [3] **Gyroscopes**, Wikipedia, 2006. Online: <http://en.wikipedia.org/wiki/Gyroscope>.
- [4] **Wiesel, W., 1989.** Spaceflight Dynamics, Wiley.
- [5] **Blakelock, J. H., 1991.** Automatic Control of Aircraft and Missiles, Wiley.
- [6] **Turkoglu, K. , 2006.** Investigation the modes of Hezarfen UAV and automatic control systems design, *BSc Thesis*, İTÜ Uçak-Uzay Bilimleri Fakültesi, Istanbul.
- [7] **Stevens B. and Lewis F. L., 2003.** Aircraft Control and Simulation, Wiley.
- [8] **Yechout, T. R., 2003.** Introduction to Aircraft Flight Mechanics, AIAA Education Series.
- [9] **Etkin, B., 1972.** Dynamics of Atmospheric Flight, Wiley.
- [10] **Astrom, K. J. and Wittenmark, B., 1995.** Adaptive control, Second Edition, Adisson Wesley.
- [11] **Krstic, M., Kanellakopoulos, P. and Kokotovic, P., 1995.** Nonlinear Adaptive Control Theory, Kannellakopoulos, Kokotovic.
- [12] **Morari, M., Schaufelberger, W., Glattfelder, A, Christophersen, F.J. and Geyer, T., 2005.** Analyse und Drehzahlregelung einer flexiblen Welle (LQR Control of a Flexible Shaft), Institut für Automatik Fachpraktikumsversuch-IfA 3.1 (Automatic Control Laboratory)-Experiment 3.1, ETH Zuerich (Swiss Federal Institute of Technology) IfA internal report, Switzerland.

- [13] **Ogata, K.**, 1997 Modern Control Engineering, Third Ed., Prentice Hall, pp.613-614.
- [14] **Vidyasagar, M.**,1993, Nonlinear Systems Analysis, 2nd ed. Upper Saddle River, NJ: Prentice-Hall.
- [15] **Cheok, K. C.**, 2007. Lyapunov method for model reference adaptive systems, Adaptive control systems lecture notes, Oakland University, Rochester, MI, USA.
- [16] **Franklin, G.F, Powell, J. D. and Emami-Naeini A.**, Feedback Control of Dynamic Systems, Addison Wesley,Third Edition, 1994, pp.551-552.
- [17] **Franklin, G.F, Powell, J. D. and Emami-Naeini A.**, Feedback Control of Dynamic Systems, Addison Wesley,Third Edition, 1994, pp.556.
- [18] **Keiviczky, T. and Balas, G.J.**, 2006. Software-enabled receding horizon control for autonomous unmanned aerial vehicle guidance, Journal of Guidance Control and Dynamics, Vol. 29, No. 3, pp.680-694.
- [19] **Richards, A. and How, J.P.**, 2006. Robust variable horizon model predictive control for vehicle maneuvering, International Journal of Robust and Non-Linear Control, Vol.16, No.7, pp.333-351.
- [20] **Khantsis, S. and Bourmistrova, A.**, 2005. UAV controller design using evolutionary algorithms, Advances in Artificial Intelligence Lecture Notes in Artificial Intelligence, No.3809, pp.1025-1030.
- [21] **Mokhtari A., M'Sirdi N.K., Meghriche K. and Belaidi A.**, 2006. Feedback linearization and linear observer for a quadrotor unmanned aerial vehicle, Advanced Robotics, Vol.20, No.1, pp.71-91.
- [22] **Li, W. and Cassandras, C.G.**, 2006. A cooperative receding horizon controller for multivehicle uncertain environments, IEEE Transactions on Automatic Control, Vol.51, No.2, pp.242-257.
- [23] **Fradkov, A. and Andrievsky, B.**, 2005. Combined adaptive controller for UAV guidance, European Journal of Control, Vol.11, No.1, pp.71-79.
- [24] **Kim, M.S. and Chung, C.S.**, 2006. The robust flight control of an UAV using MIMO QFT: GA-based automatic loop-shaping method, Systems Modeling and Simulation: Theory and Applications Lecture Notes in Computer Science, No.3398, pp.467-477.
- [25] **Singh, S.N., Zhang, R., Chandler, P. and Banda, S.**, 2003. Decentralized nonlinear robust control of UAVs in close formation, International

Journal of Robust and Non-Linear Control, Vol.13, No.11, pp.1057-1078.

- [26] **Lombaerts, T.J.J., Mulder, J.A., Voorluijs, G.M. and Decuyper, R.**, 2005. Design of a robust flight control system for a mini-UAV, AIAA Guidance, Navigation, and Control Conference, Vol.7, pp.5608-5626.
- [27] **Chen, X. and Pan, C.**, 2006. Application of H infinity control and inverse dynamic system in direct side force control of UAV, Journal of Nanjing University of Aeronautics and Astronautics, Vol.38, No.1, pp.33-36.
- [28] **Sadraey, M. and Colgren, R.**, 2005. Two DOF robust nonlinear autopilot design for a small UAV using a combination of dynamic inversion and H varies directly as loop shaping, AIAA Guidance, Navigation, and Control Conference, pp.5518-5538.
- [29] **Gurleyen, F.**, 2006. Reduced Order Dynamics Assignment for State Feedback Control and State Estimation Design by SVD of the Projections, SICE-ICASE International Joint Conference 2006, pp.1750-1757.
- [30] **Gurleyen, F. et al.**, 2006. Eyleyici arızaları ve parametre belirsizlikleri içeren uçuş kontrol sistemlerinin model referans uyarlamalı kontrol yaklaşımı ile durum izleme kontrolü, I. ULUSAL HAVACILIK VE UZAY KONFERANSI, UHUK-2006-069.
- [31] **Gurleyen, F.**, 2006. Adaptive control systems, Lecture notes, Istanbul Technical University, Istanbul, Turkey.
- [32] **Sun, Y. and Tilbury, D.**, 1996. Function rscale: Finding the scale factor to eliminate the steady-state error in system dynamics. Control tutorials for Matlab, University of Michigan, Ann Arbor, USA. <http://www.engin.umich.edu/group/ctm/extras/rscale.html>

**APPENDIX-A**

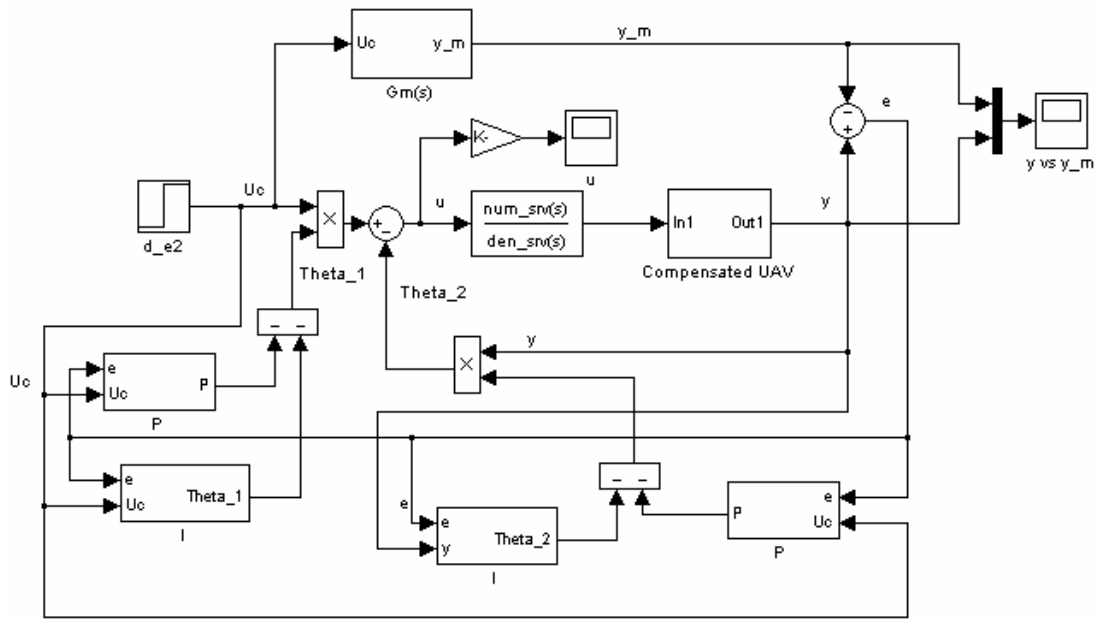


**Figure-A1** Simulink block diagram of PI adjustment algorithm based on normalized MIT rule.

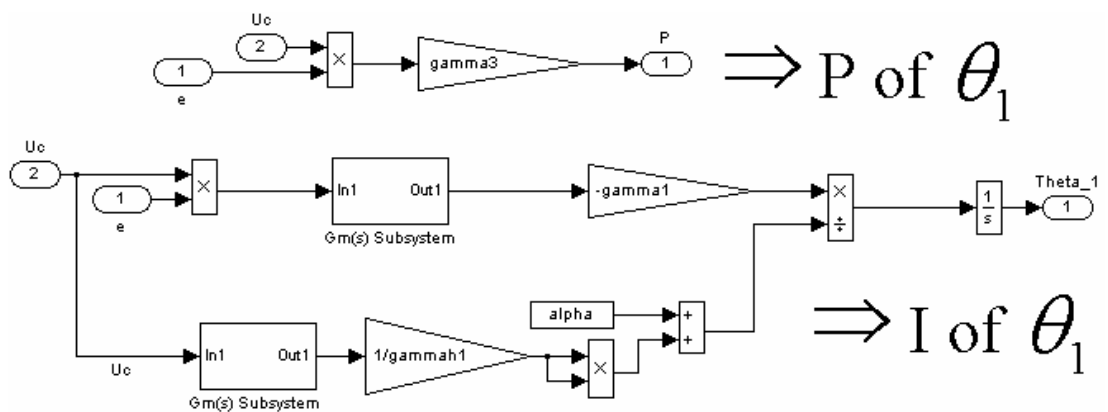


**Figure-A2** Simulink block diagram of adjustment parameter- $\theta_1$  based on normalized MIT rule.

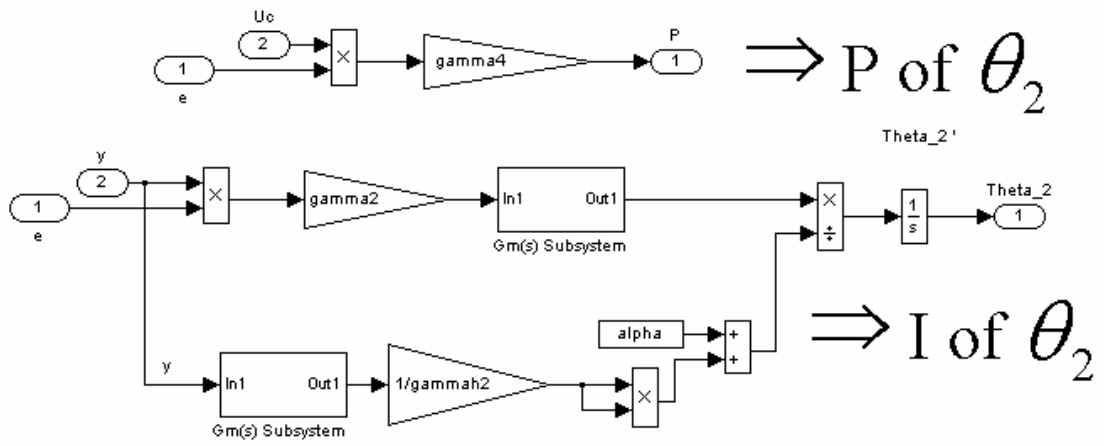


**Figure-A3** Simulink block diagram of adjustment parameter- $\theta_2$  based on normalized MIT rule.



## APPENDIX-B

### Sample Matlab-M code for longitudinal flight dynamics: MRAS design based on Lyapunov stability:

```
%%%%%%%%%%%%%%%%%%%%%%%%%%%%%%%%%%%%%%%%%%%%%%%%%%%%%%%%%%%%%%%%%%%%%%%%
%%%%%%%%%%%%%%%%%%%%%%%%%%%%%%%%%%%%%%%%%%%%%%%%%%%%%%%%%%%%%%%%%%%%%%%%
%%          FLIGH STABILITY AND CONTROL - PROJECT #1
%%
%%          Kamran Turkoglu, Istanbul Technical University,
%%          Istanbul, TURKEY, turkoglu@itu.edu.tr, kturkoglu@yahoo.com
%%          February 7th, 2007, Wed.
%%%%%%%%%%%%%%%%%%%%%%%%%%%%%%%%%%%%%%%%%%%%%%%%%%%%%%%%%%%%%%%%%%%%%%%%
%%%%%%%%%%%%%%%%%%%%%%%%%%%%%%%%%%%%%%%%%%%%%%%%%%%%%%%%%%%%%%%%%%%%%%%%

clear all, close all, clc;
syms s

% ===== %
% ===== %
% ===== LONGITUDINAL EOMS ===== %
% ===== %
% ===== %

% The constants
m=5*0.0685217659 %[slugs]%%% 1kg = 0.0685217659 slugs (MASS) (Approximate mass of
UAV is~ 3-6kg)
u=12*3.2808399 % [ft/s]%%% 1 m/s = 3.2808399 ft/s (velocity) (Approximate velovicity
of UAV is~18-19 m/sn)
g=9.807*32.1751969 % [ft / s^2] %%% Gravity constant in Emperial units ~ 9.807 m/s^2
A=0.4805*10.7639104 % [ft^2] (wing surface area) 1m^2 = 10.7639104 ft^2 (The wing
area of the UAV is ~0.1293 m^2)
rho=1.225*0.0624279606 % [lb/ft^3] %%% Density at sea level 1 kg/m^3 =
0.0624279606 lb/ ft^3
q=(rho*u^2) / 2 % Dynamic pressure
Iy=0.120396634 % 0.0888 [slug.ft^2]%%% (Moment of Inertia around y)
c=0.235*3.2808399 % [ft] %%% The chord length of the UAV = 0.235m
Lt=c*3.2808399 % [ft] The length from CG to the tail mean avg chord is ~0.235m
theta=0 % it is assumed no theta angle change (neglected), so
cos(theta)=cos(0)=1 and sin(theta)=sin(0)=0 will be taken constant
Cd=0.0132 % Drag coefficient
Cl=(m*g)/(A*q) % Lift coefficient [There is such an equation in Blakelock 1991,
pp.37, such as Cw=-Cl ]
dCl_da=0.1249 % Change oif lift coefficient with angle of attack
dCd_da=0.0389 % The change in drag coefficient with angle of attack (alpha
dCm_dit=-1.5 % This is an approximated values, not certain, ***** COULD BE ADJUSTED
*****
b=1.7*3.2808399 % [ft] %%% Wing span, from tip of the right wing to the tip of the
left wing is~1.7m
AR=(b^2)/A % Aspect Ratio, is the ratio between the square of the sapn of the wing
over the surface area of the wing
de_da=(2/(pi*AR))*(dCl_da)
K=1.1 % A constant which is generally taken 1.1 ***** COULD BE ADJUSTED *****
x=(0.25*c) % [ft] %%% distance between fixed control neutral poiunt and CG
SM=-(x/c) % static margin = xc/c

% Stability derivatives of UAV
Cxu=(-2*Cd)%-0.7507
Cx_alpha=(-dCd_da)+Cl % (this is not a certain value, might be played with that one)
Cw=-(m*g)/(A*q) % The weight coefficient of the UAV
Lt_c=Lt/c % Length of Lt over chord
Czu=-(2*Cl)
```

```

Cz_alpha_dot=(dCm_dit)*(de_da)*2
Cx_alpha=- (dCl_da)-Cd
Czq=2*K*(dCm_dit)
Cm_alpha_dot=2*(dCm_dit)*(de_da)*(Lt_c)
Cm_alpha=(SM)*(dCl_da)
Cmq=2*K*(dCm_dit)*(Lt_c)

% The elevator angle displacement, input coefficients
Cx_de=0 % neglected
Cm_de=(-0.710)
Cz_de=(c/Lt)*(Cm_de)
Ce_in=[Cx_de; Cz_de; Cm_de];

% =====
% =====
% LONGITUDINAL LINEARIZED EOMS
% =====
% =====

A_homg=[ ((m*u*s)/(A*q))-Cx_u (-Cx_alpha)
(-Cw); (-Czu) ((m*u)/(A*q)-
(c*Cz_alpha_dot)/(2*u))*s-(Cz_alpha) ((-
m*u)/(A*q)-(c*Czq)/(2*u))*s; 0 ((-
c*Cm_alpha_dot*s)/(2*u)-(Cm_alpha)
((Iy*s^2)/(A*q*c))-((c*Cmq*s)/(2*u)) ]

disp('=====')
disp('Denominator of the system')
disp('=====')
CE=det(A_homg); % Characteristic Equation (CE) of the Hoogenous solution, At the
same time this is the denominator of the whole system.

den=sym2poly(CE) % The coefficient of the denominator

disp('=====')
disp('Denominator of the system')
disp('=====')
CE=det(A_homg); % Characteristic Equation (CE) of the Hoogenous solution, At the
same time this is the denominator of the whole system.

den=sym2poly(CE) % The coefficient of the denominator

%pause, clc;

disp('=====')
disp('The roots (POLES) of the system are')
disp('=====')
poles=roots(den) % Roots of the homogenous system, POLES of the system
u1=[1 -poles(1)]; u2=[1 -poles(2)]; % Short period and Phugoid mode equations
v1=[1 -poles(3)]; v2=[1 -poles(4)]; % all together and their multiplication

conv_u12=conv(u1,u2);
conv_v12=conv(v1,v2);

if sqrt(conv_u12(3))>sqrt(conv_v12(3))
disp('=====')
disp('Characteristic equations of SHORT PERIOD in the form of ')
disp('s^2 + 2*zeta_sp*wn_sp*s + wn_sp^2 =0 is as =')
disp('=====')
conv_u12
wn_sp=sqrt(conv_u12(3))
zeta_sp=conv_u12(2)/(2*wn_sp)
Tau_sp=1/(wn_sp*zeta_sp)

disp('=====')
disp('Characteristic equations of PHUGOID MODE in the form of ')
disp('s^2 + 2*zeta_pm*wn_pm*s + wn_pm^2 =0 is as =')
disp('=====')
conv_v12
wn_pm=sqrt(conv_v12(3))
zeta_pm=conv_v12(2)/(2*wn_pm)
Tau_pm=1/(wn_pm*zeta_pm)

else

```

```

disp('=====')
disp('Characteristic equations of SHORT PERIOD in the form of ')
disp('s^2 + 2*zeta_sp*wn_sp*s + wn_sp^2 =0 is as =')
disp('=====')
conv_v12
wn_sp=sqrt(conv_v12(3))
zeta_sp=conv_v12(2)/(2*wn_sp)
Tau_sp=1/(wn_sp*zeta_sp)

disp('=====')
disp('Characteristic equations of PHUGOID MODE in the form of ')
disp('s^2 + 2*zeta_pm*wn_pm*s + wn_pm^2 =0 is as =')
disp('=====')
conv_u12
wn_pm=sqrt(conv_u12(3))
zeta_pm=conv_u12(2)/(2*wn_pm)
Tau_pm=1/(wn_pm*zeta_pm)
end

poles

%=====
% TF of theta(s) / delta_e(s)
% =====
A_te=[ ((m*u*s)/(A*q))-Cxu                                (-Cx_alpha)
      (-Cw);
      (-Czu)
      (c*Cz_alpha_dot)/(2*u)*s-(Cz_alpha)                    ((m*u)/(A*q)-
m*u)/(A*q)-(c*Czq)/(2*u)*s;                                ((-
      0
      c*Cm_alpha_dot*s)/(2*u)-(Cm_alpha)                    ((-
      ((Iy*s^2)/(A*q*c))-((c*Cmq*s)/(2*u)) ];

A_te(:,3)=Ce_in; % Using the Cramer`s rule we placed the elevator inputs in the
second column of matrix A_homg
A_te;
CE_te=-det(A_te); % Characteristic equation of theta (s)

numAte=sym2poly(CE_te) % Coefficients of NUMERATOR of theta(s) / de(s)
disp('=====')
disp('TF of theta (s) / de (s)')
disp('=====')
tf(numAte,den)
numAte=numAte/den(1);
den=den/den(1);
tf(numAte,den)
roots(den)

% =====
% ADAPTIVE CONTROLLER DESIGN PART FOR LONGITUDINAL FLIGHT
% =====
% Desired location of poles
% [short period mode]
close all

% Servo mechanism
num_srv=15;
den_srv=[1 num_srv];

% Lead compensator
num_lead=[0.6428 2.3027];
den_lead=[1.0000 12.8323];

% System matrix of the servos
num_long=conv(num_lead,(numAte*num_srv));
den_long=conv(den_lead,conv(den,den_srv));
[Along,Blong,Clong,Dlong]=tf2ss(num_long,den_long)
B=Blong;
eigs_long=eig(Along)

% Model reference system
zeta_sp_m=0.907;
wn_sp_m=8.5;
zeta_pm_m=0.907;
wn_pm_m=2.25;
rts=roots(numAte);
num_mm=(wn_sp_m^2)*(wn_pm_m^2)

```

```

num_m=(wn_sp_m^2)*(wn_pm_m^2)
den_m=conv([1 2*zeta_sp_m*wn_sp_m wn_sp_m^2],[1 2*zeta_pm_m*wn_pm_m
wn_pm_m^2]);
tf(num_m,den_m)

num_m_new=5.57271898206461*conv(num_lead,(num_m*num_srv));
den_m_new=conv(den_lead,conv(den_m,den_srv));
[Am,Bm,Cm,Dm]=tf2ss(num_m_new,den_m_new)
eigs_m=eig(Am)

%Lyapunov function
N=diag([ 700 0 0 0 0 0]);
g=3.4;
Nbar=rscale(Along,Blong,Clong,Dlong,1.37701190620988);
Nbar=Nbar(1);
P=lyap(Am',N)

% Simulation of UAV using
% Adaptive Control system Lyapunov stability rule
d_e=2;
% First simulation
SimTime=15; % [sec]
sim('UAVSimLyapLat_DeltaL_Last.mdl')
figure,plot(y.time,y.signals.values,'k:'), xlabel('Time [sec]'), ylabel('\theta
[deg]'), title('Adaptive Control system design using Lyapunov stability - Long.
dynamics'), hold on
plot(y_m.time,y_m.signals.values,'k:'), xlabel('Time [sec]'), ylabel('\theta [deg]'),
title('Adaptive Control system design using Lyapunov stability - Long. dynamics'),
hold on,
legend('y','y_m')
%axis([ 0 SimTime 0 3.0 ])

%break

SimTime=100; % [sec]
sim('UAVSimLyapLat_DeltaL_Last.mdl')
figure,
subplot(3,1,1),plot(y.time,y.signals.values,'k:'), xlabel('Time [sec]'),
ylabel('\theta [deg]'), title('Adaptive Control system design using Lyapunov
stability - Long. dynamics'), hold on
plot(y_m.time,y_m.signals.values,'k:'), xlabel('Time [sec]'), ylabel('\theta [deg]'),
title('Adaptive Control system design using Lyapunov stability - Long. dynamics'),
hold on,
legend('y','y_m')
%axis([ 0 SimTime 0.9 1.1 ])
subplot(3,1,2),plot(e.time,e.signals.values,'k:'), xlabel('Time [sec]'), ylabel('Error
[e = y - y_m]'), title('Adaptive Control system design using Lyapunov stability -
Error signal'), hold on
subplot(3,1,3),plot(u.time,u.signals.values,'k:'), xlabel('Time [sec]'),
ylabel('Actuator signal [N]'), title('Adaptive Control system design using Lyapunov
stability - Control/Servo/Actuator signal'), hold on

```

### Sample Matlab-M code for lateral flight dynamics: MRAS design based on Lyapunov stability:

```

%%%%%%%%%%%%%%%%%%%%%%%%%%%%%%%%%%%%%%%%%%%%%%%%%%%%%%%%%%%%%%%%%%%%%%%%
%%%%%%%%%%%%%%%%%%%%%%%%%%%%%%%%%%%%%%%%%%%%%%%%%%%%%%%%%%%%%%%%%%%%%%%%
%% Kamran Turkoglu, Istanbul Technical University,
%%
%% Istanbul, TURKEY, turkoglu@itu.edu.tr, kturkoglu@yahoo.com %%
%% March 21th, 2007, Wed.
%%
%% Last Modified 21 March '07, 11:01hr
%%
%%%%%%%%%%%%%%%%%%%%%%%%%%%%%%%%%%%%%%%%%%%%%%%%%%%%%%%%%%%%%%%%%%%%%%%%
%%%%%%%%%%%%%%%%%%%%%%%%%%%%%%%%%%%%%%%%%%%%%%%%%%%%%%%%%%%%%%%%%%%%%%%%

clear all, close all, clc
syms s

% ===== %
% ===== %
% ===== LATERAL EOMS ===== %
% ===== %

```

```

% ===== %
% The constants
m=5; %*0.0685217659 %[slugs]%%% 1kg = 0.0685217659 slugs (MASS) (Approximate mass of
UAV is~ 3-6kg)
u=17; %*3.2808399 % [ft/s]%%% 1 m/s = 3.2808399 ft/s (velocity) (Approximate
velocity of UAV is~18-19 m/sn)
g=9.807; %32.1751969 % [ft / s^2] %%% Gravity constant in Imperial units ~ 9.807
m/s^2
A=0.4805; %*10.7639104 % [ft^2] (wing surface area) 1m^2 = 10.7639104 ft^2 (The wing
area of the UAV is ~0.1293 m^2)
Avt=0.1323; % [m^2] - The Area of vertical tail
rho=1.225; %*0.0624279606 % [lb/ft^3] %%% Density at sea level 1 kg/m^3 =
0.0624279606 lb/ ft^3
q=(rho*u^2)/2; % Dynamic pressure
Iyy=0.120396634; % 0.0888 [slug.ft^2]%%% (Moment of Inertia around y)
c=0.235; %*3.2808399 % [ft] %%% The chord length of the UAV = 0.235m
Lt=c;%*3.2808399 % [ft] The length from CG to the tail mean avg chord is ~0.235m
theta=0; % it is assumed no theta angle change (neglected), so
cos(theta)=cos(0)=1 and sin(theta)=sin(0)=0 will be taken constant
Cd=0.0132; % Drag coefficient
Cl=(m*g)/(A*q); % Lift coefficient [There is such an equation in Blakelock 1991,
pp.37, such as Cw=-Cl ]
dCl_da=0.1249; % Change oif lift coefficient with angle of attack
dCd_da=0.0389; % The change in drag coefficient with angle of attack (alpha
dCm_dit=-1.5; % This is an approximated values, not certain, ***** COULD BE ADJUSTED
*****
b=1.7; %*3.2808399 % [ft] %%% Wing span, from tip of the right wing to the tip of
the left wing is~1.7m
AR=(b^2)/A; % Aspect Ratio, is the ratio between the square of the sapn of the wing
over the surface area of the wing
e=0.88; % Efficiency factor is between 0.8 ~ 0.9
de_da=(2/(pi*e*AR))*(dCl_da);
K=1.1; % A constant which is generally taken 1.1 ***** COULD BE ADJUSTED *****
x=(0.25*c); % [ft] %%% distance between fixed control neutral point and CG
SM=(x/c); % static margin = xc/c

% For trial Cesna T-37 has been selected
% All the values presented right here are approximated values taken from Table 3.1
pp.117, Blakelock, Aircraft and Missiles, 1991, = [1])
Cy_beta=-0.6*0.3048; % [m/sn^2] - Fuselage and vertical tail coeff.
Cl_beta=-0.045; % [1/sn^2] - Dihedral and vertical tail coeff.
Cl_p=-0.12; % [1/sn] - Wing damping coeff.
Cl_r=Cl/4; % [1/sn] - differential wing normal force coeff.
Cy_phi=Cl;
Cy_ksi=0;
Cn_beta=0.001; % [1/sn^2] - Directinal stability coeff.
Cn_p=-(Cl/8)*(1-de_da); % [1/sn] - Differential wing chord force
Cn_r=-Cd/4;
Cy_delta_r=0.0158; % [m^2/sn^2] - Rudder displacement / input in Y
Cl_delta_r=0.0131; % [1/sn^2] - Rudder displacement / input in L
Cn_delta_r=-0.08; % [1/sn^2] - Rudder displacement / input in Y
Cy_delta_a=0;
Cl_delta_a=0.6; % [1/sn^2] - Aileron displacement / input in L
Cn_delta_a=-0.01; % [1/sn^2] - Aileron displacement / input in N
Ixx=Iyy/1.4;
Izz=1.5*Iyy;
Ixz=0;

% The denominator of the Lateral motion and A matrix (taken from pp.122, Blakelock,
Aircraft and Missiles, 1991 ) is as
% Here the representation is as

% ---          ---          ---          ---
% |                | |          phi(s) |
% |                | |          psi(s) | = Cdelta_rudder or
Cdelta_aileron
% |                | |          beta(s) |
% ---          ---          ---          ---

disp('=====')
disp(' Matrix representation of the LATERAL Flight')
disp('=====')
Alat=[          ((Ixx*s^2)/(A*q*b)-(b*Cl_p*s)/(2*u))          ((-
Ixz*s^2)/(A*q*b)-(b*Cl_r*s)/(2*u))          (-Cl_beta)
;

```



```

% Rudder deflections
Ydelta_rudder=(rho*u^2*A*Cy_delta_r)/(2*m)
Ldelta_rudder=(rho*u^2*A*b*Cl_delta_r)/(2*Ixx)
Ndelta_rudder=(rho*u^2*A*b*Cn_delta_r)/(2*Izz)

% Rudder deflections
Ydelta_aileron=(rho*u^2*A*Cy_delta_a)/(2*m)
Ldelta_aileron=(rho*u^2*A*b*Cl_delta_a)/(2*Ixx)
Ndelta_aileron=(rho*u^2*A*b*Cn_delta_a)/(2*Izz)

IA=Ixz/Ixx
IB=Ixz/Izz

% Primed stability derivatives
Lbeta_prime=Lbeta+IB*Nbeta
Lp_prime=Lp+IB*Np
Lr_prime=Lr+IB*Nr
Ldelta_aileron_prime=Ldelta_aileron+IB*Ndelta_aileron
Ldelta_rudder_prime=Ldelta_rudder+IB*Ndelta_rudder

Nbeta_prime=Nbeta+IA*Lbeta
Np_prime=Np+IA*Lp
Nr_prime=Nr+IA*Lr
Ndelta_aileron_prime=Ndelta_aileron+IA*Ldelta_aileron
Ndelta_rudder_prime=Ndelta_rudder+IA*Ldelta_rudder

Ydelta_rudder_star=Ydelta_rudder/u

% =====
% LATERAL MOTION STATE SPACE REPRESENTATION
% =====
Alat_ss=[      Yv      0      -1      g/u      0;
          Lbeta_prime  Lp_prime  Lr_prime  0      0;
          Nbeta_prime  Np_prime  Nr_prime  0      0;
          0             1         0         0      0;
          0             0         1         0      0] % STATE SPACE MATRIX

% u=[ delta_aileron; delta_rudder]
Blat_ss=[      0      Ydelta_rudder_star ;
          Ldelta_aileron_prime  Ldelta_rudder_prime ;
          Ndelta_aileron_prime  Ndelta_rudder_prime ;
          0                     0             ;
          0                     0             ]; % CONTROL MATRIX

%Blat_ss(:,3:5)=0

% x=[beta; p; r; phi; psi]
Clat_ss=eye(5) % OUTPUT MATRIX - [we can select the outputs]
Clat_ss_beta = [ 1 0 0 0 0];
Clat_ss_p    = [ 0 1 0 0 0];
Clat_ss_r    = [ 0 0 1 0 0];
Clat_ss_phi  = [ 0 0 0 1 0];
Clat_ss_psi  = [ 0 0 0 0 1];

Dlat_ss=zeros(5,2)
disp('=====')
disp('Poles of the system')
disp('=====')
poles=eig(Alat_ss)';

disp('=====')
disp('Dutch Roll Mode')
disp('=====')

disp('=====')
disp('TF of RUDDER SERVO')
disp('=====')
num_r_servo=[0 5];
den_r_servo=[1 5];
tf_rservo=tf(num_r_servo,den_r_servo);

disp('=====')
disp('Rudder deflection (degrees)')
disp('=====')
d_r=2;

disp('=====')
disp('TFs for Rudder input')

```

```

disp('=====')
% x=[beta; p; r; phi; psi]
[num_r,den_r]=ss2tf(Alat_ss,Blat_ss,Clat_ss,Dlat_ss,2);

disp('=====')
disp(' Beta (s)/de_r')
disp('=====')
tf(num_r(1,:),den_r)

disp('=====')
disp('TFs of p/de_r')
disp('=====')
tf(num_r(2,:),den_r)

disp('=====')
disp('TFs of r / de_r')
disp('=====')
tf(num_r(3,:),den_r)

disp('=====')
disp('TFs of phi (s)/de_r')
disp('=====')
tf(num_r(4,:),den_r)

disp('=====')
disp('TFs of psi (s)/de_r')
disp('=====')
tf(num_r(5,:),den_r)

% =====
% TFs for the aileron and rudder input
% =====
% TFs for aileron input
[numail,denail]=ss2tf(Alat_ss,Blat_ss,Clat_ss,Dlat_ss,1);
disp('=====')
disp('TFs for Aileron input')
disp('=====')

disp('=====')
disp(' Beta (s)/de_ail')
disp('=====')
tf(numail(1,:),denail)
disp('=====')
disp('TFs of p/de_ail')
disp('=====')
tf(numail(2,:),denail)

disp('=====')
disp('TFs of r / de_ail')
disp('=====')
tf(numail(3,:),denail)

disp('=====')
disp('TFs of phi (s)/de_ail')
disp('=====')
tf(numail(4,:),denail)

disp('=====')
disp('TFs of psi (s)/de_ail')
disp('=====')
tf(numail(5,:),denail)

%figure,
%impulse(Alat_ss,Blat_ss,Clat_ss,Dlat_ss),title('Impulse response of the OL time
domain sys. in Lat. Flight')

% TFs for rudder input
[numrud,denrud]=ss2tf(Alat_ss,Blat_ss,Clat_ss,Dlat_ss,2);
disp('=====')
disp('TFs for Rudder input')
disp('=====')
disp('beta/d_r')
tf(numrud(1,:),denrud);
%figure, step(numrud(1,:),denrud)
%figure, impulse(numrud(1,:),denrud)
disp('p/d_r')

```



```

tf(numrud(2,:),denrud);
%figure, step(numrud(2,:),denrud)
%figure, impulse(numrud(2,:),denrud)
disp('r/d_r')
tf(numrud(3,:),denrud);
%figure, step(numrud(3,:),denrud)
%figure, impulse(numrud(3,:),denrud)
disp('phi/d_r')
tf(numrud(4,:),denrud);
%figure, step(numrud(4,:),denrud)
%figure, impulse(numrud(4,:),denrud)
disp('psi/d_r')
tf(numrud(5,:),denrud);
%figure, step(numrud(5,:),denrud)
%figure, impulse(numrud(5,:),denrud)

% =====
% ADAPTIVE CONTROLLER DESIGN PART FOR LONGITUDINAL FLIGHT
% =====
% Desired location of poles
% [short period mode]
close all

%TF of the servo(aileron/rudder) actuators
num_srv=15.0;
den_srv=[1.0 num_srv];

%TF of the servo(aileron/rudder) actuators
num_srv=15.0;
den_srv=[1.0 num_srv];

% System matrix of the servos
Gsys1 = pck(Alat_ss,Blat_ss,Clat_ss,Dlat_ss);
Servosys1=nd2sys(num_srv,den_srv);
Servosys=daug(Servosys1,Servosys1);
Gsys=mmult(Gsys1,Servosys);

% State space matrixes of the nominal plant with
% servos included in it
[Alat_new,Blat_new,Clat_new,Dlat_new]=unpck(Gsys);
Clat_new=eye(length(Alat_new))
Dlat_new=zeros(7,2)

% Just a simple lqr control system design
[Klat_lqr,Slat,Elat]=lqr(Alat_new,Blat_new,diag([2 2 8 178 30 10 30
]),diag([1.5 1.5])); %15.85 9 1.2 8 110 18 10
Alat_new_m=Alat_new-Blat_new*Klat_lqr;
eigsModel=eig(Alat_new-Blat_new*Klat_lqr)
d_ar=2;
SimTime=5;
sim('plqrSimModel.mdl')
%figure,plot(plqr.time,plqr.signals.values),legend('\beta','p','r','\phi','\psi')

% Lyapunov function
N=diag([ 1470 1280 8625 6200 8770 80 40])
P=lyap(Alat_new_m,N);
eigsP=eig(P);
d_e=2;

% Definition of B
B=zeros(7,2);
B(6,1)=Blat_new(6,1)
B(7,2)=Blat_new(7,2)

B'*N*B

% First simulation
SimTime=15 % [sec]
sim('UAVSimLyapLat_DeltaL_Last.mdl')
figure,plot(y.time,y.signals.values,'k'), xlabel('Time [sec]'), ylabel('\theta
[deg]'), title('Adaptive Control system design using Lyapunov stability theory -
Lateral. dynamics'), hold on
plot(y_m.time,y_m.signals.values,'k'), xlabel('Time [sec]'), ylabel('\theta [deg]'),
title('Adaptive Control system design using Lyapunov stability theory - Lateral.
dynamics'),
legend('y','y_m')
%axis([ 0 SimTime -3.0 3.0 ])

```

```

d_e=2;
%break

figure,
subplot(3,1,1),plot(y.time,y.signals.values,'k:'), xlabel('Time [sec]'),
ylabel('\theta [deg]'), title('Adaptive Control system design using Lyapunov
stability theory - Lateral. dynamics'), hold on
plot(y_m.time,y_m.signals.values,'k'), xlabel('Time [sec]'), ylabel('\theta [deg]'),
title('Adaptive Control system design using Lyapunov stability theory - Lateral.
dynamics'),
legend('y','y_m'),
subplot(3,1,2),plot(e.time,e.signals.values,'k'), xlabel('Time [sec]'), ylabel('Error
signal'), title('Adaptive Control system design using Lyapunov stability theory -
Error signal'),
subplot(3,1,3),plot(u.time,u.signals.values,'k'), xlabel('Time [sec]'), ylabel('Error
signal'), title('Adaptive Control system design using Lyapunov stability theory -
Error signal'),
legend('\delta_a','\delta_r'),

%axis([ 0 SimTime 0 3.0 ])
d_e=2;

```

## **CURRICULUM VITAE**

Kâmrân Türkođlu was born in Shumen, Bulgaria in 1981. He completed his primary school in Yenibosna İlköđretim Okulu and after 7 years of study, he graduated from Fahrettin Kerim Gökay Anadolu Lisesi in June 2000 and enrolled to the Istanbul Technical University, Astronautical Engineering Department. He has been awarded a Double Major Degree with Minor in Aeronautical Engineering Department in September 2003. He graduated from Astronautical Engineering Department in June 2005 and from Aeronautical Engineering Department in June 2006, respectively. He is still continuing his studies as a M.Sc. student in Istanbul Technical University, Aeronautical & Astronautical Engineering Department.